INVESTIGATING THE MASS SPECTROMETRIC BEHAVIOR OF NOVEL ANTINEOPLASTIC CURCUMIN ANALOGUES

A Thesis Submitted to the College of

Graduate Studies and Research

In Partial Fulfillment of the Requirements

For the Degree of Master of Science

In the College of Pharmacy and Nutrition

University of Saskatchewan

Saskatoon, SK, Canada

By

Hanan Awad Ebrahim Elsayed

PERMISSION TO USE

In presenting this dissertation in partial fulfilment of the requirements for a Postgraduate degree from the University of Saskatchewan, I agree that the Libraries of this University may make it freely available for inspection. I further agree that permission for copying of this thesis in any manner, in whole or in part, for scholarly purposes may be granted by the professor who supervised my thesis work or, in their absence, by the Head of the Department or the Dean of the College in which my thesis work was done. It is understood that any copying or publication or use of this thesis or parts thereof for financial gain shall not be allowed without my written permission. It is also understood that due recognition shall be given to me and to the University of Saskatchewan in any scholarly use which may be made of any material in my thesis.

Requests for permission to copy or to make other use of material in this dissertation in whole or part should be addressed to:

Dean of the College of Pharmacy and Nutrition

University of Saskatchewan

Saskatoon, Saskatchewan S7N 2Z4

Canada

OR

Dean of the College of Graduate Studies and Research

University of Saskatchewan

Saskatoon, Saskatchewan S7N 5A2

Canada

ABSTRACT

Curcumin analogues are novel antineoplastic agents designed by structural modifications of the natural product curcumin to enhance its therapeutic effects. Various curcumin analogues displayed a significant cytotoxic effect towards different cancer cell lines including leukemia, melanoma, and colon cancer. In order to evaluate the safety, efficiency and metabolism of the new anticancer candidates, sensitive and high throughput analytical methods are needed. Thirteen curcumin analogues with the backbone structure of 3,5-bis(benzylidene)-4-piperidone were tested. The ionization behavior of curcumin analogues was investigated to reveal the possible mechanisms for the unusual formation of the positively charged $[M-H]^+$ ions during single stage positive ion mode MALDI-MS analysis. Different ionization techniques (i.e., ESI, APCI, APPI, and MALDI) were used to evaluate this phenomenon. The results showed that curcumin analogues ionize into $[M-H]^+$ along with the expected $[M+H]^+$ species during MALDI and dopant free APPI-MS. In contrast, ESI, APCI and the dopant mediated APPI showed only the expected $[M+H]^+$ peak. Our experiments revealed that photon energy triggers the ionization of the curcumin analogues even in the absence of any ionization enhancer such as matrix, solvent or dopant. Three proposed mechanisms for the formation of $[M-H]^+$ were evaluated, two of them are probably involved in the $[M-H]^+$ formation: (i) hydrogen transfer from the analyte radical cation and (ii) hydride abstraction.

In addition to the ionization behavior, the collision induced dissociation-tandem mass spectrometric (CID-MS/MS) fragmentation behavior of curcumin analogues was evaluated showing similar dissociation pathways that centered on the piperidone ring of the 3,5-bis(benzylidene)-4-piperidone moiety. The presence of different substitutes on that moiety resulted in specific product ions for each curcumin analogue. The fragmentation patterns were

established to confirm the chemical structure of the tested compounds and identify the diagnostic product ions of each compound. Twelve common product ions were identified resulting from the breakage of various bonds within the piperidone moiety. There was a tendency for the formation of highly conjugated product ions that are stabilized via resonance. Common product ions were identified allowing for the establishment of a general MS/MS behavior for any curcumin analogue that belongs to the 3,5-bis(benzylidene)-4-piperidone structural family. The fragmentation routes and the genesis of the product ions were confirmed via MS^3 and neutral loss analysis.

In summary, the ionization of curcumin analogues provided insights into the formation of unique $[M-H]^+$ ions which were linked to photo ionization of such compounds without the need for additives, such as matrix, dopant or solvent. As such, curcumin analogues should be evaluated as MALDI matrices in the future. The CID-MS/MS analysis of curcumin analogues revealed a common fragmentation behavior of the tested compounds. It will be applied, in the future to determine metabolic by-products of the tested compounds as well as to develop targeted liquid chromatography (LC)-MS/MS methods.

ACKNOWLEDGEMENTS

I would like to thank my supervisor Dr. A. El-Aneed for his guidance, support, and patience. This thesis would not have been possible without his help and encouragement. I consider myself very fortunate to have him as a supervisor.

I would also like to thank my advisory committee members; Dr. G. McKay and Dr. R. Purves for spending their time on careful reading of my thesis and for their valuable comments. I also express thanks to my committee chair Dr. E. Krol for his help and guidance.

I sincerely acknowledge Dr. J. Amster, Ms. M. J. Stoudemayer, Dr. A. Cohen, Mr. K. Thoms, Ms. L. Usher, Dr. J. Dimmock, and Dr. U. Das for their valuable contribution to my research work. My gratitude is extended to Dr. R. Verrall and Dr. I. Badea for their support. I also acknowledge Ms. D. Michel and Dr. J. Buse for the training they provided in the mass spectrometry instrumentation.

I gratefully acknowledge the funding received towards my M.Sc. from the College of Pharmacy and Nutrition and the College of Graduate Studies and Research. I also appreciate and thank all my colleagues for their friendship and support: Ms. M. Poorghorban, Ms. M. Al-Dulaymi, Ms. M. Hamada, Mr. W. Mohammed-Saeid, Mr. M. Donkuru, Ms. S. Alwani, Ms. R. Kaur, Ms. S. Fatani, Dr. J. Singh, and Dr. J. Chitanda.

Finally I dedicated this work to my parents who always loved and supported me and to my sisters and brother for their care, love, and support.

TABLE OF CONTENTS

LIST OF SCHEMES

LIST OF FIGURES

LIST OF TABLES

LIST OF ABBREVIATIONS

AC	Alternating current
ACN	Acetonitrile
APCI	Atmospheric pressure chemical ionization
APPI	Atmospheric pressure photoionization
BHT	Butylated hydroxytoluene
CE	Collision energy
CHCA	α-Cyano-4- hydroxycinnamic acid
CI	Chemical ionization
CID	Collision induced dissociation
Cur	Curcumin
DAPPI	Desorption atmospheric pressure photoionization
DART	Direct analysis in real time
DC	Direct current
DESI	Desorption electrospray ionization
DHB	Dihydroxybenzoic acid
EI	Electron ionization
ESI	Electrospray ionization
FTICR	Fourier transform ion cyclotron resonance
HPLC	High-performance liquid chromatography
hν	Photon energy
IE	Ionization energy
IS	Internal standard
LC-MS	Liquid chromatography–mass spectrometry
LD-MS	Laser desorption-mass spectrometry
LIT	Linear ion trap
LLE	Liquid-liquid extraction
m/z	Mass to charge ratio
MALDI	Matrix assisted laser desorption ionization
MRM	Multiple reaction monitoring
MS	Mass spectrometry
MS/MS	Tandem mass spectrometry
MS^3	MS/MS/MS
MS^n	Multi-stage mass spectrometry
PAHs	Polycyclic aromatic hydrocarbons
PPT	Protein precipitation
Q	Quadrupole
Qq-LIT	Quadrupole-linear ion trap
QqQ	Triple quadrupole
Q-TOF	Quadrupole-time of flight
RF	Radio frequency
S/N ratio	Signal-to-noise ratio
SPE	Solid phase extraction
TFA	Trifluoroacetic acid
TOF	Time of flight

TOF/TOF	Tandem time of flight

CHAPTER 1
INTRODUCTION[1]

Mass spectrometry (MS) is widely used in analytical chemistry based on its ability to analyze a wide range of compounds in complex matrices with high sensitivity, selectivity, and speed. MS is applied to both small drug molecules and macromolecules and is routinely used for qualitative and quantitative applications including drug discovery [1-3], proteomics [4], metabolomics [5], genomics [6], and lipidomics [7]. MS is able to detect and quantify analytes at the pg/ml levels [8-10], hence it is routinely applied in various disciplines such as forensic science [11], toxicology [12], food safety [13], and environmental science [14].

The fast developments in MS instrumentation, including the introduction of soft ionization sources, high resolution mass analyzers, and hybrid MS instruments, allowed MS to be an ideal tool for meeting the needs of researchers in the biological and the pharmaceutical sciences. In drug discovery and development [1-3], MS identifies and structurally characterizes new drug candidates via accurate mass measurements as well as via tandem mass spectrometric (MS/MS) analysis. In addition, MS analysis is important for purity assessment of newly synthesized drug molecules and their pharmaceutical formulations [15, 16]. Such assessment allows for monitoring the synthetic process and establishing the degradation profile of the new formulation [15, 16]. In addition, MS is used to evaluate the safety and efficiency of new drug candidates during preclinical and clinical studies by monitoring their metabolic profile as well as their pharmacological and pharmacokinetic properties [1, 17].

Among various therapeutic agents, anticancer drugs remain at the forefront of drug development efforts. Global investments in anticancer treatments are expected to reach $143.7

[1] Part of the thesis introduction was recently published as a review article "*H. Awad, M. M. Khamis, and A. El-Aneed, "Mass Spectrometry, Review of the Basics: Ionization," Applied Spectroscopy Reviews, vol. 50, pp. 158-175, 2015".*

billion by 2023 [18]. In 2013 alone, the US Food and Drug Administration (FDA) approved nine of 27 new molecular entities for oncology [19]. The design of new anticancer agents usually aims to improve potency, safety, and selective toxicity towards malignant cells rather than normal cells. One target is natural products; for example, several studies have been conducted to explore the anticancer properties of curcumin and showed anti-inflammatory, antioxidant, antiproliferative, and antiangiogenic activities, with a high safety profile [20]. Curcumin (Scheme 1.1) is a natural product derived from the dietary spice turmeric that has traditionally been used in Indian folk medicine [21]. Epidemiological studies attribute the low incidence of colon cancer in India to diets rich in curcumin [22]. However, the poor bioavailability of curcumin has hampered its wide use as an anticancer agent [23]. Several approaches have been adopted to improve curcumin potency, targeting, and bioavailability [23-28]; one of which is the synthesis of structurally related compounds, namely curcumin analogues [27-29].

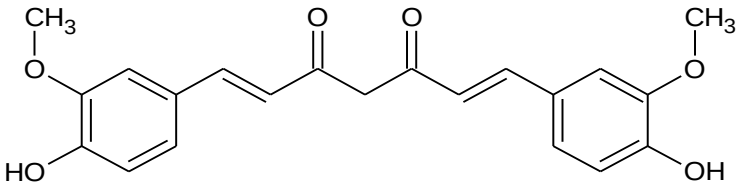

Scheme1.1. Structure of curcumin

A number of curcumin analogues showed promising *in vivo* anticancer properties including attacking cancer cells via multiple active sites and low toxicity towards normal cells [30]. All these observations support the notion that curcumin analogues are good anticancer candidates. Therefore, it is important to develop qualitative and quantitative methods for these compounds using high throughput technologies such as MS.

My proposed M.Sc. research is mainly focused on studying the MS behavior of novel curcumin analogues. The ionization behavior of curcumin analogues will be investigated to reveal the possible mechanisms for the unusual formation of the positively charged $[M-H]^+$ ions during single stage positive ion mode matrix assisted laser desorption ionization-MS (MALDI-MS) analysis of these compounds. Different ionization techniques namely, electrospray ionization (ESI), atmospheric pressure chemical ionization (APCI), atmospheric pressure photoionization (APPI), and MALDI were used. Understanding such unusual ionization behavior of curcumin analogues is important for the future development of MALDI-MS analytical methods that monitor the $[M-H]^+$ ions of these compounds in positive ion mode. The investigated mechanisms for the $[M-H]^+$ formation can also be applied to structurally-related compounds that may ionize in similar fashion.

In addition, the fragmentation behavior of curcumin analogues will be investigated using ESI tandem mass spectrometry (MS/MS). The fragmentation pattern (i.e., fingerprint) of each curcumin analogue will be established and a universal MS/MS pattern will be developed allowing for future identification and quantification of curcumin analogues.

1.1. Curcumin analogues

As mentioned earlier, curcumin analogues are therapeutic agents designed by structural modification of the curcumin molecule to enhance its therapeutic effects [29]. Various newly designed curcumin analogues displayed a significant cytotoxic effect towards different cancer cell lines including leukemia, melanoma, and colon cancer [30-33]. The evaluated molecules are 3,5-bis(benzylidene)-4-piperidone compounds, containing the 1,5-diaryl-3-oxo-1,4-pentadienyl pharmacophore (Scheme 1.2) with conjugated unsaturated ketones that act as thiol alkylators.

Since the nucleic acids are free of thiols, these compounds are targeting cellular proteins rather than attacking the nucleic acids, decreasing the possibility of mutagenicity and carcinogenicity that are usually induced by other anticancer agents [30, 32].

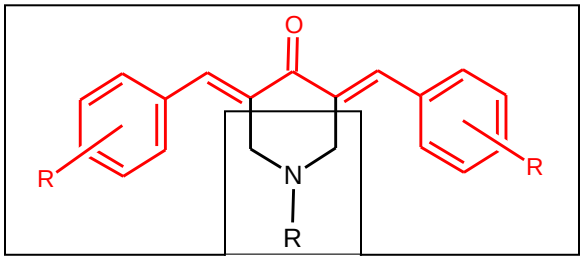

Scheme 1.2. General structure of the 3,5-bis(benzylidene)-4-piperidones (the 1,5-diaryl-3-oxo-1,4-pentadienyl pharmacophore is in the box).

The anticancer effect of curcumin analogues occurs through multiple modes of actions and multitarget sites [30]. One important cellular target for curcumin analogues is mitochondria [30]. These compounds can affect mitochondrial functions through increasing the cellular concentrations of reactive oxygen species, inhibiting oxygen consumption, and increasing the mitochondrial respiration rates, causing a decrease in its membrane potential [34].

Despite the cytotoxic properties of the 1,5-diaryl-3-oxo-1,4-pentadienyl pharmacophore (Scheme 1.2), challenges exist for the *in-vivo* use of these compounds as a result of the lipophilic nature of the 3,5-bis(benzylidene)-4-piperidone moiety [32]. This was controlled by adding substituents on the aryl groups, that in turn, changed the steric and hydrophobic properties of curcumin analogues (Scheme 1.3) [32]. Various substituents were also introduced to the piperidyl nitrogen atom of the 3,5-bis(benzylidene)-4-piperidones. The goal of N-substitution is to protect the piperidyl nitrogen atom from ionization at biological pH, since the ionized compounds cannot penetrate the membrane of the target cells [30]. In addition, N-substituents

introduce additional binding sites to the cellular target that may enhance the cytotoxicity of the drug [30, 31]. However, it is argued that such N-substituents may prevent the alignment of the 1,5-diaryl-3-oxo-1,4-pentadienyl with its primary binding site, decreasing its potency [30, 31]. Therefore, various N-substituents were introduced, and based on the N-substituent, tested curcumin analogues in this study have been categorized into four subgroups: phosphoramidates, secondary amines, mixed amines/amides, and amides (Scheme 1.3).

In addition to evaluating the cytotoxic and lipophilic properties of curcumin analogues, the photochemical properties of curcumin were also investigated. In 2013 [35], T. Qian *et al.* investigated the photolysis mechanisms of the curcumin molecule when exposed to a 355 nm laser using laser flash photolysis. The absorption spectrum of curcumin was recorded at different times after the laser pulse to monitor the generated transient species of curcumin. The results demonstrated the photoionization of curcumin (Cur) in ethanol/water mixtures producing a curcumin radical cation ($Cur^{\bullet+}$) that could be transferred into the neutral radical form ($Cur^{\bullet}$) by deprotonation. Curcumin could also be photo-excited to generate the excited singlet form (Cur^{*}) that could be transferred into the excited triplet form ($^{3}Cur^{*}$). The ratio of photoionization to photoexcitation of curcumin in ethanol/water mixtures was 3.35, indicating that photoionization is the main mechanism of curcumin photolysis [35]. Such photoionization behavior theoretically could be applied to the curcumin analogues due to structural similarities.

Phosphoramidates

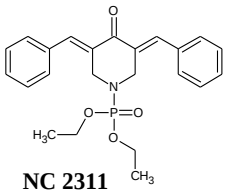

NC 2311

411.1599 Da

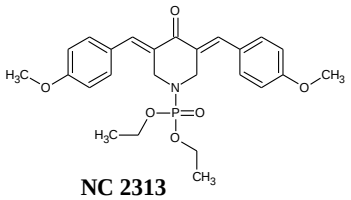

NC 2313

471.1811 Da

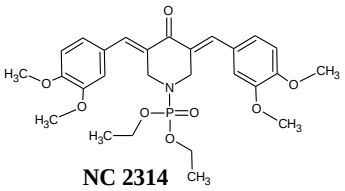

NC 2314

531.2022 Da

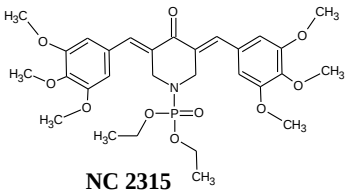

NC 2315

591.2233 Da

Secondary Amines

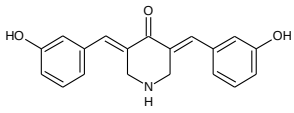

NC 2128

307.1208 Da

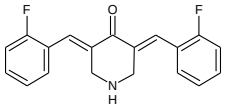

EF-24

311.1122 Da

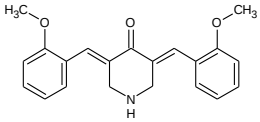

NC 2453

335.1521 Da

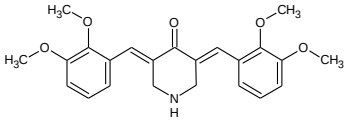

NC 2454

395.1733 Da

Mixed Amine and Amide

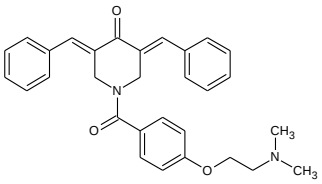

NC 2067

466.2256 Da

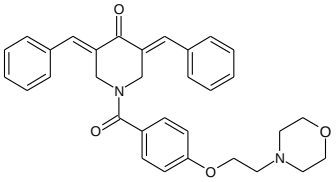

NC 2081

508.2362Da

Amides

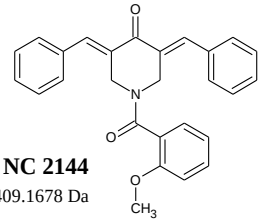

NC 2144

409.1678 Da

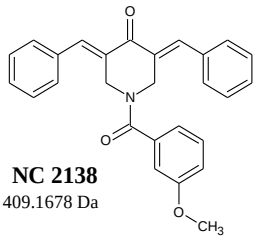

NC 2138

409.1678 Da

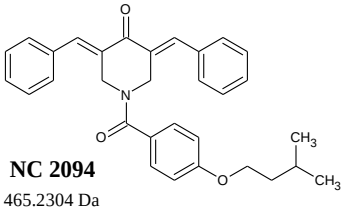

NC 2094

465.2304 Da

Scheme 1.3. Structures and monoisotopic masses of the novel antineoplastic curcumin analogues categorized by the N-substituent into four structural families: phosphoramidates, secondary amines, mixed amines/amides, and amides.

1.2. Mass spectrometry (MS)

MS is one of the most powerful analytical tools whose use is growing in numerous pharmaceutical and biological fields due to its high sensitivity, selectivity, accuracy, and high throughput capability. MS provides structural information of the analyte by measuring the mass-to-charge ratio *(m/z)* values of the charged molecules and MS/MS fragments.

1.2.1. MS ionization methods

Various ionization techniques have been used with MS including: electrospray ionization (ESI) [36, 37], atmospheric pressure chemical ionization (APCI) [38, 39], atmospheric pressure photoionization (APPI) [40] and matrix assisted laser desorption ionization (MALDI) [41, 42]. ESI and MALDI are commonly used soft ionization techniques that are able to ionize analytes with little or no fragmentation [43, 44]. ESI and APCI are readily interfaced with high-performance liquid chromatography (HPLC), therefore both are commonly used for liquid chromatography–mass spectrometry (LC-MS) [45] . Recently, APPI has been utilized in LC-MS to ionize compounds that are not well-ionized by APCI or ESI such as non-polar compounds [45]. The general principle of each ionization technique is discussed in the following sections.

1.2.1.1. Electrospray ionization (ESI)

In ESI [36, 37], the sample is introduced in solution at a typical flow rate of 1-1000 µL/min into a spray needle/capillary with a high voltage (e.g., 3–6 kV) being applied. The voltage can be either negative or positive based on the nature of the analyte, producing charged droplets that are sprayed out from the needle tip into the atmosphere (nebulization) [45]. The presence of a sheath gas (nitrogen) flowing around the needle during the nebulization process assists in directing the

droplets from the capillary tip. The charged droplets pass either through a curtain of heated inert gas (nitrogen), or through a heated capillary for complete solvent evaporation. Ions formed by ESI at atmospheric pressure pass through an orifice into the mass spectrometer for mass analysis as shown in Scheme 1.4 [45].

Two different mechanisms were proposed for ion generation in ESI, as illustrated in Scheme 1.5 [44, 46-48]: **The ion evaporation mechanism** involves solvent evaporation and coulombic fissions of the charged droplets forming smaller droplets. The gas phase ions are directly released/desorbed from the surface of the small droplets when the repulsion between charges at the droplet surface overcomes the cohesive force of the surface tension [49]. **In the charge residual model,** the molecule will not desorb from the charged droplet but it will be freed by complete evaporation of the solvent and this is more likely to happen with large molecules [50].

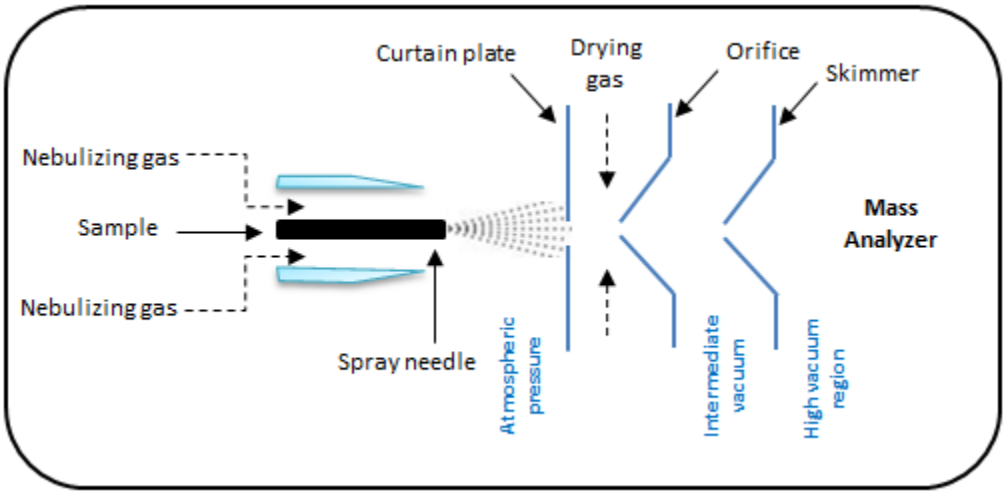

Scheme 1.4. A schematic diagram of an ESI source

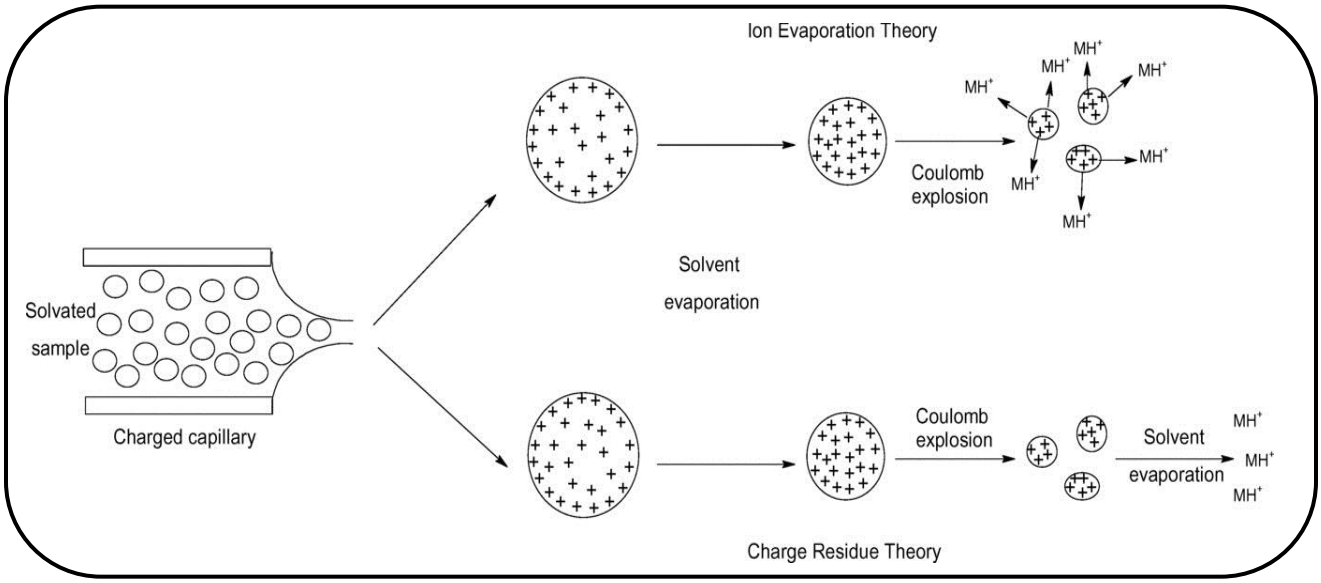

Scheme 1.5. Proposed mechanisms of ion formation during electrospray ionization [44]

ESI is suitable for a wide range of compounds with high to moderate polarity as well as varying molecular weight. For large molecules with several ionizable sites such as proteins, ESI produces multiply charged ions that allows for their analysis in mass analyzers with limited *m/z* range, such as quadrupoles [45, 51]. However, ion suppression is a major drawback when using ESI, as the presence of high concentration of analytes or salts may change the efficiency of droplet evaporation that in turns inhibit ion release into the gas phase [52, 53]. In high concentration samples, the competition between compounds for limited charges or space on the droplet surface can also decrease the efficiency of ion formation [52, 53]. To overcome ion suppression during ESI, several strategies have been applied:

I) Performing sample purification such as solid phase extraction (SPE), liquid-liquid extraction (LLE), or protein precipitation (PPT) [54-56].

II) Altering the chromatographic conditions by modifying the mobile phase additives or shifting the retention times of the analytes away from the eluting region affected by ion suppression [54-56].

III) Changing the ionization mode, such as switching to the negative ion mode where fewer compounds are ionized and matrix effect is inherently lower [54, 55]. Switching the ionization source from ESI to APCI or APPI has also been applied [57].

IV) Reducing the amount of sample being introduced to the ionization chamber via sample dilution, reducing the injection volume, or reducing the ESI flow rate [54, 55]. Nano-ESI [58] is one approach in which flow rates are substantially reduced allowing less analyte and nonvolatile compounds to be injected into the source while enhancing the desolvation process of the droplets [54, 55].

V) Using an internal standard (IS) especially an isotopically labelled IS that exhibits similar structural and physical properties to the analyte to compensate the matrix effect rather than eliminating it [54, 55].

1.2.1.2. Atmospheric pressure chemical ionization (APCI)

In APCI [38, 39], the sample solution is introduced at a flow rate typically 200-2000 µL/min into a pneumatic nebulizer that sprays the solution under atmospheric pressure. The spray droplets pass through a heated quartz tube called a desolvation/vaporization chamber to allow for the vaporization of the solvent. After desolvation, the gas phase molecules of the analyte and solvent pass through a corona discharge electrode where ionization occurs. The ionization mechanism in APCI is similar to that of chemical ionization (CI) but occurs under atmospheric pressure [45, 59]. In APCI, the vapourized solvent (S) is ionized by the corona discharge

electrode to form reactant ions (eq 1) that in turn ionize the analyte (M) by charge exchange (eq 2) or proton transfer (eq 3) as follows:

$$S + e^- \rightarrow S^{+\bullet} + 2e^- \quad (1)$$

$$S^{+\bullet} + M \rightarrow S + M^{+\bullet} \quad (2)$$

$$S^{+\bullet} + S \rightarrow [S+H]^+ + S[-H] \textbf{ then } [S+H]^+ + M \rightarrow S + [M+H]^+ \quad (3)$$

APCI is mainly applied to compounds of low to medium polarity with moderate molecular weight (up to ~1500 Da). However, it cannot be used with thermally liable compounds because of the application of heat [45] and as such is not suitable for the analysis of macromolecules such as proteins or DNA. Unlike ESI, APCI can achieve a good sensitivity at high flow rates (200 – 2000 μL/min) and APCI has a better tolerance to salts and buffers [59, 60]. The matrix effect on the ionization performance of both ESI and APCI was investigated and revealed a higher tolerance of APCI to the sample matrices in comparison with ESI [61]. These differences between ESI and APCI are mainly based on ionization mechanism differences [53]. In ESI, the analyte is ionized in the liquid phase (charged droplets) then released into the gas phase. Therefore, ion formation in ESI is more susceptible to the nonvolatile matrix components that may change droplet properties or compete for the charge or the space on the droplet surface as mentioned earlier [52, 53]. However in APCI, the analyte is introduced to the gas phase in neutral form to be ionized via chemical reactions with the reactant ions (eqs. 1, 2 and 3). This mechanism does not involve droplet formation as in ESI and therefore ion suppression factors related to the droplet properties are not applicable to APCI [38, 39].

1.2.1.3. Atmospheric pressure photoionization (APPI)

APPI is a modified form of an APCI source where the corona discharge electrode is replaced by a lamp emitting photons. In APPI [40], the sample solution is vaporized by a heated nebulizer forming gas phase molecules of the analyte and solvent that interact with the emitted photons by a discharge lamp producing the ions (Scheme 1.6). Different discharge lamps have been used with APPI; the krypton lamp is the commonly used one and generates two photon energy lines at 10.0 and 10.6 eV [40]. To selectively ionize the analyte in APPI, the emitted photon energy should be higher than the ionization energy of the analyte and lower than that of air (i.e., nitrogen and oxygen) and the used solvents (i.e., methanol, water, and acetonitrile) [62]. Such selectivity makes APPI less susceptible to ion suppression and salt buffer effects than APCI and ESI [57]. In addition, APPI is very useful for the ionization of nonpolar compounds that are not ionizable by ESI or APCI, such as polycyclic aromatic hydrocarbons (PAHs) [63]. Ghislain *et al.* compared the performance of ESI, APCI and APPI in the detection of PAHs and oxy-PAHs by direct infusion using a quadrupole time-of-flight mass spectrometer (Q-TOF-MS). The experiments confirmed the suitability of APPI in the analysis of PAHs and oxy-PAHs with a wide mass range [64]. In contrast, ESI was not able to detect these compounds. APCI was also less efficient than APPI in detecting compounds with intermediate *m/z* values, probably due to the low polarity of the detected compounds within this range [64].

Similarly, a wide range of lipids of *Leishmania donovani* were analyzed by normal phase-LC-MS using the three ionization methods (i.e., ESI, APCI, and APPI). The study showed superior performance of APPI in terms of sensitivity, signal, and signal-to-noise (*S/N*) ratio in the analysis of non/low polar lipids while ESI and APCI were better suited for the polar ones [65]. APPI can also address the issue of matrix effects in comparison with ESI and APCI. During an LC-MS analysis of estradiol in human serum and endometrial tissue, ESI showed susceptibility

to ion suppression in contrast to APPI and APCI that exhibited more tolerance towards sample matrices. In terms of *S/N* ratio and background noise, APPI was superior to APCI [66].

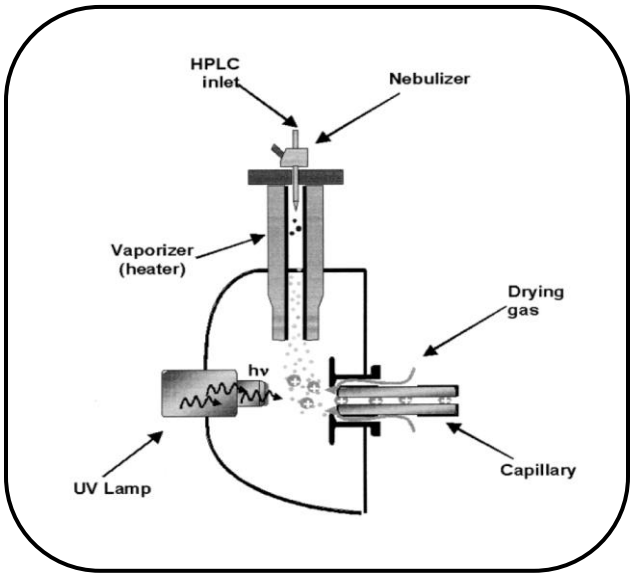

Scheme 1.6. A schematic diagram of an APPI source [57]

Ionization in APPI occurs in two ways; direct and indirect [57, 62, 67]. The analyte (M) in direct APPI directly absorbs the photon energy (*hv*) forming the radical cation ($M^{+\bullet}$) (eq 4), which reacts with a solvent molecule (S) to form the $[M+H]^+$ ion by hydrogen atom abstraction in the positive ion mode (eq 5) as follows:

$$M + hv \rightarrow M^{+\bullet} + e^- \qquad (4)$$

$$M^{+\bullet} + S \rightarrow [M+H]^+ + S[-H] \qquad (5)$$

In 2004, Jack A. Syage investigated the above proposed mechanism of $[M+H]^+$ formation during direct photoionization. In this study, Syage compared the relative abundance of $[M]^{+\bullet}$ and $[M+H]^+$ ions during direct photoionization of different compounds as vapor (with no solvent) versus using different solvents (protic e.g., CH_3OH, H_2O and aprotic solvents e.g., CCl_4). The

study confirmed the initial formation of an analyte radical ion followed by hydrogen atom abstraction from a protic solvent as a mechanism of $[M+H]^+$ formation during direct APPI. The conclusion was based on several observations including; i) significant $[M+H]^+$ formation during the photoionization of the analyte in the presence of protic solvents, but not in aprotic solvents, indicating that the protic solvents are the source of hydrogen atoms, in contrast, ii) $[M]^{+\bullet}$ was significantly formed in the absence of solvent [67].

Direct photoionization only happens with analytes of ionization energy (IE) lower than the emitted photon energy (*hv*). For example, analytes with IE < 10.2 eV can be directly photoionized by photons emitted from the krypton discharge lamp [40]. However, E. Marotta *et al.* reported unexpected photon-induced reactions during the direct APPI of furocumarins where acetonitrile participated in the $[M+H]^+$ formation of tested compounds. Acetonitrile has an ionization energy higher than the emitted photon energy (12.2 eV > 10eV), which theoretically means that the photon energy cannot ionize acetonitrile molecules and in turn cannot work as an intermediate in the protonation of furocumarins. However, the authors suggested that photon-induced isomerization of acetonitrile molecules occurred leading to the formation of other species with IE < 10 eV that consequently were able to facilitate the photoionization of furocumarins [68].

For substances with high IE values, indirect APPI is applied. This type of photoionization involves the use of a dopant (D), which is a solvent with lower ionization energy (IE) than the emitted photon energy (e.g., acetone and toluene with IE= 9.7 and 8.83 respectively), that acts as intermediate between the photons and the analytes. The dopant absorbs the photons energy (*hv*) forming the radical cation ($D^{+\bullet}$) (eq 6), which in turn ionizes the analyte (M) forming the ion by

charge exchange (eq 7) or proton transfer (eq 8) depending on the ionization energies or proton affinities of both the analyte and the solvent:

$$D + h\nu \rightarrow D^{+\bullet} + e^{-} \quad (6)$$

$$D^{+\bullet} + M \rightarrow D + M^{+\bullet} \quad (7)$$

$$D^{+\bullet} + S \rightarrow [D\text{-}H] + [S+H]^{+} \ \textbf{then} \ [S+H]^{+} + M \rightarrow S + [M+H]^{+} \quad (8)$$

1.2.1.4. Matrix assisted laser desorption ionization (MALDI)

MALDI is based on the desorption and ionization of analyte molecules incorporated into matrix crystals using a pulsed laser beam [41]. The crystals are formed by spotting a mixture of analyte/matrix solution on a sample plate to be dried by air or under vacuum. The type of matrix, technique of drying, and laser parameters are critical steps in MALDI, which may affect the analysis [69, 70]. After desorption and ionization of the analyte molecules, the formed ions are separated based on their *m/z* values in the mass analyzer. Although the detailed mechanism of ionization in MALDI is still unclear, two major models were proposed to explain the MALDI ionization process (Scheme 1.7):

1.2.1.4.1. Gas phase protonation

It was proposed that the production of analyte ions involves two steps; the first is photoionization of matrix molecules within the matrix-analyte crystals by the laser, producing matrix ions. The second step is the charge transfer from matrix ions to the neutral analytes [71-73]. In this model, matrix molecules play a major role in the formation of analyte ions and the ionization process. Therefore, various matrices have been designed for a wide range of applications. Choosing the correct matrix that suits the target analyte as well as the right laser wavelength plays an important role in analytical results. For example; α-Cyano-4-

hydroxycinnamic acid (CHCA) is widely used for peptides analysis on UV-MALDI; 2,5-Dihydroxybenzoic acid (DHB) for proteins, peptides, and carbohydrates on UV-MALDI; 3-Hydroxy-picolinic acid for DNA on UV-MALDI; and succinic acid for proteins and peptides on IR-MALDI [70, 74]. A comparison between CHCA and DHB matrices was conducted to reveal the preferred matrix for peptide mass fingerprint MALDI-MS analysis [75]. The study showed that CHCA has better sensitivity for the detection of a high number of peptides in samples with low femtomole-peptide concentrations. In contrast, DHB was better suited for the highly concentrated samples by identifying more peptides than CHCA. By evaluating the *m/z* distribution of the detected peptides, peptides with low *m/z* range (up to ~1000) were better detected by DHB in comparison with CHCA, which showed more peptides at a high *m/z* range (≥1500). The performance of both matrices confirmed the complementary nature of MALDI-MS data obtained using CHCA and DHB in peptide mass fingerprinting [75].

1.2.1.4.2. Lucky survivor model

I. Original model: In 2000, Karas *et al* [76] proposed another ionization mechanism for MALDI that may occur in parallel with the gas phase protonation model. However, the model is dependent on the solvent used for sample preparation as well as the basicity of the analyte. In this model, the analyte is ionized during sample preparation and incorporated within the matrix/sample crystals with its corresponding counter ions (e.g., Cl^- or trifluoroacetic acid anions). The ablation/desorption of the matrix-analyte crystals by laser irradiation will release clusters of the analyte ions, counter ions and matrix molecules. In the gas phase, quantitative charge neutralization between analyte, counter ions and electrons will produce the singly charged analyte ions (called lucky survivors) as a result of incomplete charge neutralization [76].

II. Refined lucky survivor model: The same principles are applied as the original model where the analyte molecules are incorporated within the matrix/sample crystals as precharged species. However, in the refined model, matrix molecules are incorporated within the desorbed clusters as ionized molecules, contributing to the counter ion neutralization process, leading to the formation of singly charged analyte ions [77].

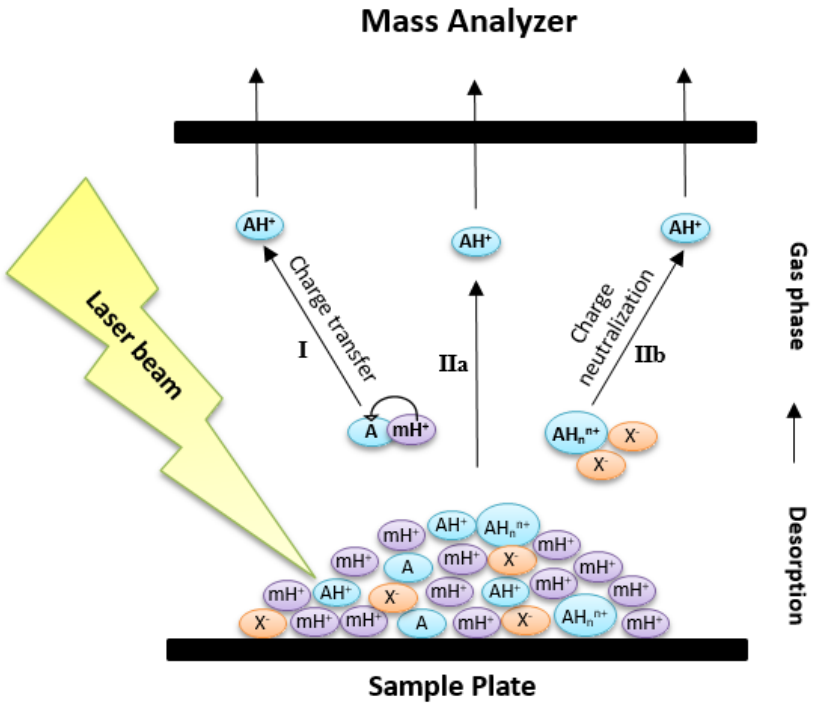

Scheme 1.7. Major proposed models for MALDI ionization; **[I]** Gas phase protonation, showing the charge transfer from the ionized matrix (mH^+) to the analyte (A). **[IIa]** Lucky survivor model, showing the direct desorption of the preformed singly charged analyte (AH^+). **[IIb]** Lucky survivor model for the multiply charged analyte (AH_n^{n+}), where incomplete neutralization by the counter ions (X^-) or electrons occur in the gas phase producing the singly charged analyte ions (AH^+). (A= analyte, m= matrix, x^- = counter ion)

Both models, the gas phase protonation and the lucky survivor, highlight the importance of the matrix for analyte ionization in MALDI-MS. In 2011, T. W. Jaskolla and M. Karas experimentally proved the simultaneous occurrence of the two previously proposed mechanisms.

In this experiment, deuterated matrix has been used to detect and differentiate between the two mechanisms. In the gas phase protonation model, charge is transferred from the deuterated matrix ion $[ma+D]^+$ to the neutral analyte, forming the deuterated analyte ion $[A+D]^+$ instead of the protonated ion $[A+H]^+$. However, the lucky survivor model indicates that the analyte molecules are already protonated during sample preparation as $[A+H]^+$ [77]. Screening the mass spectra for the presence of either $[A+H]^+$ and $[A+D]^+$ showed the presence of both, which validated the two models.

Other parameters can also determine the most prominent ionization mechanism including; pH of solvent, analyte basicity, and laser fluence [77]. A medium basic analyte (nicotinamide, *m/z* = 122.05) was investigated by MALDI-MS in different pH solutions using a deuterated matrix. The results showed that a decrease in the pH of a nicotinamide solution during sample preparation increases the $[A+H]^+$ species at *m/z* = 123.06 in comparison to the $[A+D]^+$ (Figure 1.1A). This indicates that the lucky survivor model was the prominent ionization mechanism for nicotinamide in acidic solutions. In contrast, increasing the pH of a nicotinamide solution, activated the gas phase transfer during MALDI-MS generating significant $[A+D]^+$ ions at *m/z* = 124.06 (Figure 1.1B). Laser fluence was also investigated showing a proportional relationship between laser fluence and nicotinamide ion formation via the gas phase transfer (i.e., $[A+D]^+$ ions), probably due to the enhanced ionization of matrix molecules [77].

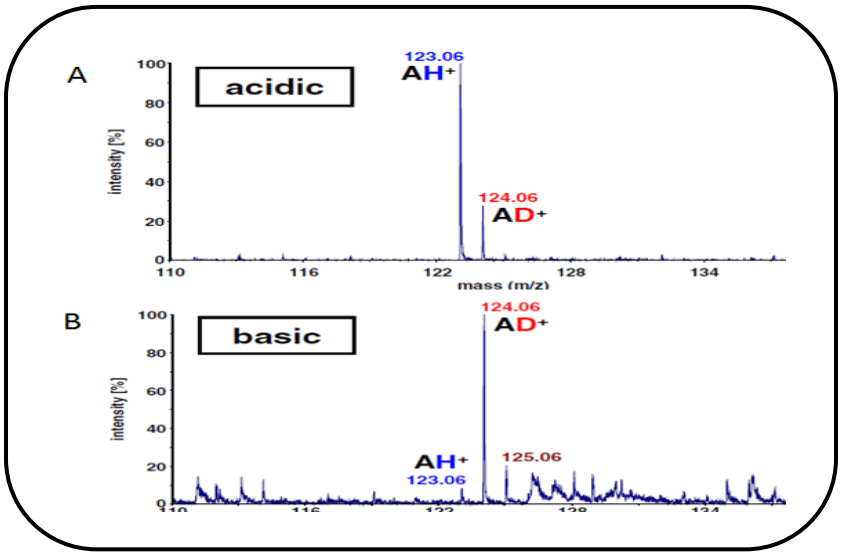

Figure 1.1. MALDI-MS spectra of nicotinamide prepared in (A) acidic solution and (B) basic solution using a deuterated matrix [77].

The type of ions generated during MS analysis is mainly based on the ionization technique, mode of ionization, and the nature of tested compounds. These ions could be protonated, deprotonated, radicals, adducts, singly charged, or multiply charged ions. The positively-charged $[M-H]^+$ ion is an ion form that has been reported with various MS-ionization techniques with no detailed mechanism for its formation. The following section will present an overview about this ion and the proposed mechanisms for its formation with each MS ionization technique.

1.2.2. $[M-H]^+$ formation during MS analysis

The positively-charged $[M-H]^+$ ion was reported during chemical ionization (CI) [78, 79] and APCI-MS [39] analysis of various compounds, mainly alkanes. Later, this ion was detected with other ionization techniques including; ESI [80, 81], MALDI [82-85], APPI [86], Desorption APPI (DAPPI) [87], Desorption ESI (DESI) [87], and direct analysis in real time (DART) [88].

Various mechanisms were proposed to explain the $[M-H]^+$ formation however, the detailed mechanism and the factors influencing $[M-H]^+$ formation are still unclear.

Generally speaking when using ESI or MALDI, basic compounds are expected to be ionized in the positive ion mode by protonation of the basic site, producing the $[M+H]^+$ ions. However, several investigations [80-88] reported unexpected ionization behavior during the positive ion mode of MS analysis for some compounds where positively charged $[M-H]^+$ ions were formed with or without the other expected species. The unusual formation of the $[M-H]^+$ ion means that the molecules have lost in net one hydrogen atom instead of accepting a proton as shown in Scheme 1.8.

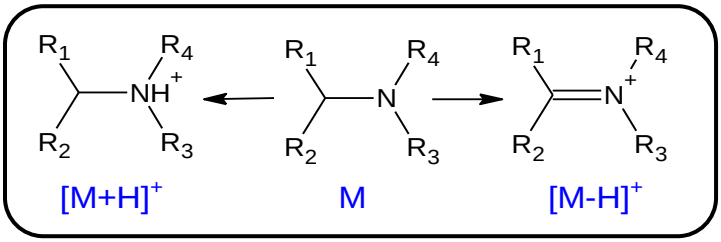

Scheme. 1.8. The proposed structures of $[M+H]^+$ and $[M-H]^+$ ions of nitrogenous compounds

$[M-H]^+$ ions were observed with different MS-ionization techniques. **In chemical ionization (CI)**, $[M-H]^+$ was significantly detected with alkanes [89]. The proposed mechanism of $[M-H]^+$ formation during CI was based on the dissociative proton transfer or hydride abstraction of the analyte by the reagent gas ions [78, 79, 90] (Scheme 1.9).

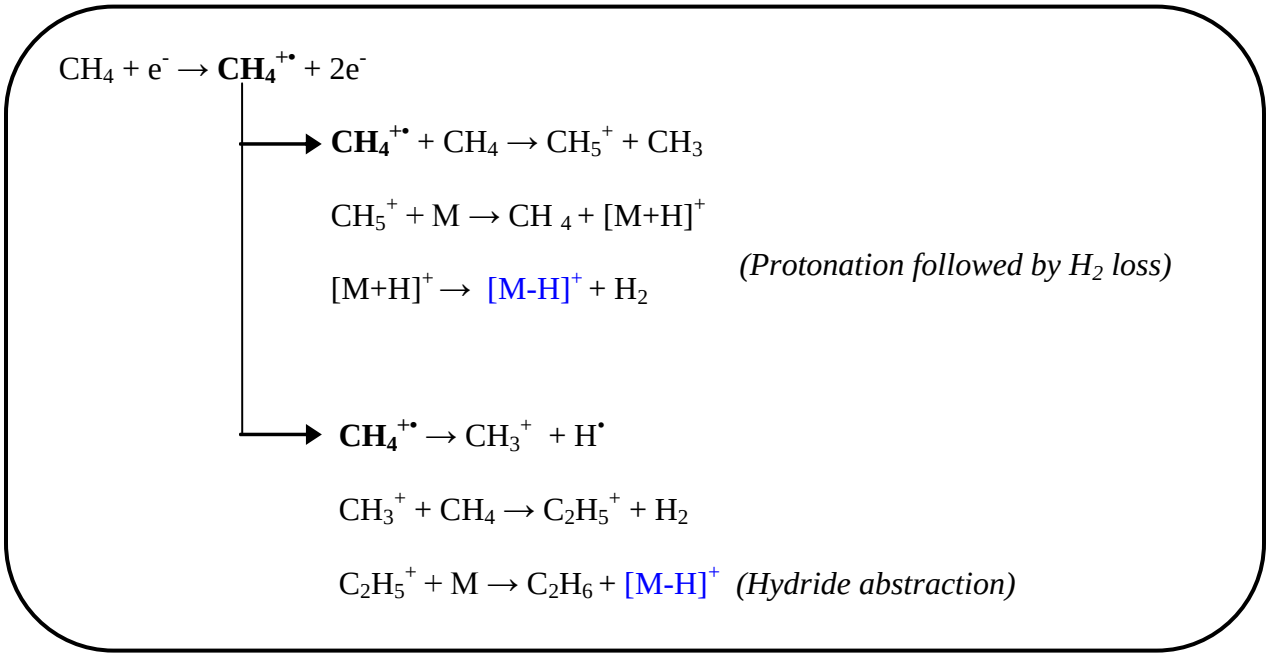

Scheme 1.9. $[M-H]^+$ ion formation during chemical ionization by methane gas ions

Similar to CI, $[M-H]^+$ was commonly observed during **APCI-MS** analysis of alkanes [91-93] and the same mechanisms were applied to explain its formation (the loss of H_2 from a protonated ion and hydride abstraction) by replacing the reagent gas ions (in CI) by other reactive ions such as protonated product ions of the solvent or the analyte (Scheme 1.10 A&B) [39, 91-94]. In addition, another mechanism was proposed for $[M-H]^+$ formation during APCI-MS involving the hydrogen transfer from the analyte radical cation to other molecules such as nitrogen [93] or oxygen species [91] (Scheme 1.10).

A) $[M+H]^+ \rightarrow [M-H]^+ + H_2$ *(Protonation followed by H_2 loss)*

B) $M + RH^+ \rightarrow [M-H]^+ + RH_2$ *(Hydride abstraction)*

C) $M^{+\bullet} + N^{+\bullet} \rightarrow [M-H]^+ + N_2H^+$

$M^{+\bullet} + O_2 \rightarrow [M-H]^+ + HO_2^{\bullet}$ *(Hydrogen transfer)*

Scheme 1.10. Proposed mechanisms for $[M-H]^+$ ion formation during APCI-MS (RH^+ is a protonated product ion of solvent or analyte)

A comparison between the sensitivity of APCI and APPI in the analysis of several neurotransmitters [86] showed that $[M-H]^+$ was the most abundant ion in the positive ion mode of **APPI-MS** spectra of beta estradiole (Scheme 1.11), especially with two solvents; water/methanol/NH_4OAc (50/50/0.1%) and water/methanol/NH_4OH (50/50/0.1%). The same ion was also observed, albeit less abundant, with APCI-MS and the same solvents. The authors suggested the H_2 loss from the $[M+H]^+$ ion as well as the hydride abstraction as possible mechanisms of $[M-H]^+$ formation [86].

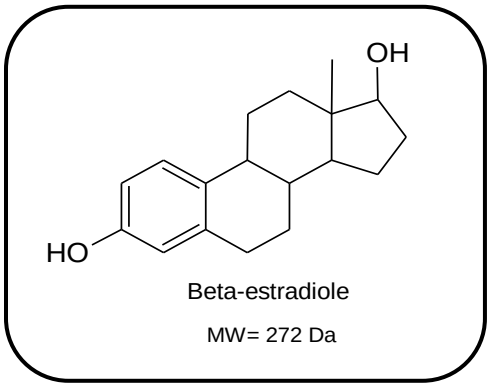

Scheme 1.11. Structure of Beta-estradiol

Using ESI-MS, Orelli *et al.* [81] and Chai *et al.* [80] reported $[M-H]^+$ ion formation during positive ion mode ESI-MS analysis of tertiary nitrogenous compounds and both proposed the hydride abstraction as a possible mechanism for $[M-H]^+$ formation through the electrochemical oxidation process [80, 81]. Orelli *et al.* suggested that the increase in the positive charge on the droplet surface during desolvation in ESI increases the surface potential making the droplet surface act as an anode where hydride abstraction can occur [81]. In the same study, the authors compared the ionization behavior of ESI with **electron ionization (EI)** where $[M-H]^+$ was detected with both techniques. For EI, a different mechanism was proposed for $[M-H]^+$ formation; the mechanism involved hydrogen transfer from the radical cations of the analyte [81].

In MALDI, Lou *et al.* [83] detected significant $[M-H]^+$ ions during single stage positive ion mode MALDI-TOF-MS analysis of tertiary amines. However, these ions were barely detected with secondary amines. Two mechanisms for $[M-H]^+$ formation were proposed: H_2 loss from the $[M+H]^+$ ion and hydrogen loss from the analyte radical cation $[M]^{+\bullet}$ (Scheme 1.12).

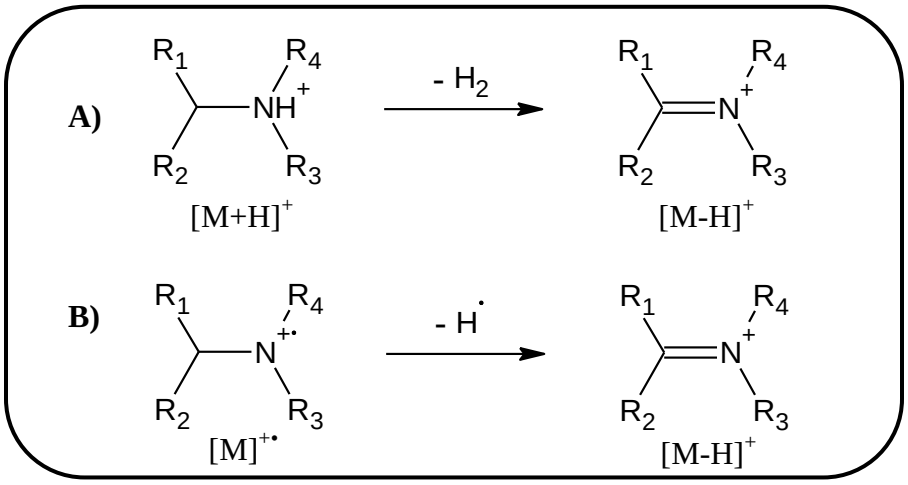

Scheme 1.12. Proposed mechanisms for $[M-H]^+$ formation during MALDI-TOF-MS [83]

More recently, C. Kang *et al.* [95] investigated the $[M-H]^+$ formation using secondary and tertiary amines with N-benzyl groups in which the methylene of the N-benzyl is labeled with deuterium (Scheme 1.13). In this work, tertiary amines with an N-benzyl group showed high-intensity of $[M-D]^+$ and $[M-H]^+$ ions in comparison with those of secondary amines that showed low abundant ions. In addition, the intensities of $[M-D]^+$ and $[M-H]^+$ and their ratios were dependent on the substituents on the N-benzyl group, for example electron donating groups (i.e., ethoxy group) showed a high level of dedeuteration of the methylene of the N-benzyl group. The authors proposed the same mechanism proposed by Lou *et al.* in Scheme 1.12B to explain the $[M-H]^+$ formation. However, it was suggested that the radical cation of the analyte could be formed directly from the neutral molecule by losing an electron or from the protonated molecule by losing a hydrogen or deuterium atom.

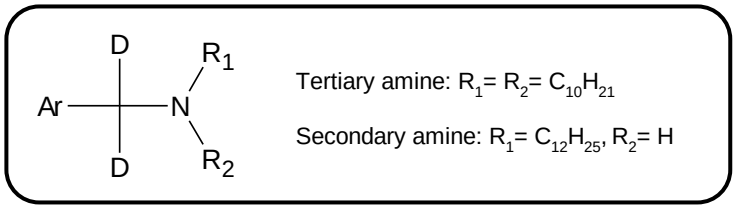

Scheme1.13. The secondary and tertiary amines with deuterated methylene of the N-benzyl group [95]

The hydride abstraction was also proposed as a possible mechanism of $[M-H]^+$ formation during MALDI-MS in several studies [84, 85]. Based on literature in the $[M-H]^+$ ion and the suggested mechanisms for its formation, it can be concluded that there are three main proposed mechanisms for $[M-H]^+$ formation; i) loss of H_2 from the protonated ion, namely dissociative proton transfer, ii) hydride abstraction from the neutral molecule and iii) hydrogen abstraction from the radical cation.

1.2.3. Mass analyzers

Ions entering a mass spectrometer pass through a mass analyzer to be separated based on their *m/z* values. There are six common types of mass analyzers that can be divided into trapping and non-trapping analyzers [45, 96]. Trapping analyzers include linear ion trap (LIT), Fourier transform ion cyclotron resonance (FTICR), and orbitrap. These analyzers are able to confine ions within the analyzing field for an indefinite time. Conversely, for non-trapping analyzers, such as quadrupole (Q), time of flight (TOF), and sector instruments, ions leave the ionization source and pass through the mass analyzer to the detector without trapping. The general principles of the commonly used mass analyzers in my research work (i.e., TOF, Q, LIT, and FTICR) will be outlined briefly in the following sections.

1.2.3.1. Time-of-flight analyzer (TOF)

In TOF, the expelled ions from the ionization source are subjected to a potential applied between an electrode and extraction grid in the acceleration region where all ions receive approximately the same kinetic energy. The accelerated ions are then allowed to travel through a field-free region with known length to reach the detector (Scheme 1.14).

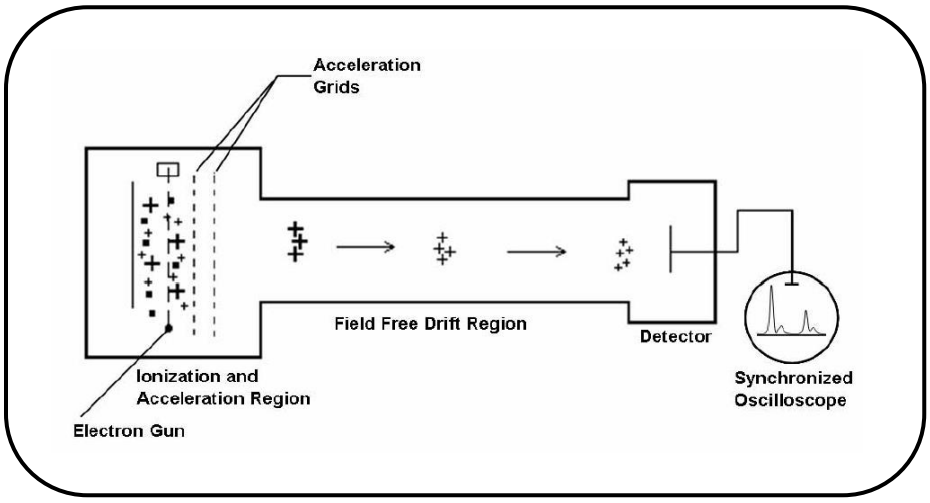

Scheme 1.14. A schematic diagram of a linear TOF-MS [97]

The ions velocities in the field-free region between the ion source and the detector depend on their *m/z* values. Therefore, the *m/z* values of ions are determined by measuring the time (t) taken by the ions in the field-free region (L) as shown in the following equation [97-100]:

$$t^2 = \frac{m}{z}\left(\frac{L^2}{2eV}\right)$$

Where: t = time of flight, m = ion mass, z = charge number of ion, L= length of the field-free region, e= charge of electron in coulombs (elementary charge), V= accelerating potential.

The above equation shows the proportional relationship between the square of time of flight (t^2) for an ion and its *m/z* value (i.e., the lower the *m/z* value of an ion, the faster it will reach the detector). This type of TOF analyzer is known as linear TOF analyzer [101].

To improve TOF performance, the reflectron TOF has been developed [102], where the ions after travelling through the tube flight, enter an electrostatic mirror (a reflectron) that reflects the ions and sends them again for a second flight distance towards the detector [102]. In this type,

the reflectron improves ion separation (resolution) by decreasing the kinetic energy variation among ions with the same *m/z* values. Ions with higher kinetic energy will enter and more deeply penetrate into the ion mirror than ions of same *m/z* values with lower kinetic energy. When the kinetic energies of the ions reach zero, ions are reaccelerated again by the reflectron electric field to be gradually repelled for another flight path to arrive at the detector at (almost) the same time [45, 97].

In TOF, the detection of ions is only based on the time taken by the ions to reach the detector. As a result, a TOF mass analyzer has no theoretical upper detection limit for *m/z* values [97]. In addition, TOF is commonly used with pulsed-ionization sources such as MALDI because of its ability to analyze all ions in a single pulse [96, 103]. However, other continuous beam ionization sources such as ESI can also be used with TOF mass analyzers via orthogonal acceleration where the continuous ion beam is transformed into discrete pulses of ions [104].

1.2.3.2. Quadrupole mass analyzer (Q)

The quadrupole mass analyzer consists of four parallel circular rods. Each opposing pair of rods is electrically connected by a combination of a constant direct current (DC) and alternating radio-frequency (RF) potentials. The applied potentials produce an opposite voltage polarity to the adjacent rods. Ions entering the quadrupole will show oscillatory movement between the rods based on their *m/z* values. Ions of a certain *m/z* value with stable trajectories will reach the detector while other ions with unstable trajectories will collide with the rods. Mathematically, calculations of which ions of given masses will have a stable trajectory can be done by using the Mathieu equations [45].

Quadrupole-based instruments are relatively low cost and small in size, utilizing low voltages for ion acceleration (2–50 V versus kV in TOF). Despite being optimal for quantification, the

sensitivity in a quadrupole mass analyzer is mass dependent and decreases with high *m/z* values. Therefore, it has a limited mass range (up to ~4000 Da) [45, 96].

1.2.3.3. Linear ion trap mass analyzer (LIT)

LIT has the basic structure of a quadrupole mass analyzer with extra trapping end cap electrodes. However, instead of detecting ions that have stable trajectories through the rods, ions are trapped in an electric field to be mass selected for detection. Ions are trapped in a LIT radially by the 2 dimensional RF quadrupole field and axially by the potentials applied to the end caps [45, 105]. Mass selective ejection of trapped ions from LIT is performed either axially or radially. Ions are expelled axially by applying alternating current (AC) voltages between the quadrupole rods and the exit lens. Ions are expelled radially by applying an appropriate AC voltage on two opposite rods with slots to eject ions out from them [45].

1.2.3.4. Fourier transform ion cyclotron resonance (FTICR)

In FTICR [106, 107], ions are trapped in a magnetic field with electric trapping plates. The trapped ions exhibit circular motions perpendicular to the magnetic field producing cyclotron frequencies that depend on their *m/z* values. Ions to be detected are excited by alternating current (AC) to increase the radius of their circular motions to be closer to the detection plates. When ions pass by the detection plates, an alternating current (named the image current) is generated producing a time domain signal that consists of all the characteristic frequencies of the measured ions. The Fourier transform operation converts the time domain signal into a frequency domain signal that results in a mass spectrum. FTICR is still the technique of choice for accurate mass measurements with mass accuracy < 1 PPM and resolution > 500,000 [45, 51]. However, the scan speed of this analyzer at high resolving power is slow as ~1 second is needed to acquire a

high resolution spectrum, unlike TOF that is able to acquire thousands of spectra in one second [45, 108, 109].

1.2.3.5. Tandem mass spectrometry

Tandem mass spectrometry performs multiple consecutive mass-analyzing steps. It is also known as MS/MS based on the number of mass analyzing stages [96, 110]. MS/MS instruments are classified into two categories: tandem-in-space and tandem-in-time instruments. **In tandem-in-space instruments**, MS/MS analyses are performed sequentially in separate mass analyzers, the non-trapping mass analyzers such as Q and TOF are usually used in designing such instruments [96]. The most commonly used tandem-in-space instruments are triple quadrupole mass spectrometers (QqQ), hybrid quadrupole time-of-flight mass spectrometers (Q-TOF) and tandem time-of-flight mass spectrometers (TOF/TOF).

QqQ is composed of two quadrupole mass analyzers separated by a quadrupole unit that acts as a collision cell where fragmentation occurs by low energy collision induced dissociation (CID) in the presence of an inert gas [111]. In most QqQ instruments, the second quadrupole is an hexapole or an octopole [45, 111]. Q-TOF is similar to QqQ but the third quadrupole analyzer is substituted by a time-of-flight mass analyzer [45, 111], allowing for accurate mass measurements. Both QqQ and Q-TOF perform low energy CID in contrast to TOF/TOF instruments that perform high energy CID [97]. In TOF/TOF, one of the common configurations currently used is the combined system of a short linear TOF, an ion deflection gate, a collision cell and a reflectron TOF [111]. The ion gate is a timed ion selector that allows the passage of selected ions to the collision cell where high energy CID is performed. The product ions then enter a longer field free region for separation producing an MS/MS spectrum [45, 97, 111].

Each tandem mass spectrometer has its own advantages, for example Q-TOF and TOF/TOF have high mass accuracy and a wide mass range [45, 111]. On the other hand, QqQ is better suited for quantification [111]. It also has the ability to perform precursor ion and neutral loss scans that allow for the confirmation of the precursor ion's structure and its fragmentation pathway [111].

In tandem-in-time instruments, trapping mass analyzers are used, such as LIT and FTICR where various MS/MS stages are performed successively in the same mass analyzer but separated in time. The main advantage of tandem-in-time instruments is their ability to perform multiple stages of fragmentation (MS^n). For MS/MS analysis, ions within a specific *m/z* range are trapped to be fragmented while other ions are ejected, and the resulted product ions are directly monitored. However, in MS^3 analysis, a specific product ion will be selected for further fragmentation and monitoring. This procedure could be repeated (i.e., MS^n analysis) [45, 111]. LIT is one of the most popular mass analyzers based on its small size, low price and high MS^n capability [110, 111]. However, its poor performance in quantitative applications and inability to perform precursor ion and neutral loss scans are its main drawbacks [110, 111]. These limitations have been overcome by introducing hybrid Qq-LIT by replacing the third Q in QqQ with a LIT allowing for all scan modes to be performed by conventional QqQ while adding the advantages of LIT [110].

1.3. Research hypotheses and objectives

The main purpose of my M.Sc. project is to investigate the ionization and tandem mass spectrometric behavior of novel antineoplastic curcumin analogues. The goal is to assess the dissociation behavior and ion formation mechanisms for curcumin analogues during MS-analysis.

1.3.1. Evaluating the ionization behavior of novel curcumin analogues using different ionization techniques; ESI, APCI, MALDI, and APPI-MS.

1.3.1.1. Hypothesis

Curcumin analogues will ionize forming $[M+H]^+$ in the positive mode and $[M-H]^-$ in the negative ion mode regardless of the type of the ionization technique and the experimental condition.

1.3.1.2. Objective

The ionization behavior of curcumin analogues using various MS ionization techniques, namely ESI, APCI, APPI (with and without dopant) and MALDI-MS will be evaluated. The ionization study will mainly involve explaining an unusual phenomenon of the predominant formation of $[M-H]^+$ species during single stage positive ion mode MALDI-MS and dopant free-APPI-MS analysis.

- Specific aim-1: Evaluate the ionization behavior of 13 curcumin analogues (Scheme 1.3) with ESI, APCI and MALDI-MS.
- Specific aim-2: Perform accurate mass measurements of $[M-H]^+$ and $[M+H]^+$ of all tested compounds using MALDI-FTICR-MS instrument.
- Specific aim-3: Evaluate the influence of various factors, namely laser intensity, the type of mass analyzer, the matrix, and the solvent in the formation of $[M-H]^+$ ions during MALDI-MS.

- Specific aim-4: Apply APPI-MS (with and without dopant) to assess the role of direct photoionization in the formation of $[M-H]^+$ ions.
- Specific aim-5: Identify the possible mechanisms for $[M-H]^+$ formation.

1.3.2. Establishment of the fragmentation patterns (i.e., fingerprints) of curcumin analogues using ESI-MS/MS.

1.3.2.1. Hypothesis

Structurally similar compounds will show similar fragmentation behavior using the same ionization technique, allowing for the establishment of a general MS/MS fragmentation pattern for the 13 tested curcumin analogues.

1.3.2.2. Objective

Establishment of the fragmentation patterns of the tested curcumin analogues using ESI-MS/MS.

- Specific aim-1: Confirm the molecular structure of tested curcumin analogues using MS, MS/MS and MS^3 analysis.
- Specific aim-2: Establish universal MS/MS (fingerprints) for the identification of tested compounds.

1.4. References

[1] W. Korfmacher and K. Yu, "Mass Spectrometry: The premier analytical tool for DMPK scientists in a drug discovery environment," LC GC North America, vol. 30, pp. 640-647, 2012.

[2] T. A. Gillespie and B. E. Winger, "Mass spectrometry for small molecule pharmaceutical product development: A review," Mass Spectrometry Reviews, vol. 30, pp. 479-490, 2011.

[3] W. A. Korfmacher, "Foundation review: Principles and applications of LC-MS in new drug discovery," Drug Discovery Today, vol. 10, pp. 1357-1367, 2005.

[4] J. R. Yates, C. I. Ruse, and A. Nakorchevsky, "Proteomics by mass spectrometry: approaches, advances, and applications," Annual Review of Biomedical Engineering, vol. 11, pp. 49-79, 2009.

[5] K. Dettmer, P. A. Aronov, and B. D. Hammock, "Mass spectrometry based metabolomics," Mass Spectrometry Reviews, vol. 26, pp. 51-78, 2007.

[6] J. R. Yates III, "Mass spectrometry: from genomics to proteomics," Trends in Genetics, vol. 16, pp. 5-8, 2000.

[7] W. J. Griffiths and Y. Wang, "Mass spectrometry: from proteomics to metabolomics and lipidomics," Chemical Society Reviews, vol. 38, pp. 1882-1896, 2009.

[8] U. Lövgren, S. Johansson, L. S. Jensen, C. Ekström, and A. Carlshaf, "Quantitative determination of peptide drug in human plasma samples at low pg/ml levels using coupled column liquid chromatography–tandem mass spectrometry," Journal of Pharmaceutical and Biomedical Analysis, vol. 53, pp. 537-545, 2010.

[9] H. Chang, Y. Wan, J. Naile, X. Zhang, S. Wiseman, M. Hecker, et al., "Simultaneous quantification of multiple classes of phenolic compounds in blood plasma by liquid chromatography–electrospray tandem mass spectrometry," Journal of Chromatography A, vol. 1217, pp. 506-513, 2010.

[10] K. J. Regina and E. D. Kharasch, "High-sensitivity analysis of buprenorphine, norbuprenorphine, buprenorphine glucuronide, and norbuprenorphine glucuronide in plasma and urine by liquid chromatography–mass spectrometry," Journal of Chromatography B, vol. 939, pp. 23-31, 2013.

[11] D. R. Ifa, A. U. Jackson, G. Paglia, and R. G. Cooks, "Forensic applications of ambient ionization mass spectrometry," Analytical and Bioanalytical Chemistry, vol. 394, pp. 1995-2008, 2009.

[12] F. T. Peters, "Recent advances of liquid chromatography–(tandem) mass spectrometry in clinical and forensic toxicology," Clinical Biochemistry, vol. 44, pp. 54-65, 2011.

[13] A. K. Malik, C. Blasco, and Y. Picó, "Liquid chromatography–mass spectrometry in food safety," Journal of Chromatography A, vol. 1217, pp. 4018-4040, 2010.

[14] F. Hernández, J. Sancho, M. Ibáñez, E. Abad, T. Portolés, and L. Mattioli, "Current use of high-resolution mass spectrometry in the environmental sciences," Analytical and Bioanalytical Chemistry, vol. 403, pp. 1251-1264, 2012.

[15] H. Lee, S. Shen, and N. Grinberg, "Identification and control of impurities for drug substance development using LC/MS and GC/MS," Journal of Liquid Chromatography & Related Technologies®, vol. 31, pp. 2235-2252, 2008.

[16] S. Singh, T. Handa, M. Narayanam, A. Sahu, M. Junwal, and R. P. Shah, "A critical review on the use of modern sophisticated hyphenated tools in the characterization of impurities and degradation products," Journal of Pharmaceutical and Biomedical Analysis, vol. 69, pp. 148-173, 2012.

[17] Y. Hsieh and W. Korfmacher, "The role of hyphenated chromatography-mass spectrometry techniques in exploratory drug metabolism and pharmacokinetics," Current Pharmaceutical Design, vol. 15, pp. 2251-2261, 2009.

[18] (June 3th). Cancer Drugs & Treatments Market - Data, Analysis and Forecasts to 2023. Available: http://gmrdata.com/cancer-drugs-to-2023.html

[19] (June 3th). APPROVED DRUGS 2013 Available: http://www.fda.gov/downloads/drugs/developmentapprovalprocess/druginnovation/ucm381803.pdf

[20] B. B. Aggarwal, A. Kumar, and A. C. Bharti, "Anticancer potential of curcumin: preclinical and clinical studies," Anticancer Research, vol. 23, pp. 363-398, 2003.

[21] B. B. Aggarwal, C. Sundaram, N. Malani, and H. Ichikawa, "Curcumin: the Indian solid gold," The molecular targets and therapeutic uses of curcumin in health and disease, pp. 1-75, 2007.

[22] K. M. Mohandas and D. C. Desai, "Epidemiology of digestive tract cancers in India. V. Large and small bowel," Indian journal of gastroenterology: official journal of the Indian Society of Gastroenterology, vol. 18, p. 118, 1999.

[23] P. Anand, A. B. Kunnumakkara, R. A. Newman, and B. B. Aggarwal, "Bioavailability of curcumin: problems and promises," Molecular pharmaceutics, vol. 4, pp. 807-818, 2007.

[24] J. Shaikh, D. D. Ankola, V. Beniwal, D. Singh, and M. N. V. Kumar, "Nanoparticle encapsulation improves oral bioavailability of curcumin by at least 9-fold when compared to curcumin administered with piperine as absorption enhancer," European Journal of Pharmaceutical Sciences, vol. 37, pp. 223-230, 2009.

[25] N. K. Gupta and V. K. Dixit, "Bioavailability enhancement of curcumin by complexation with phosphatidyl choline," Journal of pharmaceutical sciences, vol. 100, pp. 1987-1995, 2011.

[26] M. M. Yallapu, M. Jaggi, and S. C. Chauhan, "Poly (β-cyclodextrin)/Curcumin self-assembly: A novel approach to improve curcumin delivery and its therapeutic efficacy in prostate cancer cells," Macromolecular Bioscience, vol. 10, pp. 1141-1151, 2010.

[27] C. A. Mosley, D. C. Liotta, and J. P. Snyder, "Highly active anticancer curcumin analogues," The Molecular Targets and Therapeutic Uses of Curcumin in Health and Disease, pp. 77-103, 2007.

[28] P. Anand, S. G. Thomas, A. B. Kunnumakkara, C. Sundaram, K. B. Harikumar, B. Sung, et al., "Biological activities of curcumin and its analogues (Congeners) made by man and Mother Nature," Biochemical Pharmacology, vol. 76, pp. 1590-1611, 2008.

[29] S. Padhye, D. Chavan, S. Pandey, J. Deshpande, K. V. Swamy, and F. H. Sarkar, "Perspectives on chemopreventive and therapeutic potential of curcumin analogs in medicinal chemistry," Mini Reviews in Medicinal Chemistry, vol. 10, p. 372, 2010.

[30] U. Das, R. K. Sharma, and J. R. Dimmock, "1, 5-Diaryl-3-oxo-1, 4-pentadienes: A case for antineoplastics with multiple targets," Current Medicinal Chemistry, vol. 16, p. 2001, 2009.

[31] U. Das, J. Alcorn, A. Shrivastav, R. K. Sharma, E. De Clercq, J. Balzarini, et al., "Design, synthesis and cytotoxic properties of novel 1-[4-(2-alkylaminoethoxy) phenylcarbonyl]-3, 5-bis (arylidene)-4-piperidones and related compounds," European Journal of Medicinal Chemistry, vol. 42, pp. 71-80, 2007.

[32] S. Das, U. Das, P. Selvakumar, R. K. Sharma, J. Balzarini, E. De Clercq, et al., "3, 5-Bis (benzylidene)-4-oxo-1-phosphonopiperidines and related diethyl esters: potent cytotoxins with multi-drug-resistance reverting properties," ChemMedChem, vol. 4, pp. 1831-1840, 2009.

[33] U. Das, H. Sakagami, Q. Chu, Q. Wang, M. Kawase, P. Selvakumar, et al., "3, 5-Bis (benzylidene)-1-[4-2-(morpholin-4-yl) ethoxyphenylcarbonyl]-4-piperidone hydrochloride: A lead tumor-specific cytotoxin which induces apoptosis and autophagy," Bioorganic and Medicinal Chemistry Letters, vol. 20, pp. 912-917, 2010.

[34] M. Helal, U. Das, B. Bandy, A. Islam, A. J. Nazarali, and J. R. Dimmock, "Mitochondrial dysfunction contributes to the cytotoxicity of some 3, 5-bis (benzylidene)-4-piperidone derivatives in colon HCT-116 cells," Bioorganic and Medicinal Chemistry Letters, vol. 23, pp. 1075-1078, 2013.

[35] T. Qian, L. Kun, B. Gao, R. Zhu, X. Wu, and S. Wang, "Photo-ionization and photo-excitation of curcumin investigated by laser flash photolysis," Spectrochimica Acta Part A: Molecular and Biomolecular Spectroscopy, vol. 116, pp. 6-12, 2013.

[36] J. B. Fenn, M. Mann, C. K. Meng, S. F. Wong, and C. M. Whitehouse, "Electrospray ionization for mass spectrometry of large biomolecules," Science, vol. 246, pp. 64-71, 1989.

[37] M. Mann, C. K. Meng, and J. B. Fenn, "Interpreting mass spectra of multiply charged ions," Analytical Chemistry, vol. 61, pp. 1702-1708, 1989.

[38] E. Horning, M. Horning, D. Carroll, I. Dzidic, and R. Stillwell, "New picogram detection system based on a mass spectrometer with an external ionization source at atmospheric pressure," Analytical Chemistry, vol. 45, pp. 936-943, 1973.

[39] D. Carroll, I. Dzidic, R. Stillwell, K. Haegele, and E. Horning, "Atmospheric pressure ionization mass spectrometry. Corona discharge ion source for use in a liquid chromatograph-mass spectrometer-computer analytical system," Analytical Chemistry, vol. 47, pp. 2369-2373, 1975.

[40] D. B. Robb, T. R. Covey, and A. P. Bruins, "Atmospheric pressure photoionization: an ionization method for liquid chromatography-mass spectrometry," Analytical Chemistry, vol. 72, pp. 3653-3659, 2000.

[41] M. Karas, D. Bachmann, U. Bahr, and F. Hillenkamp, "Matrix-assisted ultraviolet laser desorption of non-volatile compounds," International Journal of Mass Spectrometry and Ion Processes, vol. 78, pp. 53-68, 1987.

[42] M. Karas and F. Hillenkamp, "Laser desorption ionization of proteins with molecular masses exceeding 10,000 daltons," Analytical chemistry, vol. 60, pp. 2299-2301, 1988.

[43] B. Domon and R. Aebersold, "Mass spectrometry and protein analysis," Science's STKE, vol. 312, p. 212, 2006.

[44] A. El-Aneed, A. Cohen, and J. Banoub, "Mass spectrometry, review of the basics: Electrospray, MALDI, and commonly used mass analyzers," Applied Spectroscopy Reviews, vol. 44, pp. 210-230, 2009.

[45] E. Hoffmann and V. Stroobant, Mass Spectrometry: Principles and Applications, third ed. The Atrium, Southern Gate, Chichester, West Sussex, England J. Wiley, 2007.

[46] P. Kebarle and U. H. Verkerk, "Electrospray: from ions in solution to ions in the gas phase, what we know now," Mass Spectrometry Reviews, vol. 28, pp. 898-917, 2009.

[47] P. Kebarle, "A brief overview of the present status of the mechanisms involved in electrospray mass spectrometry," Journal of Mass Spectrometry, vol. 35, pp. 804-817, 2000.

[48] N. B. Cech and C. G. Enke, "Practical implications of some recent studies in electrospray ionization fundamentals," Mass Spectrometry Reviews, vol. 20, pp. 362-387, 2002.

[49] J. V. Iribarne and B. A. Thomson, "On the evaporation of small ions from charged droplets," The Journal of Chemical Physics, vol. 64, p. 2287, 1976.

[50] M. Dole, R. L. Hines, L. L. Mack, R. C. Mobley, L. D. Ferguson, and M. B. Alice, "Gas phase macroions," Macromolecules, vol. 1, pp. 96-97, 1968.

[51] A. W.-B. a. G. Brinkmalm, Mass spectrometry: instrumentation, interpretation, and applications (A mass spectrometer's building blocks & Tandem mass spectrometry) vol. 20. Hoboken, New Jersey, USA: Wiley, 2008.

[52] T. M. Annesley, "Ion suppression in mass spectrometry," Clinical Chemistry, vol. 49, pp. 1041-1044, 2003.

[53] R. King, R. Bonfiglio, C. Fernandez-Metzler, C. Miller-Stein, and T. Olah, "Mechanistic investigation of ionization suppression in electrospray ionization," Journal of the American Society for Mass Spectrometry, vol. 11, pp. 942-950, 2000.

[54] F. Gosetti, E. Mazzucco, D. Zampieri, and M. C. Gennaro, "Signal suppression/enhancement in high-performance liquid chromatography tandem mass spectrometry," Journal of Chromatography A, vol. 1217, pp. 3929-3937, 2010.

[55] A. Van Eeckhaut, K. Lanckmans, S. Sarre, I. Smolders, and Y. Michotte, "Validation of bioanalytical LC–MS/MS assays: evaluation of matrix effects," Journal of Chromatography B, vol. 877, pp. 2198-2207, 2009.

[56] E. Chambers, D. M. Wagrowski-Diehl, Z. Lu, and J. R. Mazzeo, "Systematic and comprehensive strategy for reducing matrix effects in LC/MS/MS analyses," Journal of Chromatography B, vol. 852, pp. 22-34, 2007.

[57] K. A. Hanold, S. M. Fischer, P. H. Cormia, C. E. Miller, and J. A. Syage, "Atmospheric pressure photoionization. 1. General properties for LC/MS," Analytical chemistry, vol. 76, pp. 2842-2851, 2004.

[58] M. Wilm and M. Mann, "Analytical properties of the nanoelectrospray ion source," Analytical chemistry, vol. 68, pp. 1-8, 1996.

[59] A. Westman-Brinkmalm and G. Brinkmalm, "Mass spectrometry: instrumentation, interpretation, and applications ", R. Ekman, J. Silberring, A. Westman-Brinkmalm, and A. Kraj, Eds., ed Hoboken, New Jersey, USA: Wiley, 2008.

[60] H. Liang, R. Foltz, M. Meng, and P. Bennett, "Ionization enhancement in atmospheric pressure chemical ionization and suppression in electrospray ionization between target drugs and stable-isotope-labeled internal standards in quantitative liquid chromatography/tandem mass spectrometry," Rapid Communications in Mass Spectrometry, vol. 17, pp. 2815-2821, 2003.

[61] S. Souverain, S. Rudaz, and J.-L. Veuthey, "Matrix effect in LC-ESI-MS and LC-APCI-MS with off-line and on-line extraction procedures," Journal of Chromatography A, vol. 1058, pp. 61-66, 2004.

[62] A. Raffaelli and A. Saba, "Atmospheric pressure photoionization mass spectrometry," Mass Spectrometry Reviews, vol. 22, pp. 318-331, 2003.

[63] M. Smoker, K. Tran, and R. E. Smith, "Determination of polycyclic aromatic hydrocarbons (PAHs) in shrimp," Journal of Agricultural and Food Chemistry, vol. 58, pp. 12101-12104, 2010.

[64] T. Ghislain, P. Faure, and R. Michels, "Detection and monitoring of PAH and Oxy-PAHs by high resolution mass spectrometry: comparison of ESI, APCI and APPI source detection," Journal of The American Society for Mass Spectrometry, vol. 23, pp. 530-536, 2012.

[65] L. Imbert, M. Gaudin, D. Libong, D. Touboul, S. Abreu, P. M. Loiseau, et al., "Comparison of electrospray ionization, atmospheric pressure chemical ionization and atmospheric pressure photoionization for a lipidomic analysis of Leishmania donovani," Journal of Chromatography A, vol. 1242, pp. 75-83, 2012.

[66] P. Keski-Rahkonen, K. Huhtinen, R. Desai, D. Tim Harwood, D. J. Handelsman, M. Poutanen, et al., "LC-MS analysis of estradiol in human serum and endometrial tissue: Comparison of electrospray ionization, atmospheric pressure chemical ionization and atmospheric pressure photoionization," Journal of Mass Spectrometry, vol. 48, pp. 1050-1058, 2013.

[67] J. A. Syage, "Mechanism of $[M+ H]^+$ formation in photoionization mass spectrometry," Journal of the American Society for Mass Spectrometry, vol. 15, pp. 1521-1533, 2004.

[68] E. Marotta, R. Seraglia, F. Fabris, and P. Traldi, "Atmospheric pressure photoionization mechanisms: 1. The case of acetonitrile," International Journal of Mass Spectrometry, vol. 228, pp. 841-849, 2003.

[69] M. J. Stump, R. C. Fleming, W. H. Gong, A. J. Jaber, J. J. Jones, C. W. Surber, et al., "Matrix-assisted laser desorption mass spectrometry," Applied Spectroscopy Reviews, vol. 37, pp. 275-303, 2002.

[70] F. Hillenkamp and J. Peter-Katalinic´, MALDI MS. A practical guide to instrumentation, methods and applications. Wiley-VCH Verlag GmbH & Co. KGaA, Weinheim: Wiley Online Library, 2007.

[71] R. Knochenmuss and R. Zenobi, "MALDI ionization: the role of in-plume processes," Chemical Reviews-Columbus, vol. 103, pp. 441-452, 2003.

[72] R. Knochenmuss, "Ion formation mechanisms in UV-MALDI," Analyst, vol. 131, pp. 966-986, 2006.

[73] R. Zenobi and R. Knochenmuss, "Ion formation in MALDI mass spectrometry," Mass Spectrometry Reviews, vol. 17, pp. 337-366, 1998.

[74] R. B. Cole, Electrospray and MALDI mass spectrometry: fundamentals, instrumentation, practicalities, and biological applications, Second ed. Hoboken, New Jersey: Wiley, 2011.

[75] C. Zhang, H. Zhang, D. W. Litchfield, and K. K.-C. Yeung, "CHCA or DHB? Systematic comparison of the two most commonly used matrices for peptide mass fingerprint analysis with MALDI MS," Spectroscopy, 2010.

[76] M. Karas, M. Glückmann, and J. Schäfer, "Ionization in matrix-assisted laser desorption/ionization: singly charged molecular ions are the lucky survivors," Journal of Mass Spectrometry, vol. 35, pp. 1-12, 2000.

[77] T. W. Jaskolla and M. Karas, "Compelling evidence for lucky survivor and gas phase protonation: the unified MALDI analyte protonation mechanism," Journal of the American Society for Mass Spectrometry, vol. 22, pp. 976-988, 2011.

[78] M. S. Munson and F.-H. Field, "Chemical ionization mass spectrometry. I. General introduction," Journal of the American Chemical Society, vol. 88, pp. 2621-2630, 1966.

[79] F. H. Field, "Chemical ionization mass spectrometry," Accounts of Chemical Research, vol. 1, pp. 42-49, 1968.

[80] Y. Chai, H. Sun, J. Wan, Y. Pan, and C. Sun, "Hydride abstraction in positive-ion electrospray interface: oxidation of 1, 4-dihydropyridines in electrospray ionization mass spectrometry," Analyst, vol. 136, pp. 4667-4669, 2011.

[81] L. R. Orelli, M. B. García, I. A. Perillo, L. Tonidandel, and P. Traldi, "A comparison of the electron ionization and electrospray behaviour of some N, N′-disubstituted

hexahydropyrimidines," Rapid Communications in Mass Spectrometry, vol. 20, pp. 823-828, 2006.

[82] F. J. Cox, M. V. Johnston, and A. Dasgupta, "Characterization and relative ionization efficiencies of end-functionalized polystyrenes by matrix-assisted laser desorption/ionization mass spectrometry," Journal of the American Society for Mass Spectrometry, vol. 14, pp. 648-657, 2003.

[83] X. Lou, A. J. H. Spiering, B. F. M. de Waal, J. L. J. van Dongen, J. A. J. M. Vekemans, and E. W. Meijer, "Dehydrogenation of tertiary amines in matrix-assisted laser desorption/ionization time-of-flight mass spectrometry," Journal of Mass Spectrometry, vol. 43, pp. 1110-1122, 2008.

[84] H.-J. Yang, A. Lee, M.-K. Lee, W. Kim, and J. Kim, "Detection of small neutral carbohydrates using various supporting materials in laser desorption/ionization mass spectrometry," Bulletin of the Korean Chemical Society, vol. 31, p. 35, 2010.

[85] J. M. Nuutinen, M. Purmonen, J. Ratilainen, K. Rissanen, and P. Vainiotalo, "Mass spectrometric studies on pyridine-piperazine-containing ligands and their complexes with transition metals formed in solution," Rapid Communications in Mass Spectrometry, vol. 15, pp. 1374-1381, 2001.

[86] T. Kauppila, T. Nikkola, R. Ketola, and R. Kostiainen, "Atmospheric pressure photoionization-mass spectrometry and atmospheric pressure chemical ionization-mass spectrometry of neurotransmitters," Journal of Mass Spectrometry, vol. 41, pp. 781-789, 2006.

[87] N. M. Suni, H. Aalto, T. J. Kauppila, T. Kotiaho, and R. Kostiainen, "Analysis of lipids with desorption atmospheric pressure photoionization-mass spectrometry (DAPPI-MS) and desorption electrospray ionization-mass spectrometry (DESI-MS)," Journal of Mass Spectrometry, vol. 47, pp. 611-619, 2012.

[88] R. B. Cody, "Observation of molecular ions and analysis of nonpolar compounds with the direct analysis in real time ion source," Analytical Chemistry, vol. 81, pp. 1101-1107, 2008.

[89] A. G. Harrison, Chemical ionization mass spectrometry, Second ed. United States of America: CRC press, 1992.

[90] M. S. Munson and F. Field, "Chemical ionization mass spectrometry. IV. Aromatic hydrocarbons," Journal of the American Chemical Society, vol. 89, pp. 1047-1052, 1967.

[91] E. Marotta and C. Paradisi, "A mass spectrometry study of alkanes in air plasma at atmospheric pressure," Journal of the American Society for Mass Spectrometry, vol. 20, pp. 697-707, 2009.

[92] J. Gao, B. C. Owen, D. J. Borton II, Z. Jin, and H. I. Kenttämaa, "HPLC/APCI mass spectrometry of saturated and unsaturated hydrocarbons by using hydrocarbon solvents as the APCI reagent and HPLC mobile phase," Journal of The American Society for Mass Spectrometry, vol. 23, pp. 816-822, 2012.

[93] N. Hourani and N. Kuhnert, "Development of a novel direct-infusion atmospheric pressure chemical ionization mass spectrometry method for the analysis of heavy hydrocarbons in light shredder waste," Analytical Methods, vol. 4, pp. 730-735, 2012.

[94] S. E. Bell, R. G. Ewing, G. A. Eiceman, and Z. Karpas, "Atmospheric pressure chemical ionization of alkanes, alkenes, and cycloalkanes," Journal of the American Society for Mass Spectrometry, vol. 5, pp. 177-185, 1994.

[95] C. Kang, Y. Zhou, Z. Du, Z. Bian, J. Wang, X. Qiu, et al., "Dehydrogenation and dehalogenation of amines in MALDI-TOF MS investigated by isotopic labeling," Journal of Mass Spectrometry, vol. 48, pp. 1318-1324, 2013.

[96] G. L. Glish and R. W. Vachet, "The basics of mass spectrometry in the twenty-first century," Nature Reviews Drug Discovery, vol. 2, pp. 140-150, 2003.

[97] J. T. Watson and O. D. Sparkman, Introduction to mass spectrometry: instrumentation, applications, and strategies for data interpretation: John Wiley & Sons, 2007.

[98] B. A. Mamyrin, "Time-of-flight mass spectrometry (concepts, achievements, and prospects)," International Journal of Mass Spectrometry, vol. 206, pp. 251-266, 2001.

[99] M. Guilhaus, "Special feature: Tutorial. Principles and instrumentation in time-of-flight mass spectrometry. Physical and instrumental concepts," Journal of Mass Spectrometry, vol. 30, pp. 1519-1532, 1995.

[100] C. Weickhardt, F. Moritz, and J. Grotemeyer, "Time-of-flight mass spectrometry: State-of the-art in chemical analysis and molecular science," Mass Spectrometry Reviews, vol. 15, pp. 139-162, 1996.

[101] W. C. Wiley and I. H. McLaren, "Time-of-flight mass spectrometer with improved resolution," Review of Scientific Instruments, vol. 26, pp. 1150-1157, 1955.

[102] B. A. Mamyrin, V. I. Karataev, D. V. Shmikk, and V. A. Zagulin, "The mass-reflectron, a new nonmagnetic time-of-flight mass spectrometer with high resolution," Soviet Journal of Experimental and Theoretical Physics, vol. 37, p. 45, 1973.

[103] W. D. Lehmann, "Jürgen H. Gross: Mass spectrometry–A Textbook," Analytical and Bioanalytical Chemistry, pp. 1-2, 2011.

[104] M. Guilhaus, D. Selby, and V. Mlynski, "Orthogonal acceleration time-of-flight mass spectrometry," Mass Spectrometry Reviews, vol. 19, pp. 65-107, 2000.

[105] D. J. Douglas, A. J. Frank, and D. Mao, "Linear ion traps in mass spectrometry," Mass Spectrometry Reviews, vol. 24, pp. 1-29, 2004.

[106] M. B. Comisarow and A. G. Marshall, "Fourier transform ion cyclotron resonance spectroscopy," Chemical Physics Letters, vol. 25, pp. 282-283, 1974.

[107] M. B. Comisarow and A. G. Marshall, "Frequency-sweep Fourier transform ion cyclotron resonance spectroscopy," Chemical Physics Letters, vol. 26, pp. 489-490, 1974.

[108] A. G. Marshall, C. L. Hendrickson, and G. S. Jackson, "Fourier transform ion cyclotron resonance mass spectrometry: a primer," Mass Spectrometry Reviews, vol. 17, pp. 1-35, 1998.

[109] M. L. Gross, G. Chen, and B. Pramanik, Protein and peptide mass spectrometry in drug discovery. Hoboken, New Jersey, USA: John Wiley & Sons, 2011.

[110] J. H. Gross, "Tandem mass spectrometry," Mass Spectrometry, pp. 415-478, 2011.

[111] A. Westman-Brinkmalm and G. Brinkmalm, "Mass spectrometry: instrumentation, interpretation, and applications," R. Ekman, J. Silberring, A. Westman-Brinkmalm, and A. Kraj, Eds., ed Hoboken, New Jersey, USA: Wiley, 2008.

CHAPTER2
THE UNEXPECTED FORMATION OF $[M-H]^+$ SPECIES DURING MALDI AND DOPANT FREE-APPI MS ANALYSIS OF NOVEL ANTINEOPLASTIC CURCUMIN ANALOGUES

H. Awad, M. J. Stoudemayer, L. Usher, I. J. Amster, A. Cohen, U. Das, R. M. Whittal, J. Dimmock, A. El-Aneed

In this work, I evaluated the ionization behavior of thirteen curcumin analogues using different ionization techniques and experimental conditions. The evaluated curcumin analogues were synthesized by co-authors Dr. Das and Dr. Dimmock at University of Saskatchewan as per Dr. El-Aneed's request. I synthesized the deuterated curcumin analogue. I designed all the ionization studies in consultation with my supervisor Dr. El-Aneed. In addition, I performed all MALDI experiments using the ABI 4800 MALDI TOF/TOF™ instrument. I performed various experiments to evaluate the role of laser intensity, ionization mode, solvent, and matrix. In addition, I analyzed all the data provided by Dr. El-Aneed's collaborators. I evaluated three proposed mechanisms to explain the $[M-H]^+$ formation including loss of H_2 from the protonated $[M+H]^+$ species, hydrogen transfer from the analyte radical cation and hydride abstraction from the neutral analyte molecule. I drafted various versions of the published manuscript under the supervision of Dr. El-Aneed who revised the various versions of the manuscript.

I visited the University of Alberta working with co-author Dr. Whittal for obtaining high resolution MS data (i.e. MALDI-FTICR-MS). In addition, an APPI-TOF-MS experiment was performed, based on my suggestions by Dr. Whittal at the University of Alberta to evaluate the role of photon energy and dopant in the ionization of curcumin analogues.

The first MALDI experiment in this work was conducted in 2010 by Dr. Cohen at NRC-Halifax and Ms. L. Usher worked under the supervision of Dr. El-Aneed to theoretically study

this unique ionization mechanism focusing on four curcumin analogues. At the University of Georgia, M. J. Stoudemayer under the supervision of Dr. Amster evaluated the ionization behavior of one of the curcumin analogues (i.e. NC2138) using different MALDI-FTICR-MS experimental conditions. Ms. Stoudemayer also performed the butylated hydroxytoluene (BHT) experiments, based on my suggestion, on NC2138 and NC2144 to evaluate the radical formation mechanism using the butylated hydroxytoluene as a radical scavenger: these results were not conclusive. In addition, they provided suggestions regarding changing some of the experimental conditions such as using different solvents and various laser intensities. All co-authors were given the opportunity to provide suggestions for the final version of the manuscript I drafted under the supervision of Dr. El-Aneed.

The unexpected formation of $[M-H]^+$ species during MALDI and dopant free-APPI MS analysis of novel antineoplastic curcumin analogues

H. Awad[1], M. J. Stoudemayer[2], L. Usher[1], I. J. Amster[2], A. Cohen[3], U. Das[1], R. M. Whittal[4], J. Dimmock[1], A. El-Aneed[1*]

Published in the Journal of Mass Spectrometry (2014), 49:1139–1147

[1.] College of Pharmacy and Nutrition, University of Saskatchewan, Saskatoon, SK, S7N 5E5, Canada.

[2.] Department of Chemistry, University of Georgia, Athens, GA 30602-2556, United States

[3.] Proteomics Core Facility, Clinical Research Centre, Dalhousie University, Halifax, NS, B3H 4H7, Canada.

[4.] Department of Chemistry, University of Alberta, Edmonton, AB, T6G 2G2, Canada

* Corresponding Author:

E-mail Address: anas.el-aneed@usask.ca

Telephone: +1-306-966-2013

Keywords: MALDI-MS; APPI-MS; $[M-H]^+$; Ionization mechanism; Hydride abstraction

INTRODUCTION

Qualitative and quantitative analysis of drug molecules is a crucial step during the drug development process that requires the use of various analytical tools such as mass spectrometry (MS). Various ionization techniques have been used with MS including electrospray ionization (ESI) [1, 2], atmospheric pressure chemical ionization (APCI) [3], atmospheric pressure photoionization (APPI) [4] and matrix assisted laser desorption ionization (MALDI) [5, 6]. ESI and MALDI are the most widely used soft ionization techniques, based on their ability to ionize a wide range of biomolecules as well as small organic compounds, with minimum in-source fragmentation [7, 8]. MALDI can offer great tolerance towards contaminants, easy sample preparation and mass spectra with predominantly singly charged ions [9, 10]. For LC-MS analysis, ESI and APCI are the most widely used ionization techniques [10]. However, APPI has recently been utilized due to its ability to ionize non polar compounds that are not well-ionized by APCI or ESI [10].

In this study, we used different MS-ionization techniques to analyze some curcumin analogues that are novel drug molecules designed as anticancer agents [11, 12]. The evaluated molecules are 3,5-bis(benzylidene)-4-piperidones, containing the 1,5-diaryl-3-oxo-1,4-pentadienyl pharmacophore (Scheme 2.1) which is considered to act at a primary binding site. This group was designed to alkylate cellular thiols rather than interacting with amino or hydroxyl groups present in nucleic acid [11, 12]. In addition, substituents have been placed on the piperidyl nitrogen atom to align at auxiliary binding sites thereby increasing the cytotoxic potential of the compounds [13]. Based on the nature of the N-substituents, the curcumin analogues have been categorized into four groups: phosphoramidates, secondary amines, amides and mixed amines/amides (Scheme 2.2).

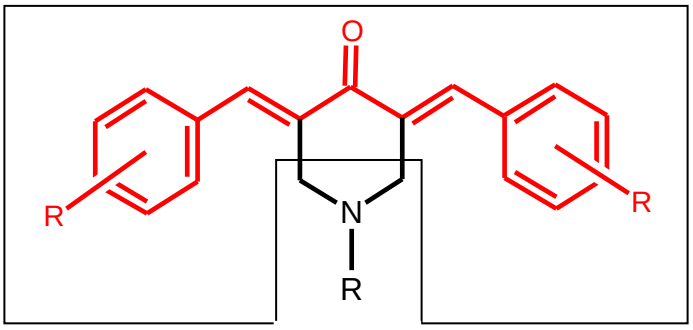

Scheme 2.1. General structure of the 3,5-bis(benzylidene)-4-piperidones (the 1,5-diaryl-3-oxo-1,4-pentadienyl pharmacophore is in the box).

Phosphoramidates

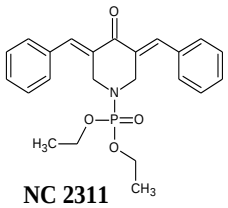

NC 2311

411.1599 Da

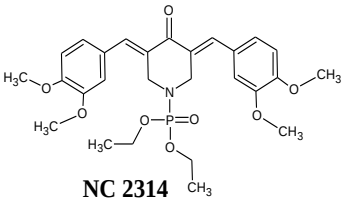

NC 2314

531.2022 Da

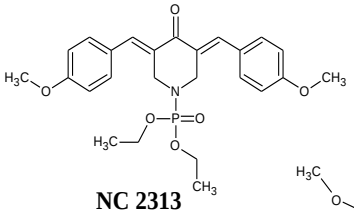

NC 2313

471.1811 Da

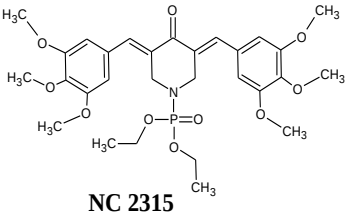

NC 2315

591.2233 Da

Secondary Amines

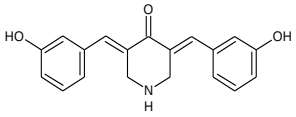

NC 2128

307.1208 Da

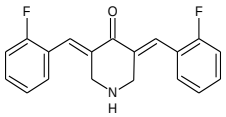

EF-24

311.1122 Da

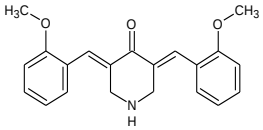

NC 2453

335.1521 Da

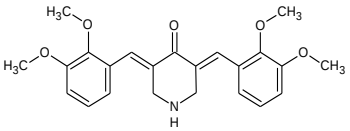

NC 2454

395.1733 Da

Mixed Amine and Amide

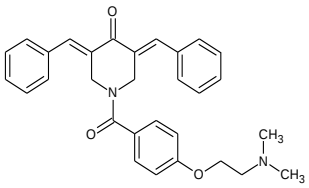

NC 2067

466.2256 Da

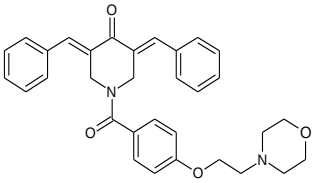

NC 2081

508.2362Da

Amides

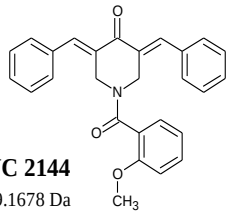

NC 2144

409.1678 Da

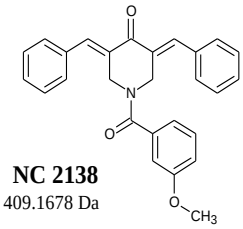

NC 2138

409.1678 Da

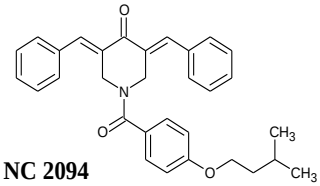

NC 2094

465.2304 Da

Scheme 2.2. Structures and monoisotopic masses of the novel antineoplastic curcumin analogues categorized by the N-substituent into four structural families: phosphoramidates, secondary amines, amides and mixed amines/amides.

The curcumin analogues are nitrogenous compounds that are expected to ionize in the positive ion mode by protonation of the basic site, producing the $[M+H]^+$ ions. Unexpectedly during single stage MALDI-MS analysis, $[M-H]^+$ ions were formed along with the expected $[M+H]^+$ species (Scheme 2.3). In addition, three curcumin phosphoramidate analogues ionized solely as $[M-H]^+$.

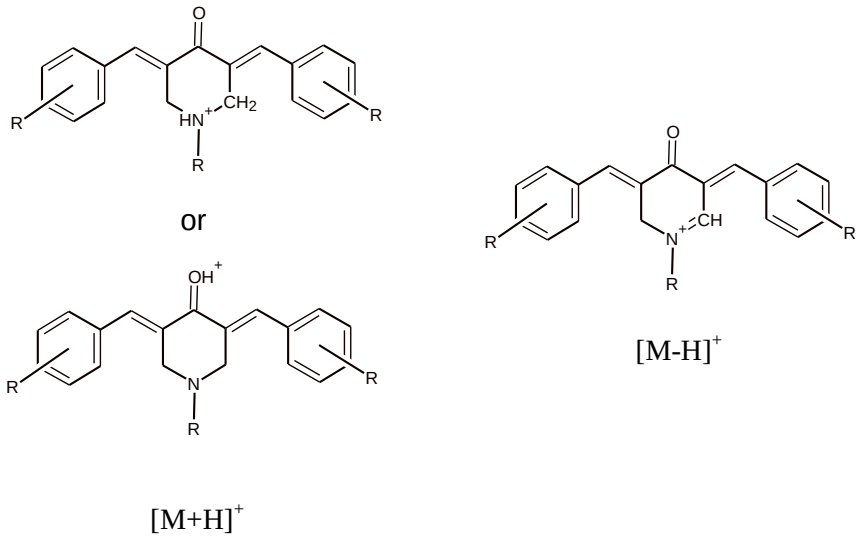

Scheme 2.3. The proposed general structures of 3,5-bis(arylidene)-4-piperidone; $[M+H]^+$ and $[M-H]^+$ ions.

The formation of positively-charged $[M-H]^+$ ions was reported significantly with alkanes during chemical ionization (CI) [14, 15] and APCI-MS [3]. Subsequently, $[M-H]^+$ ion formation has been detected with a wide range of compounds with various ionization techniques, such as ESI [16, 17], MALDI [18-22], APPI [23], Desorption APPI (DAPPI) [24], Desorption ESI (DESI) [24] and direct analysis in real time (DART) [25]. Several mechanisms have been proposed to explain the formation of $[M-H]^+$ during MS-analysis that could be summarized into three main mechanisms; i) loss of hydrogen molecule from the protonated $[M+H]^+$ ion, ii) hydrogen transfer from the analyte radical cation or iii) hydride abstraction from the neutral analyte molecule [14-23, 26-28] (Scheme 2.4).

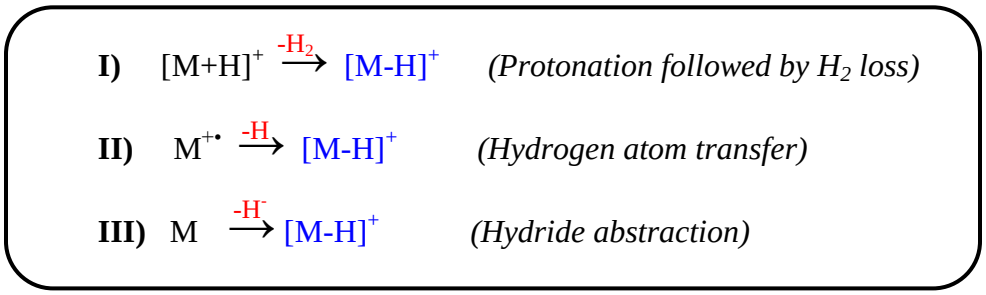

Scheme 2.4. The three general proposed mechanisms for $[M-H]^+$ formation during MS analysis.

In MALDI-MS, Lou et al. [19] detected significantly $[M-H]^+$ ions during single stage positive ion mode MALDI-TOF-MS analysis of tertiary amines. However, $[M-H]^+$ was barely detected with secondary amines. Two mechanisms for $[M-H]^+$ formation were proposed in this study: H_2 loss from the $[M+H]^+$ ion and hydrogen loss from the analyte radical cation $[M]^{+\bullet}$ (Scheme 2.4 I&II respectively). In 2013, Kang et al. [20] investigated the $[M-H]^+$ formation using secondary and tertiary amines. The study showed high-intensities of $[M-H]^+$ ion peaks with tertiary amines in comparison to secondary amines that showed low intensity peaks. The study proposed the mechanism shown in Scheme 2.4 II to explain the $[M-H]^+$ formation that involves hydrogen loss from the analyte radical cation [20]. Few papers, however, suggested the hydride abstraction of the analyte (Scheme 2.4 III) to explain the $[M-H]^+$ formation during MALDI-MS [21, 22].

In our work, the ionization behavior of biologically active curcumin analogues (Scheme 2.2) were studied using various ionization techniques, namely ESI, APCI, APPI (with and without a dopant), and MALDI. Significant $[M-H]^+$ peaks were detected with MALDI and dopant free APPI-MS. Therefore, we investigated the role of the matrix and the solvent in $[M-H]^+$ formation by applying laser desorption ionization (LD)-MS and solvent free LD-MS. In addition, the

influence of laser intensity, the type of mass analyzer and the ionization mode were evaluated. Our aim is to expand on the previously reported formation of the $[M-H]^+$ ion and understand the various factors that may contribute to its formation.

Understanding the unusual ionization behavior of curcumin analogues is important for the future development of qualitative and quantitative MS based methods to analyze these drug candidates or any structurally-related compounds that may behave in a similar way. In addition, the unusual ionization behavior of curcumin analogues revealed interesting observations that may contribute in understanding the detailed mechanism of MALDI that is currently still not totally clear.

EXPERIMENTAL

Curcumin analogues were synthesized by the methods described previously [12, 13]. The compounds are categorized by the N-substituent as phosphoramidates, secondary amines, amides and mixed amines/amides (Scheme 2.2).

ESI-MS analysis

ESI-MS analysis was conducted on an AB SCIEX 4000 QTRAP® instrument (Qq-LIT-MS). Samples were prepared in concentration of 0.2 mg/mL in 100% acetonitrile (ACN). Samples were directly injected at a flow rate of 10 µL/min using a Harvard syringe pump. The instrument was operated in the positive ion mode with ion spray voltage 5500 V at room temperature and a declustering potential of 100V.

APCI-MS analysis

Samples with a concentration of 0.2 mg/mL in water: acetonitrile (50:50, v/v) were injected into an AB SCIEX 4000 QTRAP® instrument (Qq-LIT-MS) by switching the ionization source from ESI into APCI. The instrument was operated in the positive ion mode with a APCI probe temperature at 200°C, nebulizer current of 3 μA and a declustering potential of 100 V.

APPI-MS analysis

Samples were injected into an Agilent 6220 orthogonal time-of-flight-MS equipped with an APPI source. The instrument was operated in the positive ion mode with a krypton lamp generating two photon energy lines at 10.0 and 10.6 eV. The vaporizer was set to 350°C while the drying gas was set at 10L/min with the gas heater set to 300°C. The carrier solvent was 100% acetonitrile for the no dopant samples (0.2 mg/mL dissolved in 100% ACN) and 95% ACN/5% acetone for the dopant samples (0.001 mg/mL dissolved in 100% ACN) at a flow rate of 0.2 mL/min.

MALDI-MS analysis

Samples were prepared at a concentration of 1μg/mL by dissolving the curcumin analogue in 100% ACN. 2,5-Dihydroxybenzoic acid (DHB) was used as a matrix with a concentration of 10 mg/mL in H_2O:ACN:TFA (50:50:0.1, v/v/v). Samples were prepared by mixing the above working solutions of analyte and matrix in a ratio of 1:1 (v/v). Samples were spotted on MALDI stainless steel plate, dried and introduced into an ABI 4800 MALDI TOF/TOF™ instrument equipped with a Nd:YAG laser, 355 nm wavelength, 3 to 7 ns pulse width and a 200 Hz firing rate. The laser intensity was set at 4200, delay time 25 ns and the accelerating voltage at 20 kV. Mass spectra were acquired in the reflector positive ion mode by summing the spectra of 800

laser shots. For investigating the possible mechanism of $[M-H]^+$ formation during MALDI-MS analysis, samples were run under different conditions including negative ion mode and different laser intensities (4000-5000).

LD-MS and solvent free LD-MS analysis

In LD-MS analysis, curcumin analogues were dissolved in 100% ACN at a concentration of 0.2 mg/ml and introduced into an ABI 4800 MALDI TOF/TOF™ instrument without using a matrix. In solvent-free LD-MS, powders of curcumin analogues were smeared on a MALDI stainless steel plate with no matrix or solvent and introduced into the ABI 4800 MALDI TOF/TOF™ instrument. In both LD-MS and solvent free LD-MS, samples were run under the same instrument parameters described above for the MALDI-MS analysis.

The solvent free LD-MS analysis experiment was duplicated using MALDI-FTICR-MS (Bruker 9.4T Apex-Qe FTICR-MS) to investigate the influence of the mass analyzer on $[M-H]^+$ formation in the absence of other factors such as matrix and solvent. The FTICR instrument was equipped with a 355 nm Nd:YAG laser and operated in the positive ion mode with laser power range 45-75%. Mass spectra were acquired by summing the spectra of 25 laser shots. Exact mass measurements of the curcumin analogues were performed after externally calibrating the FTICR instrument with polyethylene glycol 600 and DCTB (trans-2-[3-(4-tert-butylphenyl)-2-methyl-2-propenylidene]malononitrile).

RESULTS AND DISCUSSION

Ionization of curcumin analogues

The curcumin analogues showed various ionization behaviors based on the ionization methods. In the single stage positive ion mode ESI-MS and APCI-MS, all curcumin analogues were ionized as expected yielding the protonated ion, $[M+H]^+$. Interestingly, in the single stage positive ion mode of MALDI-MS, curcumin analogues were ionized in two forms showing both $[M-H]^+$ and $[M+H]^+$ species. Figure 2.1 shows the MALDI-MS spectrum for one of the curcumin analogues (NC 2067 will be used as a representative structure with a monoisotopic mass of 466.2 Da) showing two major peaks $[M-H]^+$ and $[M+H]^+$ at *m/z* = 465.2 and 467.1 respectively. The authenticity of the observed $[M-H]^+$ and $[M+H]^+$ ions was verified via exact mass measurements using an FT-ICR-MS instrument (Table 2.1). A peak at *m/z* = 269.1 was also observed representing a $[M+3H]^+$ ion. An $[M+3H]^+$ ion has been reported and investigated by Calba et al. during MALDI-MS studies [29, 30], and they proposed that hydrogen atoms transfer from the matrix to the analyte molecule as a possible mechanism for its formation. The $[M+3H]^+$ ion was not observed with all tested curcumin analogues and since our aim is to evaluate the formation of $[M-H]^+$; therefore, it will not be discussed further in this work.

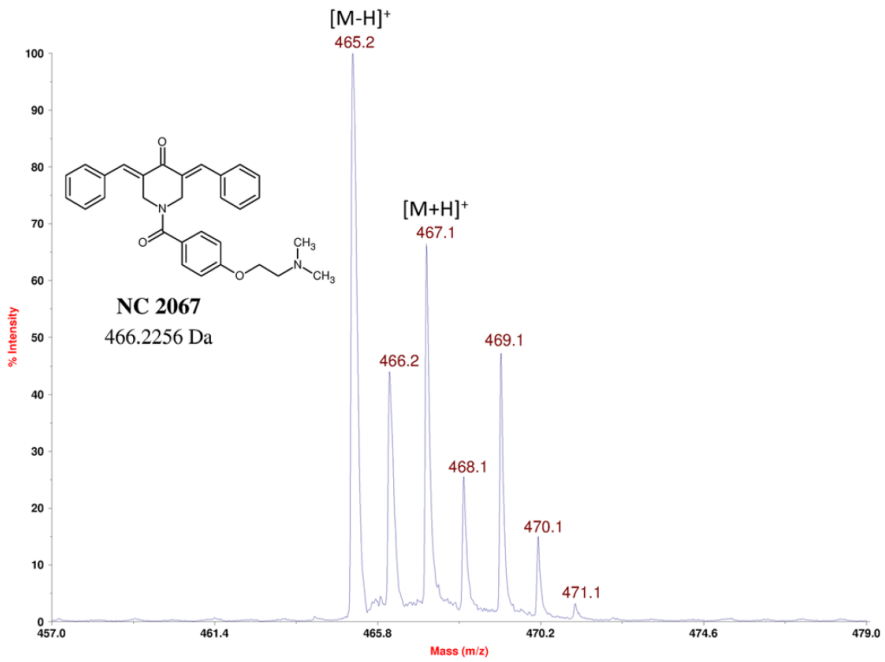

Figure 2.1. **MALDI-MS** spectrum of curcumin analogue (NC 2067 with monoisotopic mass= 466.2 Da) showing two forms of ions $[M-H]^+$ and $[M+H]^+$ (*m/z* 465.2 and 467.1, respectively).

Compound	Theoretical, *m/z*		Observed, *m/z*		Accuracy (ppm)	
	$[M-H]^+$	$[M+H]^+$	$[M-H]^+$	$[M+H]^+$	$[M-H]^+$	$[M+H]^+$
NC2311	410.15157	412.16722	410.15177	412.16763	0.48	0.99
NC2313	470.17270	472.18835	470.17301	N/A	0.66	N/A
NC2314	530.19383	532.209479	530.19388	N/A	0.10	N/A
NC2315	590.21496	592.230609	590.21511	N/A	0.26	N/A
NC2128	306.11247	308.12812	306.11220	308.12788	0.87	0.78
EF-24	310.10380	312.11945	310.10431	312.11928	0.54	1.64
NC2453	334.14377	336.15942	334.14397	336.15967	0.60	0.75
NC2454	394.16490	396.18055	394.16527	396.18087	0.94	0.81
NC2067	465.21727	467.23292	465.21771	467.23359	0.96	1.43
NC2081	507.22783	509.24348	507.22802	509.24375	0.36	0.52
NC2144	408.15942	410.17507	408.15984	410.17540	1.04	0.79
NC2138	408.15942	410.17507	408.15978	410.17536	0.87	0.71
NC2094	464.22202	466.23767	464.22248	466.23820	0.99	1.13

Table 2.1. The mass accuracy of $[M-H]^+$ and $[M+H]^+$ ions for each curcumin analogue using Bruker 9.4T Apex-Qe MALDI-FTICR-MS.

To explain the detailed mechanism of $[M-H]^+$ formation during MALDI-MS, several experiments were conducted to explore the factors that may influence the formation of $[M-H]^+$ ions including laser intensity, the type of the mass analyzer, ionization mode, matrix and solvent.

Monitoring the change in $[M-H]^+$ formation with the change in laser intensity, vacuum pressure or length of time between formation and detection can be explored with different mass analyzers (trapping or non-trapping analyzer). For example, in the Fourier transform ion cyclotron resonance (FT-ICR) instrument, ions are formed at a vacuum pressure of approximately 1.5 Torr and stored in an external hexapole for several milliseconds prior to injection to the low pressure region of the ICR cell. In comparison, ions are formed in the TOF/TOF at less than μTorr pressures and the time from ion formation to detection is on the μs time scale. Changes in pressure and time may influence the relative abundance of the ion types observed. By using different mass analyzers (i.e. FTICR instead of TOF) and changing the laser intensity of MALDI-TOF-MS within the range (4000 - 5000) did not alter the results, as both $[M-H]^+$ and $[M+H]^+$ ions were observed, indicating that neither the laser intensity (within the tested range) or the mass analyzer has a significant role in $[M-H]^+$ formation. In addition, changing the mode of ionization to the negative ion mode was investigated to monitor any unusual ion formation. However, the negative ion mode of MALDI-MS resulted in the formation of the radical anion $[M]^{-\bullet}$ and the expected $[M-H]^-$ of all tested compounds with no unusual formation of other ions (data not shown).

In order to study the influence of the matrix on the $[M-H]^+$ ion formation, MALDI-MS experiment was repeated with two different matrices (i.e. α-Cyano-4-hydroxycinnamic acid and 3-Hydroxy-4-Nitrobenzoic acid) for NC2138 as a representative compound. The experiments showed the same results of 2,5-dihydroxybenzoic acid as both $[M-H]^+$ and $[M+H]^+$ ions were

observed (data not shown). Interestingly, the formation of $[M-H]^+$ and $[M+H]^+$ ions were not changed even in the absence of matrix during an LD-MS experiment of all tested curcumin analogues except the disappearance of $[M+3H]^+$ peak (Figure 2.2).

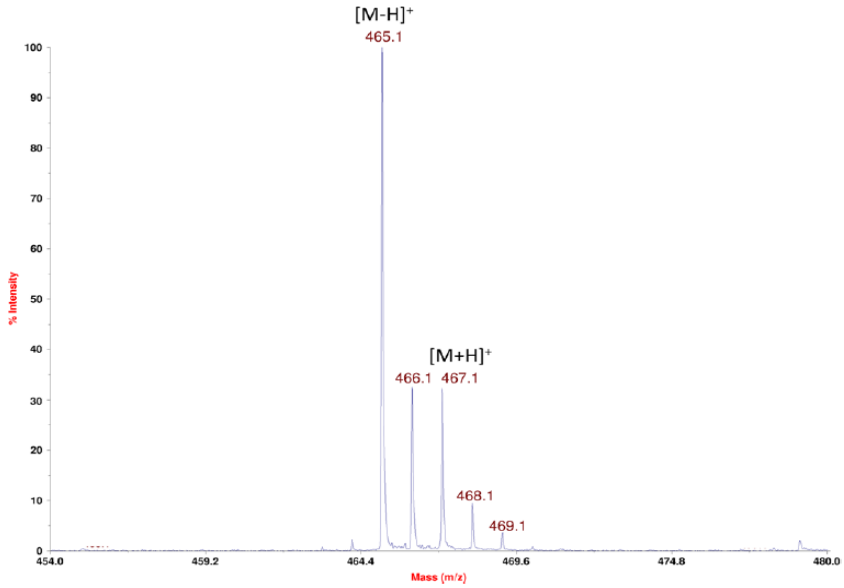

Figure 2.2. **LD-MS** spectrum of curcumin analogue (NC2067) showing two forms of ions $[M-H]^+$ and $[M+H]^+$ (*m/z* 465.1 and 467.1 respectively).

LD-MS experiment supported the significant role of matrix in $[M+3H]^+$ formation as previously described by Calba et al. [29, 30]. In contrast, matrix was not significant for the $[M-H]^+$ and $[M+H]^+$ formation. The relative intensity of $[M+H]^+$ was, however, increased, as expected, when using a matrix (Figures 2.1 & 2.2). Two more ratios of analyte: matrix were investigated in our MALDI-MS experiments (1:100 and 1:1000 molar ratios) in order to monitor the change in $[M+H]^+/[M-H]^+$ relative peak intensities. The results showed significant increase in the $[M+H]^+/[M-H]^+$ intensities with the higher ratio of analyte: matrix due to increase in the protonated ion form $[M+H]^+$ of our compounds (data not shown).

Based on the lucky survivor model of MALDI [31, 32], the solvent may also play a role in ion formation by ionizing the analyte during sample preparation. Therefore, we investigated different solvent mixtures during sample and matrix preparations in MALDI-MS. For example 100%ACN or H_2O:ACN:TFA (50:50:0.1) were applied for sample preparation while ACN:H_2O (50:50) and H_2O:ACN:TFA (50:50:0.1) for matrix solution. Changing the solvent system of both sample and matrix solutions did not change the MALDI-MS results as both ions $[M-H]^+$ and $[M+H]^+$ were formed. However, as expected, the $[M+H]^+$ peak intensity was enhanced by using a proton donor solvent such as TFA. To further evaluate the role of the solvent in the $[M-H]^+$ ion formation, solvent free LD-MS was applied. In this method, the curcumin analogue powder was smeared on a stainless steel MALDI plate without a solvent or a matrix. Interestingly, both $[M-H]^+$ and $[M+H]^+$ ions were formed (Figure 2.3), indicating that neither the matrix nor the solvent play a decisive role for the formation of $[M-H]^+$ or $[M+H]^+$ ions of the tested compounds.

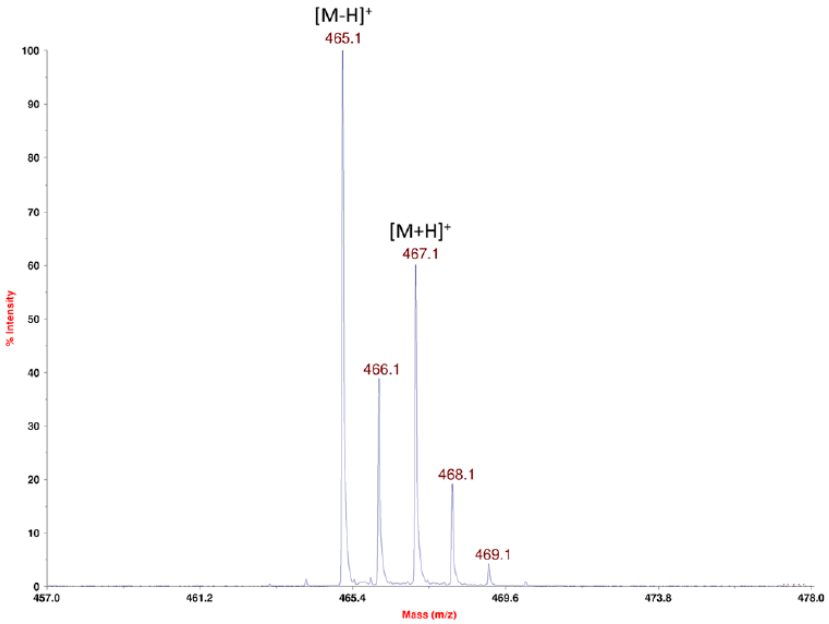

Figure 2.3. **Solvent free LD-MS** spectrum of curcumin analogue (NC2067) showing two forms of ions $[M-H]^+$ and $[M+H]^+$ (*m/z* 465.1 and 467.1 respectively).

The above findings indicate that the two major models that explain the ionization mechanism of MALDI; gas phase protonation [33-35], and lucky survivor model [31, 32], cannot explain the $[M-H]^+$ or $[M+H]^+$ formation of the tested curcumin analogues, as both models highlighted the importance of the matrix and solvent, respectively, for analyte ionization during MALDI-MS.

The unusual formation of $[M-H]^+$ ions during the positive ion mode of MALDI-MS means that the curcumin analogues have lost in net one hydrogen atom instead of accepting a proton. It can be argued that ring fusion may be occurring during ionization and the observed $[M-H]^+$ is simply $[M-2H+H]^+$. Therefore, we analyzed a newly designed deuterated curcumin analogue in which 10 hydrogen atoms of the two benzene rings were replaced with deuterium atoms giving MW = 285 Da (Figure 2.4). During the positive ion mode LD-MS of the deuterated compound, two major peaks were observed at 284.1 and 286.1 Da, indicating that the tested compound was ionized as proposed in Scheme 2.3 by losing a hydrogen in net forming the $[M-H]^+$ and by accepting a proton forming the $[M+H]^+$ respectively (Figure 2.4). This experiment confirmed that the major peak of $[M-H]^+$ at *m/z* 284.1 was formed by double bond formation between the nitrogen atom and the adjacent carbon atom rather than any possible ring fusion. However, a minor peak was detected at *m/z* 283.1 which is probably the protonated form of the ring fused structure $[M-D-H+H]^+$ (Figure 2.4).

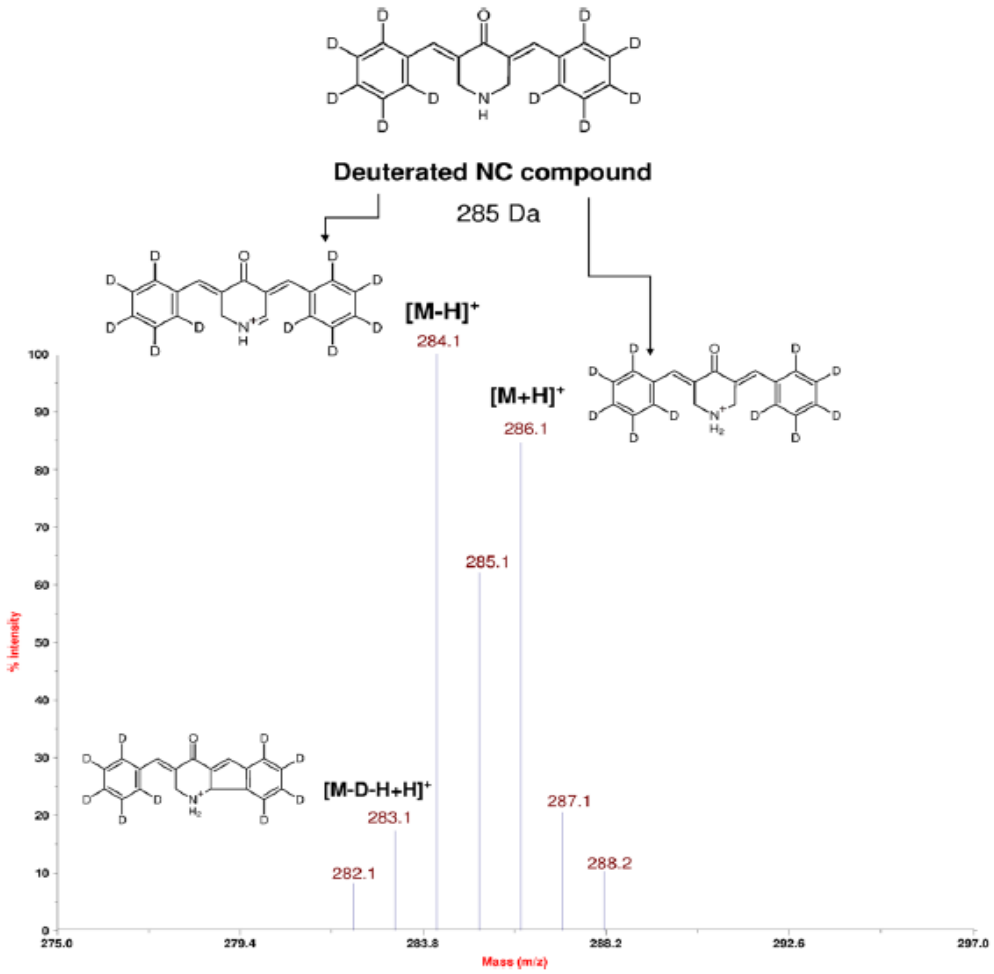

Figure 2.4. **LD-MS** spectrum of the deuterated NC compound showing two forms of ions $[M-H]^+$ and $[M+H]^+$ (*m/z* 284.1 and 286.1 respectively).

By excluding all the factors (i.e. matrix, solvent, laser intensity and analyzer type) that evidently did not significantly contribute to the formation of $[M-H]^+$ or $[M+H]^+$ ions, it was important to investigate direct photoionization as a possible factor of such unusual ionization behavior. Therefore, another ionization technique that depends on photoionization was used, namely APPI. During APPI-MS, the ionization behavior of the curcumin analogues was dopant-dependent. In the presence of dopant (5% acetone in ACN), curcumin analogues were mainly ionized as $[M+H]^+$ as in ESI and APCI (Figure 2.5A). However, in the absence of a dopant, the

ionization behavior was similar to that observed during MALDI-MS producing the two forms of ions $[M-H]^+$ and $[M+H]^+$ (Figure 2.5B). An explanation for such APPI-dopant related behavior is detailed later.

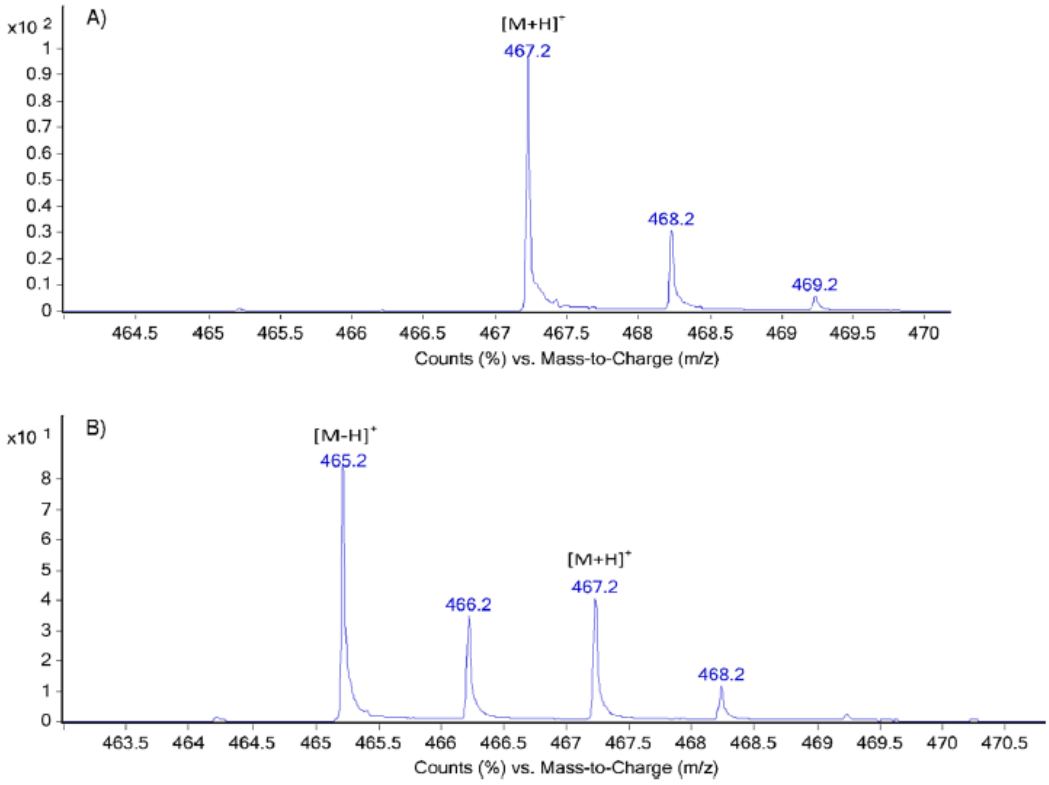

Figure 2.5: **APPI-MS** spectrum of curcumin analogue (NC2067) **using 5% acetone as a dopant** showing only $[M+H]^+$ ion **(A)**. **APPI-MS** spectrum of curcumin analogue (NC2067) **without a dopant** showing two forms of ions $[M-H]^+$ and $[M+H]^+$ **(B)**.

Proposed mechanisms for $[M-H]^+$ and $[M+H]^+$ ion formation

The above experiments showed that tested curcumin analogues were able to ionize in two forms as $[M-H]^+$ and $[M+H]^+$ even in the absence of any ionization enhancer such as a matrix or a solvent in MALDI; or a dopant in APPI. Such ionization behavior may indicate the involvement of direct photoionization as a possible mechanism for the formation of both ions.

The formation of the $[M+H]^+$ ion by direct photoionization is expected with compounds of low ionization energy that are able to absorb the photon energy [36-38], as follows:

$$M + h\nu \rightarrow M^{+\bullet} + e^- \qquad (1)$$

$$M^{+\bullet} + S \xrightarrow{H} [M+H]^+ + S[-H] \qquad (2)$$

The analyte molecule (M) absorbs the photon energy ($h\nu$) forming the radical cation ($M^{+\bullet}$) (eq 1), which in turn reacts with a solvent molecule (S) to form the $[M+H]^+$ ion by hydrogen atom transfer (eq 2). This mechanism could explain the $[M+H]^+$ formation during dopant free APPI-MS and LD-MS. However, in the absence of a solvent (S) (i.e. solvent free LD-MS), the most likely reaction could be a hydrogen atom transfer from another neutral analyte molecule instead of the solvent as illustrated in (eq 3).

$$M^{+\bullet} + M \xrightarrow{H} [M+H]^+ + M\,[-H] \qquad (3)$$

As illustrated in equations (1), (2) and (3), radicals play an important role in $[M+H]^+$ ion formation by direct photoionization. Radicals were significantly observed with all curcumin analogues, except one, during dopant free APPI-MS; whereas in MALDI-MS, only a few compounds showed such radicals. The absence of radicals during MALDI-MS could be explained by the fast conversion of these species into the more stable protonated form $[M+H]^+$ or that the laser photon energy was not sufficient to generate the radicals in the positive ion mode

and the excited state of the analyte (M^*) was formed instead of the radicals (eq 4) to be followed by proton transfer (eq 5).

$$M + h\nu \rightarrow M^* \qquad (4)$$

$$M^* + M \xrightarrow{H^+} [M\text{-}H]^- + [M+H]^+ \qquad (5)$$

The proposed mechanisms for the direct photoionization of the curcumin analogues during MALDI, LD, and solvent free LD-MS is similar to the principles that govern the ionization of a matrix [33]. The matrix is directly photoionized by the laser producing the matrix radicals or the excited state of the matrix molecules, which in turn ionize the analyte in the gas phase [33]. Therefore, we explored the curcumin analogues as matrix candidates. However the curcumin analogues remained able to self-ionize without the ionization of the other tested analytes (tetracycline and prednisolone were tested; data not shown).

In the above proposed mechanisms, we explained the $[M+H]^+$ formation of the tested curcumin analogues by direct photoionization during LD-MS, solvent free LD-MS, and dopant free-APPI-MS. However, the above explanations do not explain the unusual formation of $[M-H]^+$ and its possible mechanism. As mentioned, $[M-H]^+$ ions were previously reported with various ionization techniques including MALDI [18-22] and APPI [23]. Most publications focused on three mechanisms to explain the $[M-H]^+$ formation; i) loss of H_2 from the protonated analyte, ii) hydrogen atom transfer from the analyte radical cation or iii) hydride abstraction from the

neutral analyte molecule (Scheme 2.4). For the curcumin analogues, conversion of the $[M+H]^+$ ion into $[M-H]^+$ via H_2 loss (Scheme 2.4I) could be rationalized by the fact that $[M-H]^+$ ions are highly conjugated species and therefore are more stable in comparison to $[M+H]^+$ (Scheme 2.3). However, this proposed mechanism was not completely supported by our experimental results for three reasons; i) the conversion of $[M+H]^+$ into $[M-H]^+$ was not detected with all tested compounds during MALDI-MS as three compounds (NC2313, NC2314 and NC2315) were only detected as $[M-H]^+$ with no $[M+H]^+$ formation (Figure 2.6). ii) Such conversion was not detected with dopant mediated-APPI-MS experiment; however, it was detected with the same technique in the absence of a dopant, acknowledging that the $[M+H]^+$ ion was formed in both experiments. iii) The fragmentation spectra of $[M+H]^+$ ions of all tested curcumin analogues using ESI-MS/MS at various collision energies did not show $[M-H]^+$ as a possible product ion via H_2 loss (data not shown). Such observations do not support the proposed H_2 loss mechanism (Scheme 2.4I); however it cannot be completely excluded as multiple mechanisms may be occurring simultaneously.

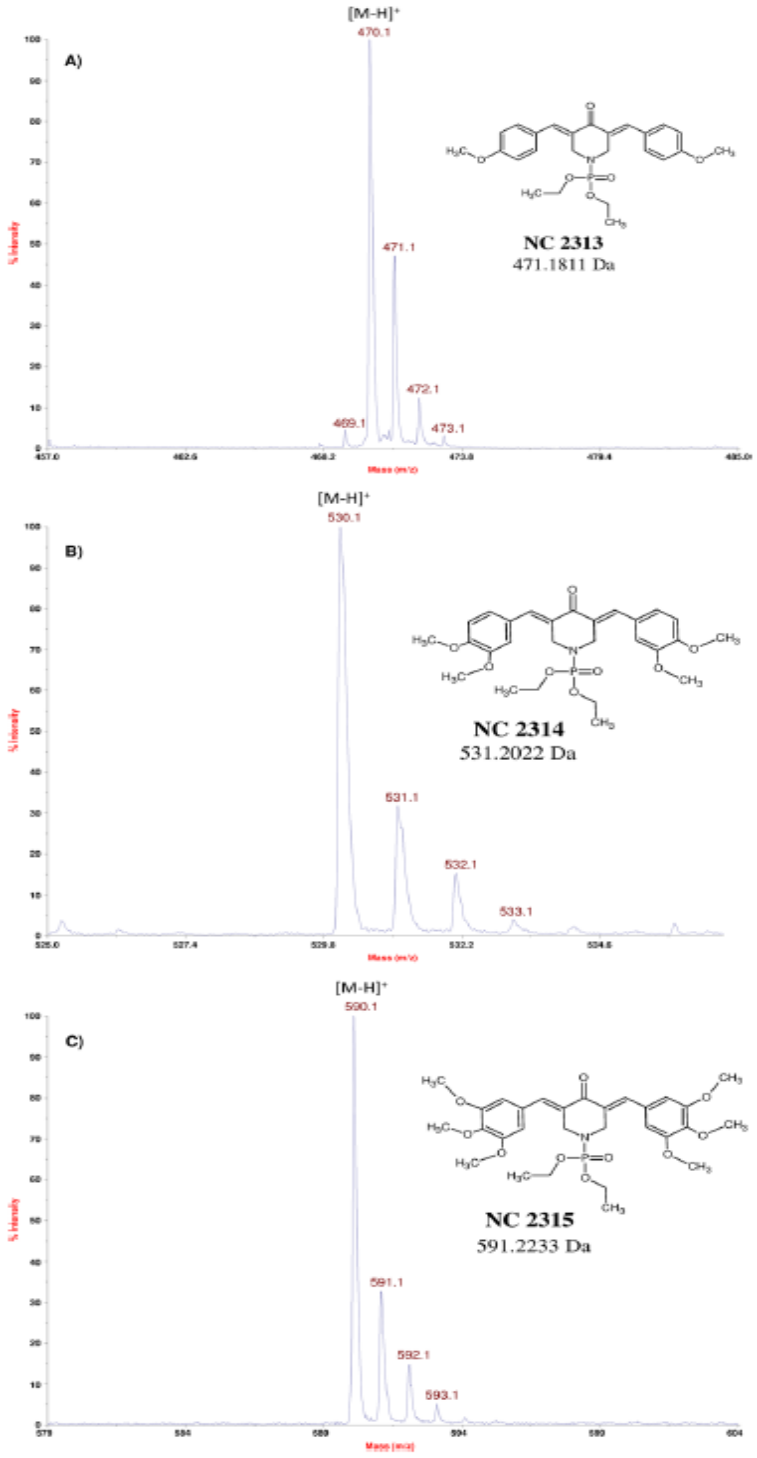

Figure 2.6. Formation of $[M-H]^+$ in absence of $[M+H]^+$ during the solvent free LD-MS analysis of NC 2313 **(A)**, NC2314 **(B)** & NC2315 **(C)**.

The disappearance of $[M+H]^+$ ions with the three curcumin analogues (NC2313, NC2314 and NC2315) was surprising as these three compounds were substituted with multiple methoxy groups (Scheme 2.2). The methoxy groups in the three tested compounds are electron donating groups which can theoretically increase the ability of the nitrogen to share its lone pairs of electrons, making them more susceptible to accept a proton; hence, forming the $[M+H]^+$ ions. Conventional chemistry may not be sufficient to explain the reason behind such observation as the rules governing gas-phase chemistry may be different than those governing bench-based chemical reactions. At this stage, we are not able to explain the reason behind such an observation.

Another proposed mechanism for $[M-H]^+$ ion formation includes hydrogen atom transfer from the analyte radical cation into other molecules such as oxygen [26] or nitrogen species [27] (Scheme 2.4II). This mechanism is similar to the previously proposed mechanism of $[M+H]^+$ formation by direct photoionization (eq 1, 2 & 3) except that the analyte radical cation ($M^{+\bullet}$) will lose a hydrogen atom instead of accepting one to form the $[M-H]^+$ ion. The hydrogen transfer mechanism may explain the change in the ionization behavior of the curcumin analogues during APPI-MS based on the use of a dopant as illustrated in Scheme 2.5. In the absence of a dopant, the analyte is directly photoionized forming both $[M+H]^+$ and $[M-H]^+$ by hydrogen transfer from/to the analyte radical cation ($M^{+\bullet}$) (Scheme 2.5A). However in the presence of a dopant, such as acetone or toluene that has low ionization energy in comparison to the tested analytes, the dopant will be more susceptible to photoionization forming the dopant radical cation ($D^{+\bullet}$), which acts as an intermediate between the photons and the analyte forming the $[M+H]^+$ ion by proton transfer (indirect photoionization) (Scheme 2.5B) [36]. This could explain the disappearance of $[M-H]^+$ ions during the dopant-APPI-MS.

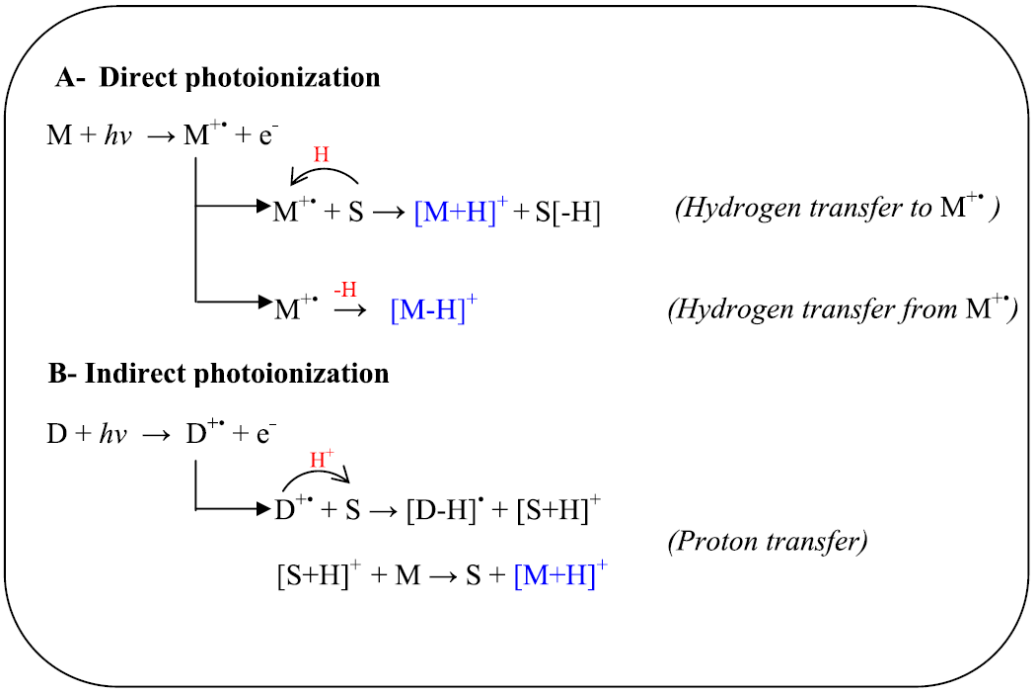

Scheme 2.5. Summary of direct **(A)** and indirect **(B)** photoionization during APPI-MS analysis of curcumin analysis (M = analyte, S = Solvent, D = Dopant and *hv* = Photon energy).

The last possible mechanism for $[M-H]^+$ formation is hydride abstraction (Scheme 2.4III) . In this mechanism, the curcumin analogue is probably photo-excited by the photon energy producing the excited molecular state (M^*), followed by a hydride abstraction by a protonated molecule (RH^+) such as a protonated product ion of analyte or solvent (eq 6).

$$M^* + RH^+ \xrightarrow{H^-} [M-H]^+ + RH_2 \qquad (6)$$

It was suggested that $[M-H]^+$ formation during MALDI-MS is a result of a reaction involving the analyte and the matrix resulting in the hydride abstraction [21]. However in our work, $[M-H]^+$ ions were formed even in the absence of a matrix (i.e., LD-MS) indicating that other ions could be involved in this mechanism.

The unique chemical structures of the curcumin analogues should also be considered to facilitate the hydride abstraction reaction, particularly when no matrix or solvent were used. The backbone structure of curcumin analogues is based on the 3,5-bis(benzylidene)-4-piperidyl group (Scheme 2.1), which shows active sites that are able to perform a redox reaction with another curcumin analogue via hydride abstraction. Scheme 2.6 shows how hydrogen abstraction could occur between two curcumin analogues and the corresponding formed ions including the $[M-H]^+$ ion.

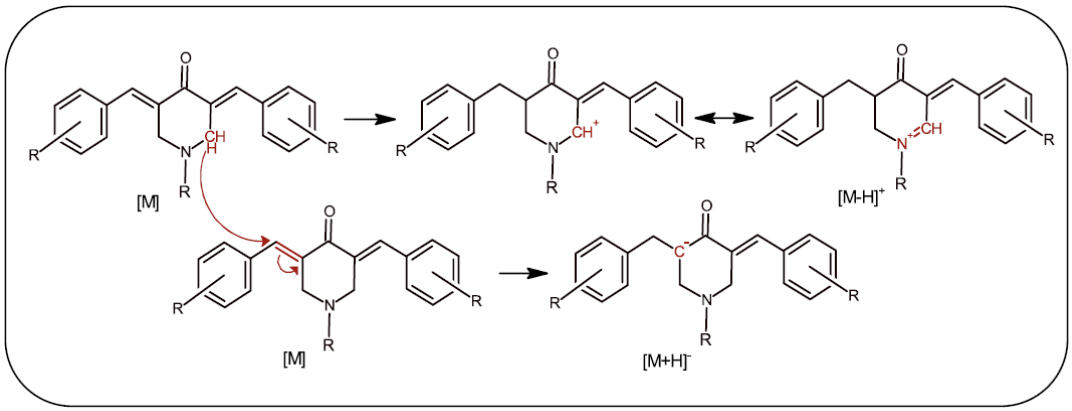

Scheme 2.6. Formation of $[M-H]^+$ by hydrogen abstraction between two curcumin analogues.

CONCLUSION

Curcumin analogues that belong to the 3,5-bis(benzylidene)-4-piperidone structural family showed diverse ionization behaviors in the positive ion mode of various MS-ionization techniques. The four tested categories of curcumin analogues (phosphoramidates, secondary amines, amides and mixed amines/amides) showed an unusual significant peak of $[M-H]^+$ with MALDI and dopant free-APPI-MS in contrast to ESI, APCI, and dopant mediated APPI that showed no, or barely detected, a $[M-H]^+$ peak. Interestingly, the tested compounds were able to form both $[M-H]^+$ and $[M+H]^+$ ions even in the absence of a matrix and solvent during solvent

free LD-MS analysis. Evidence indicated that photon energy during MALDI, LD, solvent free LD and dopant free-APPI-MS was the trigger for the ionization of the tested curcumin analogues. However, several publications reported the $[M-H]^+$ formation with other compounds using non-photoionization based techniques such as CI, APCI and ESI, indicating that the trigger of such ion formation is dependent on the structural features of the analyte .

In this study, the $[M-H]^+$ structure of the tested compounds was established by analyzing a specially designed deuterated compound to confirm the double bond formation between the nitrogen atom and the adjacent carbon atom. The three main proposed mechanisms for the $[M-H]^+$ formation were investigated showing opposing observations to the H_2 loss mechanism (i) that states the $[M-H]^+$ is formed via the H_2 loss from $[M+H]^+$ species. However the other two proposed mechanisms namely the hydrogen transfer from the analyte radical cation (ii) and hydride abstraction from the neutral analyte molecule (iii) were still applicable.

The ionization behavior of the curcumin analogues and structurally-related compounds should be taken into account during the development of MS-based qualitative or quantitative analytical methods. In addition, studying the ionization behavior of curcumin analogues with various ionization techniques and under different conditions improves our knowledge on ion formation mechanisms during MS-analysis including the unexpected formation of $[M-H]^+$ species.

REFERENCES

1. Fenn JB, Mann M, Meng CK, Wong SF, Whitehouse CM: Electrospray ionization for mass spectrometry of large biomolecules. Science 1989, 246:64-71.

2. Mann M, Meng CK, Fenn JB: Interpreting mass spectra of multiply charged ions. Analytical Chemistry 1989, 61:1702-1708.

3. Carroll D, Dzidic I, Stillwell R, Haegele K, Horning E: Atmospheric pressure ionization mass spectrometry. Corona discharge ion source for use in a liquid chromatograph-mass spectrometer-computer analytical system. Analytical Chemistry 1975, 47:2369-2373.

4. Robb DB, Covey TR, Bruins AP: Atmospheric pressure photoionization: an ionization method for liquid chromatography-mass spectrometry. Analytical Chemistry 2000, 72:3653-3659.

5. Karas M, Bachmann D, Bahr U, Hillenkamp F: Matrix-assisted ultraviolet laser desorption of non-volatile compounds. International Journal of Mass Spectrometry and Ion Processes 1987, 78:53-68.

6. Karas M, Hillenkamp F: Laser desorption ionization of proteins with molecular masses exceeding 10,000 daltons. Analytical chemistry 1988, 60:2299-2301.

7. Domon B, Aebersold R: Mass spectrometry and protein analysis. Science's STKE 2006, 312:212.

8. El-Aneed A, Cohen A, Banoub J: Mass spectrometry, review of the basics: Electrospray, MALDI, and commonly used mass analyzers. Applied Spectroscopy Reviews 2009, 44:210-230.

9. Han X, Aslanian A, Yates III JR: Mass spectrometry for proteomics. Current opinion in chemical biology 2008, 12:483-490.

10. Hoffmann E, Stroobant V: Mass spectrometry: Principles and applications. third edn. The Atrium, Southern Gate, Chichester, West Sussex, England J. Wiley; 2007.

11. Das U, Sharma RK, Dimmock JR: 1, 5-Diaryl-3-oxo-1, 4-pentadienes: A case for antineoplastics with multiple targets. Current Medicinal Chemistry 2009, 16:2001.

12. Das S, Das U, Selvakumar P, Sharma RK, Balzarini J, De Clercq E, Molnár J, Serly J, Baráth Z, Schatte G: 3, 5-Bis (benzylidene)-4-oxo-1-phosphonopiperidines and related diethyl esters: Potent cytotoxins with multi-drug-resistance reverting properties. ChemMedChem 2009, 4:1831-1840.

13. Das U, Alcorn J, Shrivastav A, Sharma RK, De Clercq E, Balzarini J, Dimmock JR: Design, synthesis and cytotoxic properties of novel 1-[4-(2-alkylaminoethoxy) phenylcarbonyl]-3, 5-bis (arylidene)-4-piperidones and related compounds. European Journal of Medicinal Chemistry 2007, 42:71-80.

14. Munson MS, Field F-H: Chemical ionization mass spectrometry. I. General introduction. Journal of the American Chemical Society 1966, 88:2621-2630.

15. Field FH: Chemical ionization mass spectrometry. Accounts of Chemical Research 1968, 1:42-49.

16. Orelli LR, García MB, Perillo IA, Tonidandel L, Traldi P: A comparison of the electron ionization and electrospray behaviour of some N, N′-disubstituted hexahydropyrimidines. Rapid Communications in Mass Spectrometry 2006, 20:823-828.

17. Chai Y, Sun H, Wan J, Pan Y, Sun C: Hydride abstraction in positive-ion electrospray interface: oxidation of 1, 4-dihydropyridines in electrospray ionization mass spectrometry. Analyst 2011, 136:4667-4669.

18. Cox FJ, Johnston MV, Dasgupta A: Characterization and relative ionization efficiencies of end-functionalized polystyrenes by matrix-assisted laser desorption/ionization mass spectrometry. Journal of the American Society for Mass Spectrometry 2003, 14:648-657.

19. Lou X, Spiering AJH, de Waal BFM, van Dongen JLJ, Vekemans JAJM, Meijer EW: Dehydrogenation of tertiary amines in matrix-assisted laser desorption/ionization time-of-flight mass spectrometry. Journal of Mass Spectrometry 2008, 43:1110-1122.

20. Kang C, Zhou Y, Du Z, Bian Z, Wang J, Qiu X, Gao L, Sun Y: Dehydrogenation and dehalogenation of amines in MALDI-TOF MS investigated by isotopic labeling. Journal of Mass Spectrometry 2013, 48:1318-1324.

21. Yang H-J, Lee A, Lee M-K, Kim W, Kim J: Detection of small neutral carbohydrates using various supporting materials in laser desorption/ionization mass spectrometry. Bulletin of the Korean Chemical Society 2010, 31:35.

22. Nuutinen JM, Purmonen M, Ratilainen J, Rissanen K, Vainiotalo P: Mass spectrometric studies on pyridine-piperazine-containing ligands and their complexes with transition metals formed in solution. Rapid Communications in Mass Spectrometry 2001, 15:1374-1381.

23. Kauppila T, Nikkola T, Ketola R, Kostiainen R: Atmospheric pressure photoionization-mass spectrometry and atmospheric pressure chemical ionization-mass spectrometry of neurotransmitters. Journal of Mass Spectrometry 2006, 41:781-789.

24. Suni NM, Aalto H, Kauppila TJ, Kotiaho T, Kostiainen R: Analysis of lipids with desorption atmospheric pressure photoionization-mass spectrometry (DAPPI-MS) and desorption electrospray ionization-mass spectrometry (DESI-MS). Journal of Mass Spectrometry 2012, 47:611-619.

25. Cody RB: Observation of molecular ions and analysis of nonpolar compounds with the direct analysis in real time ion source. Analytical Chemistry 2008, 81:1101-1107.

26. Marotta E, Paradisi C: A mass spectrometry study of alkanes in air plasma at atmospheric pressure. Journal of the American Society for Mass Spectrometry 2009, 20:697-707.

27. Hourani N, Kuhnert N: Development of a novel direct-infusion atmospheric pressure chemical ionization mass spectrometry method for the analysis of heavy hydrocarbons in light shredder waste. Analytical Methods 2012, 4:730-735.

28. Gao J, Owen BC, Borton II DJ, Jin Z, Kenttämaa HI: HPLC/APCI mass spectrometry of saturated and unsaturated hydrocarbons by using hydrocarbon solvents as the APCI reagent and HPLC mobile phase. Journal of The American Society for Mass Spectrometry 2012, 23:816-822.

29. Calba P, Muller J, Inouye M: H-atom transfer following analyte photoionization in matrix-assisted laser desorption/ionization processes. Rapid Communications in Mass Spectrometry 1998, 12:1727-1731.

30. Calba P, Muller J, Hachimi A, Lareginie P, Guglielmetti R: Spirooxazines as a molecular probe for the study of matrix-assisted laser desorption/ionization processes. Part I: Study of the interaction effect between the molecular probe and the matrix. Rapid Communications in Mass Spectrometry 1997, 11:1602-1611.

31. Karas M, Glückmann M, Schäfer J: Ionization in matrix-assisted laser desorption/ionization: singly charged molecular ions are the lucky survivors. Journal of Mass Spectrometry 2000, 35:1-12.

32. Jaskolla TW, Karas M: Compelling evidence for lucky survivor and gas phase protonation: the unified MALDI analyte protonation mechanism. Journal of the American Society for Mass Spectrometry 2011, 22:976-988.

33. Zenobi R, Knochenmuss R: Ion formation in MALDI mass spectrometry. Mass Spectrometry Reviews 1998, 17:337-366.

34. Knochenmuss R, Zenobi R: MALDI ionization: the role of in-plume processes. Chemical Reviews-Columbus 2003, 103:441-452.

35. Knochenmuss R: Ion formation mechanisms in UV-MALDI. Analyst 2006, 131:966-986.

36. Syage JA: Mechanism of $[M+H]^+$ formation in photoionization mass spectrometry. Journal of the American Society for Mass Spectrometry 2004, 15:1521-1533.

37. Fesenko T, Laguta I, Kuzema P, Stavinskaya O: Laser desorption/ionization time-of-flight mass spectrometric analysis of some synthetic flavonoids and their complexes with Zn and Fe. Journal of Materials Science (Lithuanian version) 2010, 16:272-277.

38. Kamel A, Jeanville P, Colizza K: Mechanism of $[M+H]^+$ formation in atmospheric pressure photoionization mass spectrometry: Identification of propionitrile in acetonitrile with high mass accuracy measurement and tandem mass spectrometry and evidence for its involvement in the protonation phenomenon. Journal of the American Society for Mass Spectrometry 2008, 19:1579-1589.

CHAPTER3
ESTABLISHMENT OF TANDEM MASS SPECTROMETRIC FINGERPRINT OF NOVEL ANTINEOPLASTIC CURCUMIN ANALOGUES USING ELECTROSPRAY IONIZATION

H.Awad[1], U. Das[1], J. Dimmock[1], A. El-Aneed[1*]

In this work, I investigated, under the supervision of Dr. El-Aneed, the CID-MS/MS fragmentation behavior of thirteen curcumin analogues using tandem ESI-Qq-LIT-MS. I established the fragmentation pattern of each compound, which was confirmed by the MS^3 experiments and neutral loss scans. The molecular structures of the tested compounds were confirmed and the diagnostic product ions were identified to be used for qualitative and quantitative analysis of these compounds. Similar fragmentation behavior was observed among the thirteen curcumin analogues that mainly centered on the cleavage of the piperidone ring of the 3,5-bis(benzylidene)-4- piperidone allowing for establishing a general MS\MS pattern for these compounds. I performed all the MS experiments in this work. I also drafted the manuscript with Dr. El-Aneed who revised the various versions of the paper. Drs. Das and Dimmock synthesized the tested curcumin analogues based on Dr. El-Aneed's request.

Establishment of tandem mass spectrometric fingerprint of novel antineoplastic curcumin analogues using electrospray ionization

H.Awad[1], U. Das[1], J. Dimmock[1], A. El-Aneed[1*]

[1.] College of Pharmacy and Nutrition, University of Saskatchewan, Saskatoon, SK, S7N 5E5, Canada.

* Corresponding Author:

E-mail Address: anas.el-aneed@usask.ca

Telephone: +1-306-966-2013

INTRODUCTION

In the last few decades, the anticancer drug market showed significant growth due to the constant and crucial need for more selective, potent and, safe anticancer agents. Natural products represent one of the valuable sources for the development of novel anticancer agents [1, 2]. Biologically active compounds can either be extracted from its natural source or designed as structural analogues for naturally existing compounds [1, 2]. For example, curcumin is a natural component of the spice turmeric that showed various biological activities including anticancer, anti-inflammatory, antioxidant, and anti-microbial effects [3, 4]. The poor bioavailability of curcumin has limited its efficiency as anticancer agent [5]. Consequently, curcumin analogues were designed by structural modification of the curcumin molecule to enhance bioavailability and potency [6, 7].

A number of curcumin analogues showed promising anticancer properties towards different cancer cell lines including melanoma and colon and pancreatic cancer cells [8-11]. The evaluated curcumin analogues in this study are 3,5-bis(benzylidene)-4-piperidone compounds, containing the 1,5-diaryl-3-oxo-1,4-pentadienyl pharmacophore (Scheme 3.1) that acts as thiol alkylator and responsible for the selective antitumor effect of these compounds [11-14]. For more effective antitumor activity, a series of novel curcumin analogues were designed with various substituents on the aryl groups and the piperidyl nitrogen atom of the 3,5-bis(benzylidene)-4-piperidone (Scheme 3.2). The aryl substituents were added to change the steric and hydrophobic properties of curcumin analogues in order to enhance their *in-vivo* use [14]. On the other hand, the N-substituents were introduced to enhance the drug penetration to target cells by protecting the piperidyl nitrogen atom from ionization at biological pH as the ionized molecules cannot

penetrate the cell membrane [12]. In addition, N-substituents represent additional binding sites to the target cells that may enhance the cytotoxicity of the drug candidate [12, 13].

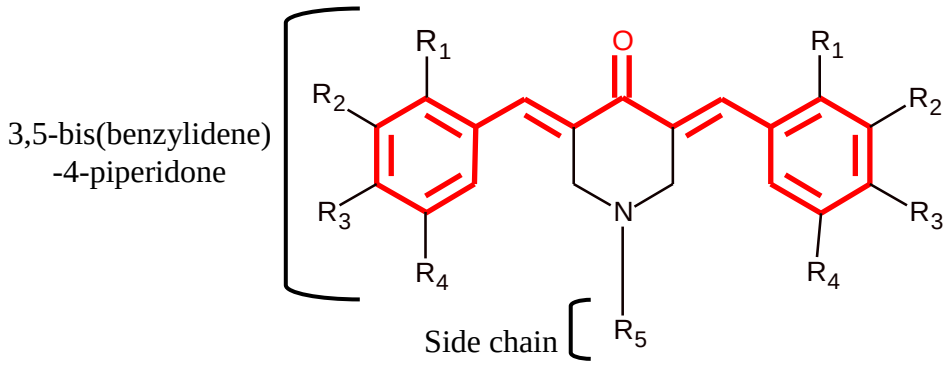

Scheme 3.1. Schematic representation of the 3,5-bis(benzylidene)-4-piperidone with the N-substituent as side chain (1,5-diaryl-3-oxo-1,4-pentadienyl pharmacophore highlighted in bold red)

Phosphoramidates

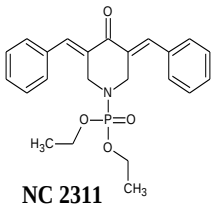

NC 2311

411.1599 Da

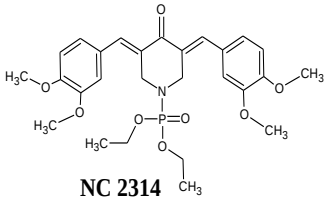

NC 2314

531.2022 Da

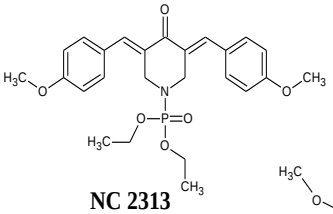

NC 2313

471.1811 Da

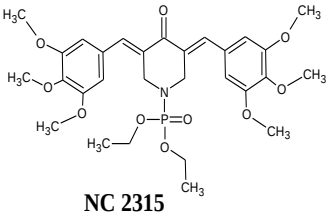

NC 2315

591.2233 Da

Secondary Amines

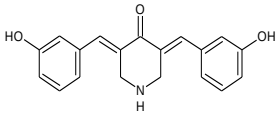

NC 2128

307.1208 Da

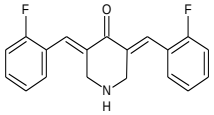

EF-24

311.1122 Da

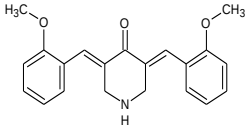

NC 2453

335.1521 Da

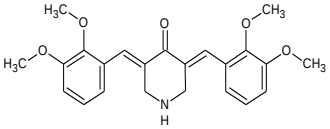

NC 2454

395.1733 Da

Mixed Amine and Amide

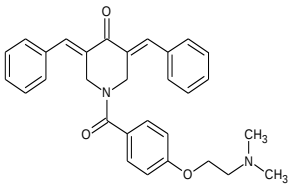

NC 2067

466.2256 Da

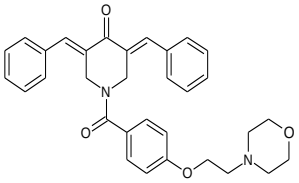

NC 2081

508.2362Da

Amides

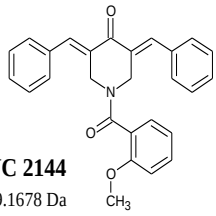

NC 2144

409.1678 Da

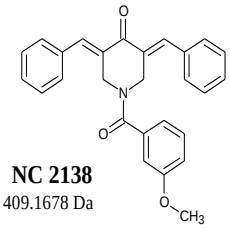

NC 2138

409.1678 Da

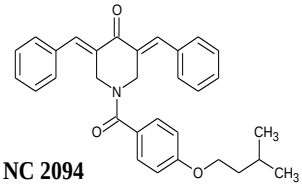

NC 2094

465.2304 Da

Scheme 3.2. Structures and monoisotopic masses of the novel antineoplastic curcumin analogues categorized by the N-substituent into four structural families: phosphoramidates, secondary amines, mixed amines/amides and amides.

To evaluate the safety and efficiency of the newly designed compounds during preclinical and clinical studies, efficient analytical methods are required. Mass spectrometry (MS) is widely used in the drug discovery and development process based on its sensitivity, selectivity and high throughput capability [15, 16]. MS structurally characterizes the target analytes via accurate mass measurements (single stage MS analysis) as well as via collision-induced dissociation tandem mass spectrometric (CID-MS/MS) analysis [17]. The establishment of CID-MS/MS fragmentation patterns for structurally-related compounds allow for the confirmation of their molecular structure and the identification of diagnostic product ions to be used subsequently for qualitative and quantitative analysis. For example, our research group illustrated a universal MS/MS dissociation behavior of a series of structurally-related cationic surfactants used as drug delivery agents [18, 19]. The data was subsequently used to develop targeted MS-based quantification methods that were employed within cellular lysate to assess the uptake and removal of these cationic lipids [20, 21]. In fact, the development of a general MS/MS dissociation behavior will allow for the prediction of the fragmentation patterns of newly synthesized compounds with structural similarities.

Recently, we investigated the ionization behavior of 13 curcumin analogues (Scheme 3.2) illustrating a unique ionization mechanism that resulted in the formation of what we proposed to be positively charged $[M-H]^+$ ions during single stage matrix assisted laser desorption ionization-MS (MALDI-MS) and atmospheric pressure photo ionization (APPI)-MS analysis [22]. Conversely, only the expected $[M+H]^+$ species were observed during electrospray (ESI) and atmospheric pressure chemical ionization (APCI) [22]. In this subsequent study, we are evaluating the CID-ESI-MS/MS fragmentation behavior of the $[M+H]^+$ species of curcumin analogues (Scheme 3.2). Due to the wide array of structures for currently investigated curcumin

analogues in the literature [23-26], our main aim is to identify common CID-MS/MS fragmentation patterns among diverse structures. We identified for the first time a general MS/MS dissociation behavior that will allow for the analysis of other structurally-related compounds. In addition, our data will facilitate future studies, concerning metabolite identification as well as the development of multiple reaction monitoring (MRM) quantification methods.

EXPERIMENTAL

Materials

Curcumin analogues were synthesized by using previously reported synthetic methods [13, 14]. The compounds are categorized based on the nature of the N-substituent as phosphoramidates, secondary amines, mixed amines/amides and, amides (Scheme 3.2).

Mass spectrometric analysis

Single-stage MS analysis

Stock solutions of each curcumin analogue were prepared to a concentration of 1mg/mL in 100% acetonitrile (ACN). Each sample was further diluted by 500–1000× prior to single stage and tandem MS analysis. Curcumin analogues were analyzed using an Applied Biosystems API QSTAR® XL instrument, which is a quadrupole time-of-flight hybrid mass spectrometer (Qq-TOF-MS) equipped with ESI source.

Samples were injected into the Qq-TOF-MS at flow rate of 10 µL/min using a Harvard Syringe Pump. The system was operated in the positive ion mode with an ionspray voltage of

5000 V, a declustering potential of 40 V and, a focusing potential of 120 V. Exact mass measurements of the curcumin analogues were performed using the Qq-TOF-MS with a two point external calibration. External calibration was performed prior to analyzing the curcumin analogues. Two singly charged calibration standards were used; Cesium iodide (CsI, purity 99.9%, $[M]^+$ *m/z* 132.9055, CAS Number 7789-17-5, Sigma-Aldrich, Oakville, ON, Canada) and Sex pheromone inhibitor iPD1 ($C_{39}H_{72}N_8O_{11}$, purity >94%, $[M+H]^+$ *m/z* 829.5320, CAS Number 120116-56-5, Bachem Bioscience Inc., PA, USA).

Tandem MS analysis

Tandem mass spectrometric analysis of curcumin analogues was conducted on the AB SCIEX 4000 QTRAP® instrument, which is a hybrid triple quadrupole–linear ion trap mass spectrometer (Qq-LIT-MS). The MS/MS, multi-stage-MS (MS^3), enhanced product ion scan and, neutral loss scan analysis were performed for each sample to confirm the precursor ion's structure and its fragmentation pathway. MS/MS was also acquired using the QSTAR® system (Qq-TOF-MS); however, the data was not as informative as minor fragmentation was observed in the QSTAR in comparison to the rich MS/MS data obtained by the QTRAP. This is due to the fact that the Qq-LIT-MS allows for the accumulation of ions in the linear ion trap when applying the "enhanced" product ion scan. Such capabilities are not possible with the Qq-TOF-MS instrument.

In both instruments, collision induced dissociation (CID) was conducted in the positive ion mode with an ionspray voltage of 5500 V, a declustering potential of 40-70 V and, a collision energy (CE) of 20-35 V using nitrogen as a collision gas. Parameters of the MS/MS analysis

were optimized to ensure the formation of the product ions while maintaining the presence of the precursor ion. The exact collision energy used for each analyte is shown in Appendix B.

RESULTS AND DISCUSSION

Single-stage MS analysis

In positive ion full scan ESI-MS analysis, curcumin analogues showed an abundant protonated ion, $[M+H]^+$. The exact masses of curcumin analogues were measured using the ESI-Qq-TOF-MS, showing mass accuracies of less than 6 ppm mass error using the two point-external calibration (Table 3.1). This confirms the molecular structure of tested compounds, particularly when combined with MS/MS analysis, detailed below. The ability to achieve such high mass accuracy was attributed to applying external calibration of the instrument directly prior to analyzing tested compounds. In fact, such results were comparable to recent structural work in which internal calibration was employed showing mass accuracy of less than 5 ppm when analyzing cationic surfactants using the QSTAR system [19].

Compound	Molecular formula	Mono-isotopic mass	$[M+H]^+$ *m/z*, theoretical	$[M+H]^+$ *m/z*, observed	Mass accuracy (ppm)
NC2311	$C_{23}H_{26}NO_4P$	411.1599	412.167223	412.1679	1.64
NC2313	$C_{25}H_{30}NO_6P$	471.1811	472.188353	472.1894	2.22
NC2314	$C_{27}H_{34}NO_8P$	531.2022	532.209482	532.2084	2.03
NC2315	$C_{29}H_{38}NO_{10}P$	591.2233	592.230612	592.234	5.72
NC2128	$C_{19}H_{17}NO_3$	307.1208	308.12812	308.1278	1.04
EF-24	$C_{19}H_{15}F_2NO$	311.1122	312.119447	312.1203	2.73
NC2453	$C_{21}H_{21}NO_3$	335.1521	336.15942	336.1581	3.93
NC2454	$C_{23}H_{25}NO_5$	395.1733	396.18055	396.1798	1.89
NC2067	$C_{30}H_{30}N_2O_3$	466.2256	467.23292	467.2336	1.46
NC2081	$C_{32}H_{32}N_2O_4$	508.2362	509.243484	509.2441	1.21
NC2144	$C_{27}H_{23}NO_3$	409.1678	410.17507	410.1756	1.29
NC2138	$C_{27}H_{23}NO_3$	409.1678	410.17507	410.1752	0.32
NC2094	$C_{31}H_{31}NO_3$	465.2304	466.237671	466.2383	1.35

Table 3.1. The mass accuracy of $[M+H]^+$ ions of the tested curcumin analogues using ESI-Qq-TOF-MS

Tandem MS analysis

The fragmentation behavior of curcumin analogues was evaluated using low-energy collision induced dissociation (CID) of ESI-Qq-LIT-MS in the positive ion mode. All tested curcumin analogues have the same backbone structure of 3,5-bis(benzylidene)-4-piperidone (Scheme 3.1) that showed similar fragmentation behavior with bond cleavage occurring at the piperidone ring during the MS/MS analysis. The differences among curcumin analogue structures was based on the difference in the substituents of the aryl groups and the piperidyl nitrogen atom of the 3,5-

bis(benzylidene)-4-piperidone (Scheme 3.2). Such differences resulted in specific product ions during MS/MS analysis that could be used as diagnostic product ions for the qualitative and quantitative MS/MS-analysis of these compounds. The side chain of curcumin analogues (N-substituents) was also dissociated during the low energy CID-MS/MS analysis. However, the side chain fragmentation did not follow a general pattern due to the dramatic differences in their chemical structures.

The detailed general fragmentation behavior of curcumin analogues was discussed in two sections; 3,5-bis(benzylidene)-4-piperidone fragmentation and side chain fragmentation to highlight the common MS/MS pathways among various curcumin analogues. It should be emphasized that we are identifying common dissociation behavior among various structures of curcumin analogues that can allow for the analysis of other compounds.

3,5-bis(benzylidene)-4-piperidone fragmentation

NC 2067 will be used as a representative model for curcumin analogue MS/MS analysis as this compound showed the highest number of common product ions generated via the fragmentation of the 3,5-bis(benzylidene)-4-piperidone moiety. NC2067 showed 11 product ions (F1-11) produced during the ESI-Qq-LIT-MS/MS analysis (Figure 3.1). The fragmentation centered on the piperidone ring (highlighted in bold blue in Figure 3.1A) of the 3,5-bis(benzylidene)-4-piperidone moiety and each detected product ion was formed by breaking specific bonds of that ring as illustrated in the structure within Table 3.2. Table 3.2 shows the 12 common product ions detected during the MS/MS analysis of the 13 curcumin analogues (NC2067 showed 11 out of the 12 identified common product ions).

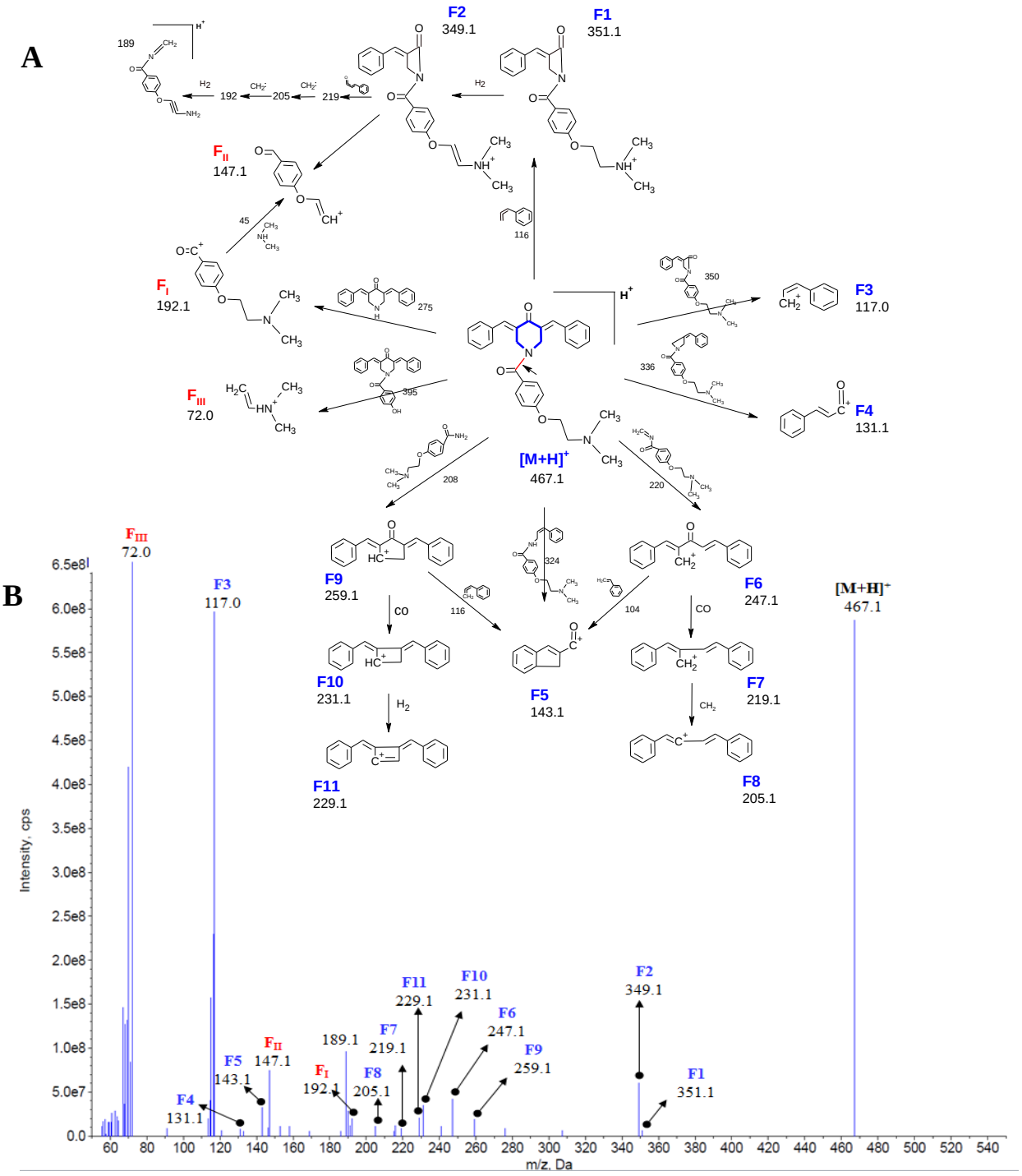

Figure 3.1. The proposed fragmentation pattern (A) and the ESI-Qq-LIT-MS/MS spectrum (B) of NC2067 (the piperidone ring of NC2067 is highlighted in bold blue and the side chain bond is identified with an arrow)

Precursor ion $[M+H]^+$	Product ions	Broken Bonds
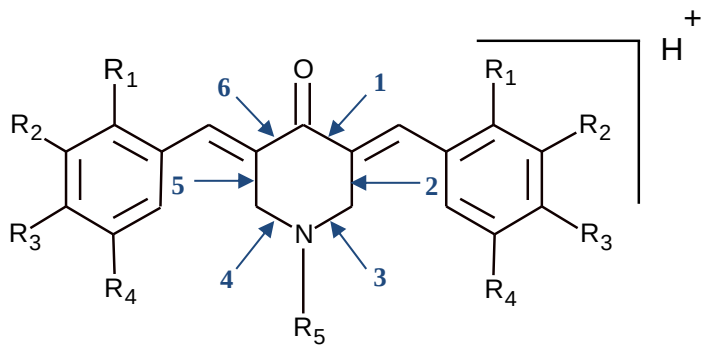	F1	1 & 3
	F2	1 & 3
	F3	1 & 3
	F4	1 & 5
	F5	1 & 4
	F6	2 & 4
	F7	1, 2, 4 & 6
	F8	1, 2, 5 & 6
	F9	3 & 4
	F10	1, 3, 4 & 6
	F11	1, 3, 4 & 6
	F12	1 & 2

Table 3.2. The fragmentation sites in the 3,5-bis(benzylidene)-4-piperidone and the corresponding product ions during the ESI-MS/MS of the tested curcumin analogues.

Initial dissociation of the piperidone ring occurs via a cleavage of the bonds (1 and 3). Two mechanisms can occur at the same time producing either the minor product ion observed at 351.1 (F1) or the highly abundant product ion observed at 117 (F3). The proposed two mechanisms are shown in Scheme 3.3 in which the charge is presumably localized on the nitrogen atom. The first mechanism involves the neutral loss of C_9H_8 (116 Da) (Scheme 3.3A). This occurs via electron movements resulting in the species observed at 351.1 where the positive charge is relocalized to the carbon of the carbonyl functional group while a neutral species is eliminated. However, F1 ion is quickly converted into the more abundant highly conjugated stable diagnostic product ion at *m/z* 349.1 (F2) by losing a hydrogen molecule (Figure 3.1A).

The second mechanism involving cleavages of bonds 1 and 3 of the piperidone ring (Scheme 3.3B) involves the production of the product ion F3 observed at *m/z* 117.0. In this mechanism, hydrogen rearrangement occurs; however, charge localization is directed towards the smaller species while the relatively large 350 Da species is eliminated as a cyclized neutral moiety. The F3 ion is one of the most abundant product ions that has been detected with all curcumin analogues (Table 3.3). This could be due to the stable conjugated structure of this small ion that enables it to resist additional fragmentation. The mechanism shown in Scheme 3.3 that includes rearrangement, electron movements and cyclization is the driving principle for the formation of the majority of the piperidone-driven fragmentation.

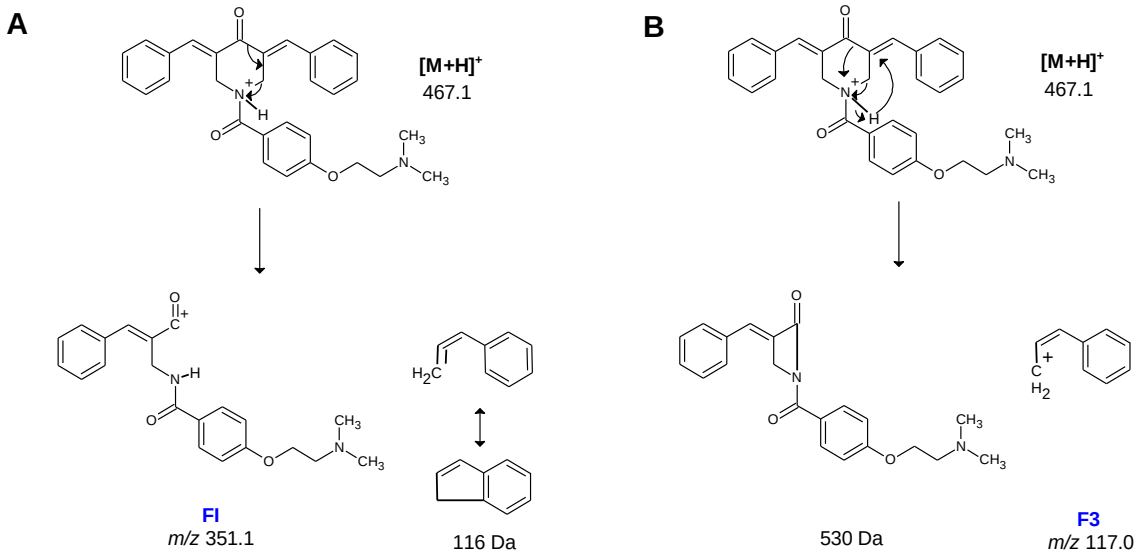

Scheme 3.3. The two proposed mechanisms for the formation of the product ions F1 at *m/z* 351.1 (A) and F3 at *m/z* 117.0 (B).

The 3,5-bis(benzylidene)-4-piperidone fragmentation													
Compound	**Precursor ion P = $[M+H]^+$**	**F1 ($P-C_5H_8$)**	**F2 ($F1-H_2$)**	**F3 ($P-N^1$)**	**F4 ($P-N^2$)**	**F5 ($P-N^3$)**	**F6 ($P-N^4$)**	**F7 (F6-CO)**	**F8 ($F7-CH_2$)**	**F9 ($P-N^5$)**	**F10 (F9-CO)**	**F11 ($F10-H_2$)**	**F12 ($P-N^6$)**
2311	412.2	296	-	117	131	143	247	219	205	259	231	229	308
2313	472.2	-	-	147	161	-	307	-	-	-	-	-	-
2314	532.2	-	-	177	191	203	-	-	-	379	-	-	368
2315	592.2	-	-	207	221	233	427	-	-	439	-	409	398
2067	467.2	351	349	117	131	143	247	219	205	259	231	229	-
2081	509.2	-	391	117	-	143	247	219	205	259	231	229	-
2144	410.2	294	-	117	131	143	247	219	205	259	231	229	-
2138	410.2	-	-	117	131	143	247	219	205	259	231	229	306
2094	466.2	-	-	117	-	-	247	219	205	259	231	229	-
2453	336.2	-	-	147	161	173	-	-	-	-	-	-	-
2454	396.2	-	-	177	191	203	-	-	-	-	-	-	-
EF24	312.2	-	-	135	149	161	283	-	-	-	-	-	-
2128	308.2	-	174	133	147	159	-	-	-	-	-	-	-

$N^1 = C_{10}H_4NO + R_1+R_2+R_3+R_4+R_5$ $N^3 = C_9H_6N + R_1+R_2+R_3+R_4+R_5$ $N^5 = NH_2+R_5$
$N^2 = C_{10}H_6N + R_1+R_2+R_3+R_4+R_5$ $N^4 = CH_2N+R_5$ $N^6 = C_8H_4 + R_1+R_2+R_3+R_4$

Table 3.3. The product ions of the 3,5-bis(benzylidene)-4-piperidone moiety during the ESI-MS/MS of the tested curcumin analogues.

In addition to F3, two other product ions that were observed among most compounds are ions observed at *m/z* 131.1 (F4) and 143.1 (F5) by breaking the piperidone bonds at (1 and 5) and (1 and 4) respectively (Tables 3.2 and 3.3). Similar to F3, both F4 and F5 are small ions with high conjugation within their structures (Figure 3.1A).

The product ion F6 observed at *m/z* 247.1 is formed through cleavage of bonds (2 and 4), followed by a sequential elimination of a carbonyl group CO and methylene CH_2 resulting in the formation of ions, F7 at *m/z* 219.1 and F8 at *m/z* 205.1. Another sequential fragmentation that was observed in eight curcumin analogues includes the formation of the ion designated F9 observed at *m/z* 259, which in the case of NC2067 was formed by breaking bonds (3 and 4) and cyclization (Figure 3.1A & Tables 3.2 and 3.3). F9 ion usually loses a carbonyl group to form another product ion (F10) at *m/z* 231.1 that in turns losses a hydrogen molecule to generate F11 at *m/z* 229.1. As it can be seen among the majority of observed product ions, the dissociation behavior is driven by the formation of highly conjugated structures during the CID-MS/MS analysis of curcumin analogues.

The same fragmentation behavior of the 3,5-bis(benzylidene)-4-piperidone moiety of NC2067 was detected with other curcumin analogues (Table 3.3). This behavior enables the establishment of a general fragmentation pattern for these compounds based on the CID-MS/MS of the 3,5-bis(benzylidene)-4-piperidone moiety as shown in Table 3.3. However, the number of detected product ions varied between curcumin analogues based on their structural differences. It can be speculated that the difference in the substituents of the aryl groups and the piperidyl nitrogen atom between curcumin analogues affect the stability of the piperidone ring and make it more or less susceptible to dissociation. For example, product ion designated as (F12) was detected with few curcumin analogues (not with NC2067) by breaking the piperidone ring bonds

at (1 and 2). The absence of few product ions within some curcumin analogues could also be due to the fast conversion of these product ions into more stable species. For example, in Table 3.3, the product ion (F10) was not detected with NC2315 curcumin analogue however, the product ion (F11) which is generated from (F10) by the loss of hydrogen molecule was detected with this compound. This indicates that the product ion (F10) was formed during the fragmentation of NC2315 and completely converted into F11.

To confirm the sequence of the proposed fragmentation (Figure 3.1B), MS^3 analysis was performed. Table 3.4 shows a summary for MS^3 experiments of NC2067; illustrating that one product ion could be formed from different sources. For example, the product ion observed at *m/z* 143.1 was formed from two other product ions (*m/z* 259.1 and 247.1) in addition to its possible direct formation from the precursor ion. On the other hand, a unique product ion has been formed only during the MS/MS analysis of NC2067 (not shown in Table 3.3) with *m/z* value= 189.1. MS^3 analysis confirmed that this ion is produced from the ion observed at *m/z* 349.1 via serial fragmentation (Figure 3.1A).

Precursor ion I	Precursor ion II	MS/MS/MS product ions
467.1	349.1	189.1, 147.1
	259.1	231.1, 229.1, 143.1
	247.1	219.1, 205.1, 143.1
	231.1	229.1
	192.1	147.1

Table 3.4. Summary of MS^3 experiments for NC2067

In addition to MS^3 experiments, neutral loss scans were performed to confirm the precursor ion's structure and the proposed fragmentation pathway. For example, the product ion (F3) was proposed to be directly formed by neutral loss of 350 Da from the precursor ion (467.1 Da) (Figure 3.1A). This pathway was confirmed by scanning the neutral loss of 350 Da during the MS/MS analysis of NC2067, showing the 467.1 as a precursor ion for the product ion (F3). The purpose of this work is to develop a general fragmentation behavior of all tested curcumin analogues. However, a relatively detailed MS/MS fragmentation, primary focusing on the abundant ions, along with the associated spectrum of all curcumin analogues are shown in Appendix B. We underlined the product ions that can serve as diagnostic species during qualitative/quantitative analysis of these compounds.

The fragmentation of curcumin analogues with secondary amines (i.e. NC2453, NC2454, EF24, NC2128) (Scheme 3.2) partially followed the general pathway presented in Table 3.3 by showing mainly the product ions of F3, F4 and F5. The absence of the side chain in these compounds may have resulted in the observed variations in their MS/MS dissociation behavior. The CID-MS/MS fragmentation of the secondary amine curcumin analogues also centered on the piperidone ring but in a different fashion than other compounds with side chains (Table 3.5).

Precursor ion $[M+H]^+$	Product ions	Broken Bonds
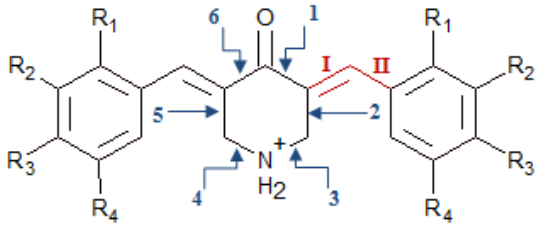	F1'	3 & 4
	F2'	1 & 6
	F3'	1, 3, 4 & 6
	F4'	1, 2, 3, 4, 5 & 6
	F5'	I
	F6'	II
	F7'	II, 3 & 4
	F8'	II, 1, 3, 4 & 6
	F9'	I, 3 & 4
	F10'	R

Compound	Precursor ion P = $[M+H]^+$	F1' (P-NH_3)	F2' (P-CO)	F3' (F2'-NH_3)	F4' (F3'-C_2H_2)	F5' (P-N_1)	F6' (P-N_2)	F7' (F6'-NH_3)	F8' (F7'-CO)	F9'	F10' (P-RH)
2453	336.2	-	308	291	265	121	228	211	183	215	304
2454	396.2	379	368	351	325	151	258	241	213	245	364
EF24	312.2	-	284	267	-	109	216	-	171	203	292
2128	308.2	291	280	263	237	107	214	197	169	201	290

$N_1 = C_{12}H_7NO + R_1 + R_2 + R_3 + R_4$ $N_2 = C_6H_2 + R_1 + R_2 + R_3 + R_4$

Table 3.5. The fragmentation sites in the 3,5-bis(benzylidene)-4-piperidone and the corresponding product ions during the ESI-MS/MS of the secondary amine curcumin analogues.

In Figure 3.2, the MS/MS spectrum of NC 2128 was used as a representative compound showing the direct loss of the amino and the carbonyl groups from the precursor ion *m/z* 308.0 via breaking the bonds (3 and 4) and bonds (1 and 6) resulting in the product ions F1' and F2' observed at *m/z* 291.0 and 280.0 respectively. The product ion F2' showed sequential elimination of the amino group forming F3' observed at *m/z* 263.0 that in turns loses acetylene group to yield F4' at *m/z* 237.0.

In addition, two unique product ions (i.e. F5' and F6') were detected, generated by the fragmentation of the benzylidene group of the 3,5-bis(benzylidene)-4-piperidone moiety via breaking the bonds (I and II) (Table 3.5). Curcumin analogues can exist in resonance forms as the double bond designated I (Table 3.5) can resonate as shown in Figure 3.2A. In effect, bond I is converted from a double bond into a single bond that can be easily dissociated into the product ion F5' at *m/z* 107.0 (Figure 3.2A). Unlike F5', product ion F6' at *m/z* 214.1 can undergo additional dissociating via the loss of the amino group producing F7' at *m/z* 197.1 which in turns loses the carbonyl group forming F8' at *m/z* 169.1.

Similar to F6', in which dissociation occurred at bond II, F9' at *m/z* 201.1 is another product ion that was formed by the cleavage of the bond II. The loss of the aryl substituent (RH) is one of the common product ions that have been detected with the MS/MS analysis of the secondary amines curcumin analogues. In the case of NC2128, such a loss constitutes a loss of water producing F10' at *m/z* 290.0. There are two possible mechanisms that explain the formation of F10' presented in Figure 3.2. The proposed mechanisms are dependent on the site of protonation of the precursor ion that may take place either on the amino group or the hydroxyl group of NC2128. In the latter case, the loss of water yields to production of F10' species in which the positive charge is localized within the aromatic ring, enhancing the stability of this ion via

resonance. Other structures were proposed in case the charge was localized on the secondary amine functional group (Figure 3.2). Other product ions are self-explanatory and are shown in Figure 3.2A such as ions observed at *m/z* 273.0 and 245.1. Table 3.6 illustrates the performed MS^3 and neutral loss experiments confirming the proposed fragmentation pathway as presented in Figure 3.2. The detailed fragmentation and associated spectrum of curcumin analogues bearing secondary amine functional groups are shown in Appendix B.

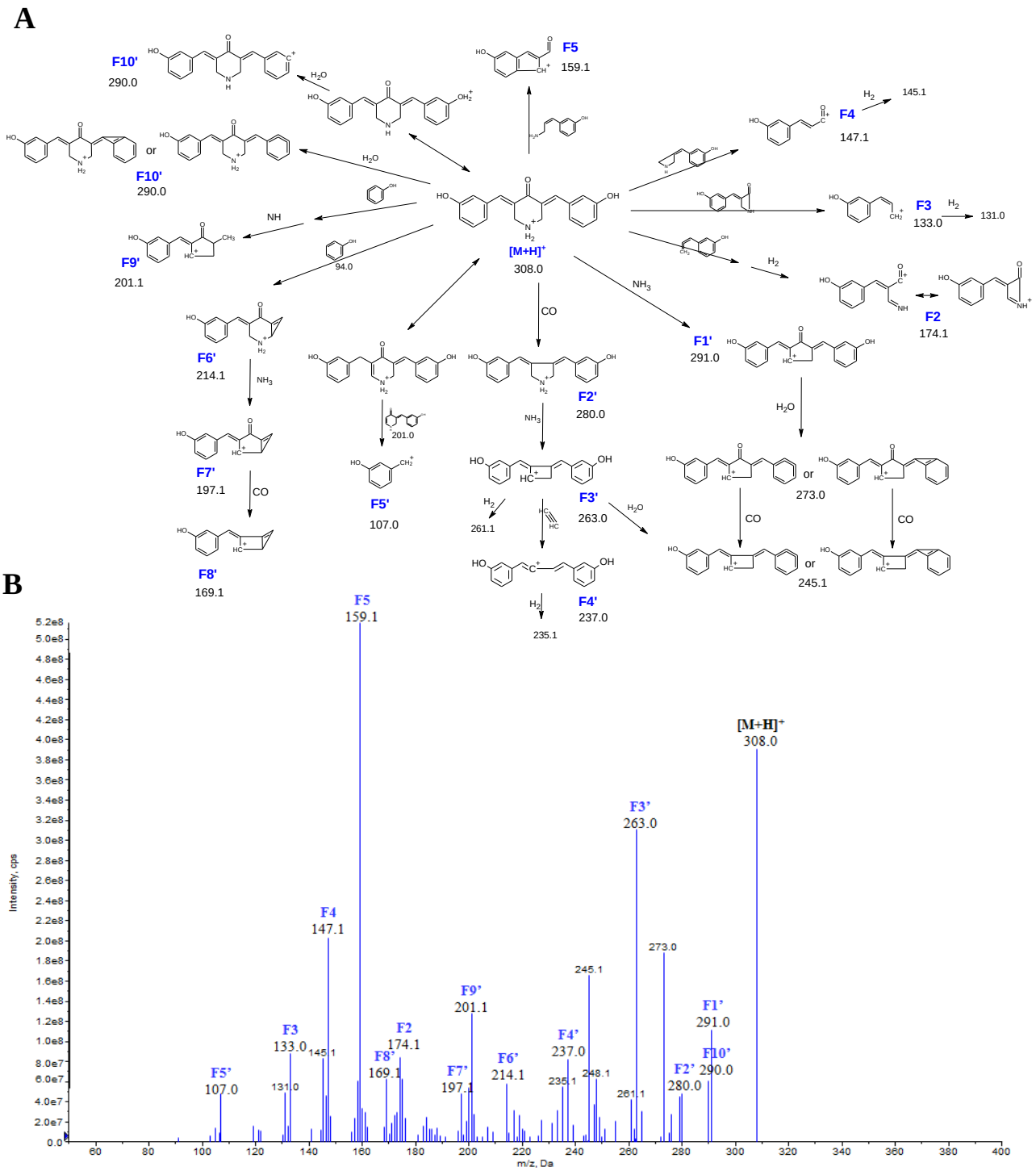

Figure 3.2. The proposed fragmentation pattern (A) and the ESI-Qq-LIT-MS/MS spectrum (B) of NC 2128 secondary amine curcumin analogue.

MS^3 analysis		
Precursor ion I	**Precursor ion II**	**MS^3 product ions**
308.0	291.0	273.0, 263.0, 245.1, 197.1, 169.1, 159.1, 147.1
	273.0	245.1
	280.0	263.0, 245.1, 237.0, 235.1
	263.0	245.1, 237.0, 235.1
	214.1	197.1
	197.1	169.1
Neutral loss scan		
Neutral loss		**Precursor ion**
201 (forming product ion F5')		308.0
94 (forming product ion F6')		308.0

Table 3.6. Summary of MS^3 and neutral loss experiments for NC2128

Side chain fragmentation

The side chain dissociation behavior of the tested curcumin analogues was based on the structural features of each side chain. In Figure 3.1A, the side chain fragmentation of NC2067 was focused on the amide bond (bond is identified with an arrow) with the neutral loss of the 3,5-bis(benzylidene)-4-piperidone moiety (275 Da), generating the ion of the side chain (F_I) at *m/z* = 192.1. Other side chain product ions (F_{II} and F_{III}) were observed at *m/z* 147.1 and 72.0, respectively, as shown in Figure 3.1A. The MS^3 and the neutral loss scan experiments were performed to confirm the fragmentation pathway of these ions. For example, the product ion (F_{II}) at *m/z* 147.1 was formed from the ion (F_I) at *m/z* 192.1 and also from (F2) at *m/z* 349.1 (Table 3.4). On the other hand, a neutral loss of 395 Da was investigated, confirming the proposed direct formation of the product ion (F_{III}) at *m/z* 72 from the precursor ion (Figure 3.1A).

The same fragmentation behavior of the side chain of NC2067 was also observed with other curcumin analogues that belong to amides and mixed amine/amide categories as presented in Table 3.7A. The generated (F_I) from NC2067 and NC2094 at *m/z* 192 and 191 respectively were characteristic to their precursor ions and with good ion count to possibly serve as diagnostic product ions for these compounds. Another abundant (F_I) product ion was detected at *m/z* 135 during the MS/MS analysis of NC2144 and NC2138 (Table 3.7A). However, this ion cannot be used to differentiate between NC2144 and NC2138 since an identical product ion at *m/z* 135 is formed.

In the phosphoramidate curcumin analogues, the side chain product ions were formed in different fashion than the previously discussed compounds (Table 3.7B). In this group, the product ion (F_i) was formed via the loss of the ethylene group from the side chain of the precursor ion, followed by sequential loss of other ethylene group to form the (F_{ii}) ion. The dissociation was ended by the neutral loss of water molecule forming (F_{iii}) ion (Table 3.7B). In addition to the proposed side chain fragmentation, another structure was proposed for the (F_i) ion through the neutral loss of carbonyl group from the 3,5-bis(benzylidene)-4-piperidone moiety instead of side chain fragmentation (shown in Appendix B).

The side chain fragmentation

A) Amides and mixed amines/amides curcumin analogues

NC 2067 F_I=192 Da

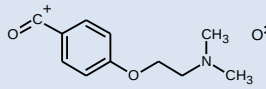

NC 2081 F_I=234 Da

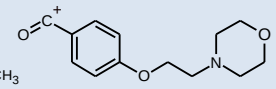

NC 2094 F_I=191 Da

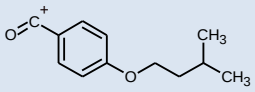

NC 2144 F_I=135 Da

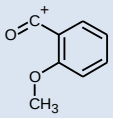

NC 2138 F_I=135 Da

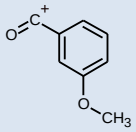

Compound	Precursor ion $P = [M+H]^+$	F_I $[R_5]^+ = (P- C_{19}H_{17}NO)$	F_{II}	F_{III}
2067	467.2	192	**(F_I - C_2H_7N)** = 147	**(F_I - $C_7H_4O_2$)** = 72
2081	509.2	234	**(F_I - C_4H_9NO)** = 147	**(F_I - $C_7H_4O_2$)** = 114
2094	466.2	191	**(F_I - C_5H_{10})** = 121	-
2144	410.2	135	-	-
2138	410.2	135	-	-

B) Phosphoramidate curcumin analogues

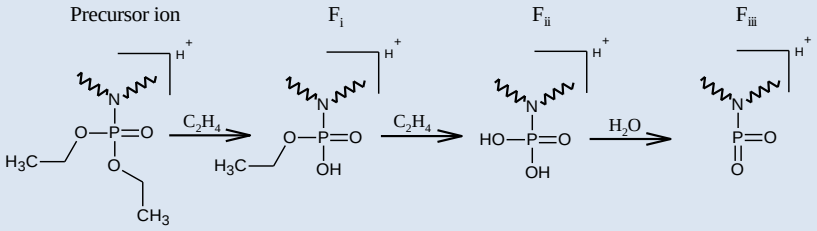

Compound	Precursor ion $P = [M+H]^+$	F_i ($P-C_2H_4$)	F_{ii} ($F_i-C_2H_4$)	F_{iii} ($F_{ii}-H_2O$)
2311	412.2	384	356	338
2313	472.2	444	416	-
2314	532.2	504	-	-
2315	592.2	564	-	-

Table 3.7. The product ions of the curcumin analogues' side chains during their ESI-MS/MS **(A)** amides and mixed amines/amides categories, showing the structures of (F_I) product ion **(B)** phosphoramidate curcumin analogues, showing the fragmentation pathway of the phosphoramidate side chain.

The protonation site

The presence of different substituents on the aryl groups and the piperidyl nitrogen atom of curcumin analogues resulted in change in the basic properties of each atom in the structures of these compounds. It was not conclusive to determine which atom will show high electron density and will be able to accept a proton during the single stage positive ion mode MS analysis. However, during CID-MS/MS analysis of curcumin analogues such as NC2311 with precursor ion $[M+H]^+$ = 412.1, a minor product ion at *m/z* 394.1 was observed (shown in Appendix B). This fragment was a result of direct loss of water molecule (18 Da) from the precursor ion, indicating that the precursor ion has a hydroxyl group which is only possible if the protonation site was the oxygen atom as presented in Scheme 3.4. This observation was detected with NC2311, NC2314 and NC2315 proving that oxygen atom is a possible site for protonation during curcumin analogues ionization.

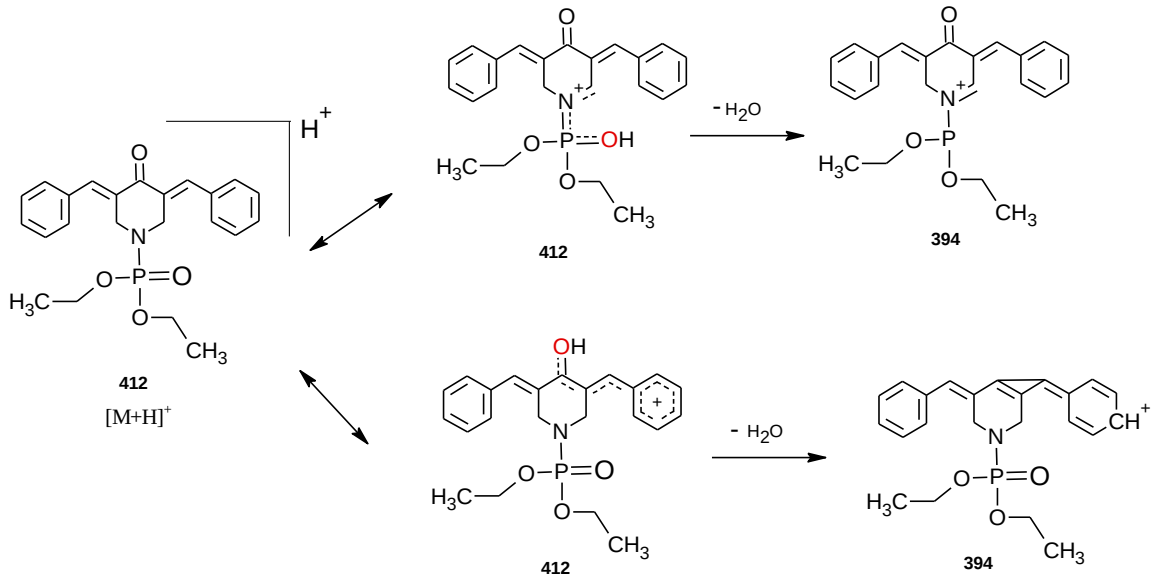

Scheme 3.4. The direct loss of water molecule from the precursor ion of NC2311 (412) and the formation of a product ion with *m/z* value at 394.

CONCLUSION

In this work, exact mass measurement confirmed the elemental composition of the 13 novel antineoplastic curcumin analogues with mass accuracy <6 ppm. The Qq-LIT-MS/MS fragmentation pattern was established for each compound confirming its chemical structure and revealing its diagnostic product ions that are characteristic for each compound. The established fragmentation patterns were confirmed via MS^3 and neutral loss experiments that confirmed the proposed chemical structure of product ions and fragmentation pathway. A similar fragmentation behavior was observed among all tested curcumin analogues that mainly centered on the cleavage of the piperidone ring. However, such behavior was affected by the different substituents on curcumin analogues.

The fragmentation similarity allowed for the establishment of a general fragmentation pattern for these compounds that will be beneficial in future quantitative and qualitative analysis. This pattern is a MS-fingerprint pattern that can be used for the identification of these compounds or other compounds belonging to the 3,5-bis(benzylidene)-4-piperidone structural family. In addition, the use of the diagnostic product ions in quantification of curcumin analogues via multiple-reaction monitoring (MRM) analysis will ensure selectivity especially in the presence of complex matrices during preclinical and clinical studies.

REFERENCES

1. Gordaliza M: Natural products as leads to anticancer drugs. Clinical and Translational Oncology 2007, 9:767-776.

2. Coseri S: Natural products and their analogues as efficient anticancer drugs. Mini Reviews in Medicinal Chemistry 2009, 9:560-571.

3. Aggarwal BB, Kumar A, Bharti AC: Anticancer potential of curcumin: preclinical and clinical studies. Anticancer Research 2003, 23:363-398.

4. Maheshwari RK, Singh AK, Gaddipati J, Srimal RC: Multiple biological activities of curcumin: a short review. Life Sciences 2006, 78:2081-2087.

5. Anand P, Kunnumakkara AB, Newman RA, Aggarwal BB: Bioavailability of curcumin: problems and promises. Molecular Pharmaceutics 2007, 4:807-818.

6. Padhye S, Chavan D, Pandey S, Deshpande J, Swamy KV, Sarkar FH: Perspectives on chemopreventive and therapeutic potential of curcumin analogs in medicinal chemistry. Mini Reviews in Medicinal Chemistry 2010, 10:372.

7. Anand P, Thomas SG, Kunnumakkara AB, Sundaram C, Harikumar KB, Sung B, Tharakan ST, Misra K, Priyadarsini IK, Rajasekharan KN: Biological activities of curcumin and its analogues (Congeners) made by man and Mother Nature. Biochemical Pharmacology 2008, 76:1590-1611.

8. Nagaraju GP, Zhu S, Wen J, Farris AB, Adsay VN, Diaz R, Snyder JP, Mamoru S, El-Rayes BF: Novel synthetic curcumin analogues EF31 and UBS109 are potent DNA hypomethylating agents in pancreatic cancer. Cancer Letters 2013, 341:195-203.

9. Kanwar SS, Yu Y, Nautiyal J, Patel BB, Padhye S, Sarkar FH, Majumdar AP: Difluorinated-curcumin (CDF): a novel curcumin analog is a potent inhibitor of colon cancer stem-like cells. Pharmaceutical Research 2011, 28:827-838.

10. Faião-Flores F, Suarez JAQ, Maria-Engler SS, Soto-Cerrato V, Pérez-Tomás R, Maria DA: The curcumin analog DM-1 induces apoptotic cell death in melanoma. Tumor Biology 2013, 34:1119-1129.

11. Das S, Das U, Michel D, Gorecki DK, Dimmock JR: Novel 3, 5-bis (arylidene)-4-piperidone dimers: Potent cytotoxins against colon cancer cells. European Journal of Medicinal Chemistry 2013, 64:321-328.

12. Das U, Sharma RK, Dimmock JR: 1, 5-Diaryl-3-oxo-1, 4-pentadienes: A case for antineoplastics with multiple targets. Current Medicinal Chemistry 2009, 16:2001.

13. Das U, Alcorn J, Shrivastav A, Sharma RK, De Clercq E, Balzarini J, Dimmock JR: Design, synthesis and cytotoxic properties of novel 1-[4-(2-alkylaminoethoxy) phenylcarbonyl]-3, 5-bis (arylidene)-4-piperidones and related compounds. European Journal of Medicinal Chemistry 2007, 42:71-80.

14. Das S, Das U, Selvakumar P, Sharma RK, Balzarini J, De Clercq E, Molnár J, Serly J, Baráth Z, Schatte G: 3, 5-Bis (benzylidene)-4-oxo-1-phosphonopiperidines and related diethyl esters: Potent cytotoxins with multi-drug-resistance reverting properties. ChemMedChem 2009, 4:1831-1840.

15. Hsieh Y, Korfmacher W: The role of hyphenated chromatography-mass spectrometry techniques in exploratory drug metabolism and pharmacokinetics. Current Pharmaceutical Design 2009, 15:2251-2261.

16. Korfmacher W, Yu K: Mass Spectrometry: The premier analytical tool for DMPK scientists in a drug discovery environment. LC GC North America 2012, 30:640-647.

17. Donkuru M, Chitanda JM, Verrall RE, El-Aneed A: Multi-stage tandem mass spectrometric analysis of novel β-cyclodextrin-substituted and novel bis-pyridinium gemini surfactants designed as nanomedical drug delivery agents. Rapid Communications in Mass Spectrometry 2014, 28:757-772.

18. Buse J, Badea I, Verrall RE, El-Aneed A: Tandem mass spectrometric analysis of the novel gemini surfactant nanoparticle families G12-s and G18: 1-s. Spectroscopy Letters 2010, 43:447-457.

19. Buse J, Badea I, Verrall RE, El-Aneed A: Tandem mass spectrometric analysis of novel diquaternary ammonium gemini surfactants and their bromide adducts in electrospray-positive ion mode ionization. Journal of Mass Spectrometry 2011, 46:1060-1070.

20. Buse J, Badea I, Verrall RE, El-Aneed A: A general liquid chromatography tandem mass spectrometry method for the quantitative determination of diquaternary ammonium gemini surfactant drug delivery agents in mouse keratinocytes' cellular lysate. Journal of Chromatography A 2013, 1294:98-105.

21. Buse J, Purves RW, Verrall RE, Badea I, Zhang H, Mulliga CC, Peru KM, Bailey J, Headley JV, El-Aneed A: The development and assessment of high-throughput mass spectrometry-based methods for the quantification of a nanoparticle drug delivery agent in cellular lysate. Journal of Mass Spectrometry 2014, 49:1171–1180.

22. Awad H, Stoudemayer MJ, Usher L, Amster IJ, Cohen A, Das U, Whittal RM, Dimmock J, El-Aneed A: The unexpected formation of $[M-H]^+$ species during MALDI and dopant free-APPI MS analysis of novel antineoplastic curcumin analogues. Journal of Mass Spectrometry 2014, 49:1139–1147.

23. Du Z-Y, Wei X, Huang M-T, Zheng X, Liu Y, Conney AH, Zhang K: Anti-proliferative, anti-inflammatory and antioxidant effects of curcumin analogue A2. Archives of Pharmacal Research 2013, 36:1204-1210.

24. Chen B, Zhu Z, Chen M, Dong W, Li Z: Three-dimensional quantitative structure–activity relationship study on antioxidant capacity of curcumin analogues. Journal of Molecular Structure 2014, 1061:134-139.

25. Xia Y-Q, Wei1, X-Y, Li W-L, Kanchana K, Xu C-C, Chen D-H, Chou P-H, Jin R, Wu J-Z, Liang G: Curcumin analogue A501 induces G2/M arrest and apoptosis in non-small cell lung cancer cells. Asian Pacific Journal of Cancer Prevention 2014, 15:6893-6898.

26. Zhu S, Moore TW, Lin X, Morii N, Mancini A, Howard RB, Culver D, Arrendale RF, Reddy P, Evers TJ: Synthetic curcumin analog EF31 inhibits the growth of head and neck squamous cell carcinoma xenografts. Integrative Biology 2012, 4:633-640.

CHAPTER 4
GENERAL DISCUSSION

4.1. General discussion

A variety of curcumin analogues have been designed over the last decade with promising pharmacological effects including anticancer [1], anti-inflammatory [2], and antioxidant effects [3]. The recent progress in the curcumin analogues research requires the use of sensitive, fast, and accurate analytical tools to evaluate potency, selectivity, and safety of the newly designed agents during preclinical and clinical studies. Mass spectrometry is an ideal analytical platform that can achieve the desired analysis of these compounds especially in complex biological matrices [4-6]. In our work, thirteen curcumin analogues with the 3,5-bis(benzylidene)-4-piperidone backbone structure (Scheme 1.3) were designed as anticancer agents and provided by Dr. Dimmock and his research team [7, 8]. These novel curcumin analogues showed cytotoxic effects against different cancer cell lines and are being evaluated as potential anticancer candidates [8-10]. Current evaluation studies include pharmacokinetic and metabolic studies that are important to determine effective drug concentrations, route of administration, and metabolic fate of these bioactive compounds [11, 12]. To my knowledge, there is only one LC-ESI-MS/MS that has been developed to characterize the pharmacokinetic and metabolic properties of one of the thirteen curcumin analogues, namely EF-24 [11]. In this study, the EF-24 plasma stability, protein binding, and pharmacokinetics were characterized. In addition, the *in-vitro* metabolism of the EF24 was evaluated in mouse liver microsomes showing the hydroxylated and reduced forms of EF24 as metabolites. This method was based on identifying the protonated ion form $[M+H]^+$ of EF-24 at *m/z* 312 and applying the multiple reaction monitoring (MRM) mode by monitoring the *m/z* 312 → 149 transition of EF-24 [11].

The development of MS based analytical methods for the analysis of the tested curcumin analogues requires studying the ionization and the CID-MS/MS behavior of such compounds. MS analysis allows for the selective identification and accurate quantification of the target analyte(s) in low concentrations within complex biological matrices. In my work, the ionization and the CID-MS/MS behavior of the thirteen curcumin analogues were investigated aiming to improve knowledge of the MS behavior of these compounds for future MS method development.

4.1.1. The ionization behavior of thirteen curcumin analogues during single stage positive ion mode using different ionization techniques

Curcumin analogues were unusually ionized during the single stage positive ion mode of MALDI-MS, showing two forms of ions; $[M-H]^+$ and $[M+H]^+$. The mass accuracy of both ions was measured using a MALDI-FTICR-MS instrument, showing mass accuracies of < 2 ppm (Table 2.1). The unexpected formation of $[M-H]^+$ was investigated over three different research streams: 1) Proposing a structure for the $[M-H]^+$ ion of curcumin analogues; 2) Evaluating the ionization behavior of curcumin analogues using various MALDI experimental conditions and other ionization techniques; 3) Proposing mechanisms for the $[M-H]^+$ and $[M+H]^+$formation.

Proposed structure of $[M-H]^+$

The $[M-H]^+$ chemical structure (Scheme 2.3) was proposed by double bond formation between the nitrogen atom and the adjacent carbon atom while the positive charge is localized on the nitrogen atom. The proposed structure was confirmed by analyzing a deuterated curcumin analogue with 10 deuterium atoms in the two benzyl rings that allowed for monitoring the site of hydrogen release.

Ionization behavior of curcumin analogues using various MALDI experimental conditions and other ionization techniques

The $[M-H]^+$ ions were not detected during the single stage positive ion mode of ESI and APCI-MS analyses of curcumin analogues, indicating that the $[M-H]^+$ phenomenon is related to the MALDI ionization mechanism. Different MALDI experimental conditions were evaluated including different solvents, matrices, matrix/analyte ratios, mass analyzer (i.e., FTICR instead of TOF), ionization mode (i.e., negative mode), and laser intensities (i.e., 4000-5000 arb. unit). All experiments showed both ions $[M-H]^+$ and $[M+H]^+$ during MALDI-MS indicating that the ionization of curcumin analogues is not significantly affected via varying MALDI conditions. Two more experiments were performed; LD-MS and solvent free LD-MS to explore the role of solvent and matrix in the $[M-H]^+$ formation. Both experiments revealed that neither solvent nor matrix play a significant role in the formation of such ions. Finally, another photoionization based technique was used (i.e., APPI) to evaluate the role of photoionization in the $[M-H]^+$ formation showing that the $[M-H]^+$ formation is significantly affected by photon energy. The ionization behavior of curcumin analogues during APPI-MS was dopant dependent where $[M-H]^+$ formed in absence of dopant and disappeared with dopant mediated APPI-MS (Scheme 2.5).

Proposed mechanisms for the $[M-H]^+$ and $[M+H]^+$ formation

Three proposed mechanisms for $[M-H]^+$ formation (Scheme 2.4) were evaluated showing opposing observations to one of these mechanisms (i.e., loss of H_2 from the protonated analyte). However, the other two proposed mechanisms (hydrogen atom transfer from the analyte radical cation and hydride abstraction) were still applicable as possible mechanisms for the $[M-H]^+$ formation. On the other hand, the detailed mechanism of $[M+H]^+$ formation of curcumin analogues in the absence of solvent and matrix during solvent free LD-MS was explained. This

mechanism was based on direct photoionization or photo-excitation of curcumin analogue molecules forming the radical cation or excited state of the analyte, followed by hydrogen subtraction or proton transfer respectively as presented in equations (1-5) on pages (61-62).

In summary, the formation of $[M-H]^+$ was primarily dependent on photoionization/photo-excitation using either MALDI or APPI. On the other hand, the formation of the expected $[M+H]^+$ was generally present in all evaluated ionization mechanisms including ESI, APCI, MALDI and APPI. The formation of radical ions ($M^{+\bullet}$) was confined to APPI-MS, providing insights into the mechanism that lead to the formation of $[M-H]^+$ ions. To advance the development of MS-based analytical methods for curcumin analogues, CID-MS/MS behavior of each species must be evaluated. In this work, I focused on assessing the CID-MS/MS dissociation behavior of curcumin analogues during ESI-MS/MS analysis using a Qq-LIT-MS instrument.

4.1.2. Tandem mass spectrometric analysis of the thirteen curcumin analogues

MS single stage analysis allowed for the identification of the thirteen curcumin analogues by measuring their exact masses. The molecular formula of the thirteen curcumin analogues were confirmed by monitoring the $[M+H]^+$ ions in the single stage positive ion mode of ESI-Qq-TOF-MS. The mass accuracy error was less than 6 ppm for all tested compounds using a two point-external calibration (Table 3.1).

In addition to single stage-MS, the structural features of curcumin analogues were evaluated by investigating their ESI-Qq-LIT-MS/MS fragmentation behavior. In this work, the CID-MS/MS fragmentation pattern of each curcumin analogue was established and the diagnostic product ions were identified to be used sequentially for qualitative and quantitative

analysis of these compounds (Appendix B-Schemes 1-13). Similar CID-MS/MS dissociation behavior was observed with all tested curcumin analogues that was mainly based on the cleavage of the piperidone ring of the 3,5-bis(benzylidene)-4- piperidone moiety. As a result, a general fragmentation pattern was established for the thirteen curcumin analogues, presenting twelve common product ions (Table 3.3). The number of detected product ions varied between curcumin analogues as a result of the difference in the substituents on the aryl and the piperidyl nitrogen atom of the 3,5-bis(benzylidene)-4- piperidone. For example, the absence of the substitution on the piperidyl nitrogen atom in the case of the secondary amine curcumin analogues (Scheme 1.3) resulted in less detected common product ions (3 out of 12). However, other product ions were detected with these compounds that also centered on the cleavage of the piperidone ring but in different fashion as presented in Table 3.5. Side chain fragmentation of curcumin analogues showed characteristic product ions with good intensities that could serve as diagnostic ions (Table 3.7). The established MS/MS pathways were confirmed via MS^3 analysis and neutral loss scans.

In summary, MS analysis confirmed the molecular structures of the tested compounds as well as established a universal MS/MS dissociation behavior. The reported data will serve as a foundation allowing for method development as well as metabolite identification of curcumin analogues.

4.2. Summary

Studying the MS ionization and MS/MS dissociation behaviors of the thirteen curcumin analogues allowed for a better understanding of the ionization mechanism and MS/MS fragmentation behaviors of tested compounds. The data can be applied in the development of

MS-based analytical methods. In this work, the unexpected ionization behavior of curcumin analogues was investigated to demonstrate the factors involved in the $[M-H]^+$ and $[M+H]^+$ ion formation and their proposed formation mechanisms. We provided a detailed mechanism study evaluating the roles of the matrix/dopant, solvents/additives, and laser energy. Photon energy was crucial for the observed unique ionization behavior. Studying the ionization of curcumin analogues with various ionization techniques and under different conditions improves knowledge regarding ion formation mechanisms during MS-analysis including the unexpected formation of $[M-H]^+$ species. The ionization behavior of the curcumin analogues and structurally-related compounds should be taken into account during the development of MS-based qualitative or quantitative analytical methods.

In addition, the MS/MS fragmentation patterns of the tested curcumin analogues were established confirming their chemical structures and providing fingerprint MS/MS patterns with diagnostic product ions that can be used for selective identification and quantification of these compounds. A general MS/MS fragmentation pattern was established based on the similar fragmentation behavior of the tested curcumin analogues. It can serve as a benchmark for metabolite identification and to predict the MS/MS of structurally related compounds [13-16].

4.3. Future directions

4.3.1. Investigating curcumin analogues as possible MALDI matrices

The ability of the evaluated curcumin analogues to self-ionize by direct absorption of the photon energy during MALDI-MS as well as APPI-MS may indicate that these compounds can be used as possible future MALDI matrices. Recently, a curcumin molecule was successfully applied as a MALDI matrix for the analysis of several different analytes (i.e., drugs, lipids,

peptides, and proteins) as well as for MALDI imaging applications [17]. The evaluated curcumin analogues in this study were designed by structural modification of the curcumin molecule showing the same conjugated unsaturated ketone structure. Such structural similarity may indicate that these compounds can also, similar to curcumin, be used as MALDI matrices.

4.3.2. Qualitative and quantitative analysis of the tested curcumin analogues and structurally-related compounds

MALDI based analytical methods can be developed for the analysis of the thirteen curcumin analogues by monitoring the $[M-H]^+$ ions instead of the $[M+H]^+$. As $[M-H]^+$ ions were detected with high intensities in comparison to the $[M+H]^+$, this may help enhance the sensitivity/selectivity of the developed method as well as the limit of detection/quantification. In addition, three curcumin analogues were ionized only as $[M-H]^+$ without the formation of the $[M+H]^+$ ions which means that MALDI-based identification and quantification of these compounds cannot be achieved by monitoring $[M+H]^+$ ions (Figure 2.6).

The established ESI-MS/MS fingerprints of the tested curcumin analogues can be used for the identification of these compounds during their preclinical and clinical evaluation. In addition, the general fragmentation pattern can be applied to other curcumin analogues recently designed by other research groups and belonging to the 3,5-bis(benzylidene)-4-piperidone structural family [13-16]. The identified diagnostic product ions from the established MS/MS pattern of each curcumin analogue are important for the quantification of these compounds via multiple-reaction monitoring (MRM) analysis. Using unique transitions during the MRM-quantification ensures selectivity of the method especially in the presence of complex matrices.

4.4. References

[1] D. K. Agrawal and P. K. Mishra, "Curcumin and its analogues: potential anticancer agents," Medicinal Research Reviews, vol. 30, pp. 818-860, 2010.

[2] A.-M. Katsori, M. Chatzopoulou, K. Dimas, C. Kontogiorgis, A. Patsilinakos, T. Trangas, et al., "Curcumin analogues as possible anti-proliferative & anti-inflammatory agents," European Journal of Medicinal Chemistry, vol. 46, pp. 2722-2735, 2011.

[3] K. M. Youssef, M. A. El-Sherbeny, F. S. El-Shafie, H. A. Farag, O. A. Al-Deeb, and S. A. A. Awadalla, "Synthesis of curcumin analogues as potential antioxidant, cancer chemopreventive agents," Archiv der Pharmazie, vol. 337, pp. 42-54, 2004.

[4] W. A. Korfmacher, "Foundation review: Principles and applications of LC-MS in new drug discovery," Drug Discovery Today, vol. 10, pp. 1357-1367, 2005.

[5] W. Korfmacher and K. Yu, "Mass Spectrometry: The premier analytical tool for DMPK scientists in a drug discovery environment," LC GC North America, vol. 30, pp. 640-647, 2012.

[6] T. A. Gillespie and B. E. Winger, "Mass spectrometry for small molecule pharmaceutical product development: A review," Mass Spectrometry Reviews, vol. 30, pp. 479-490, 2011.

[7] U. Das, J. Alcorn, A. Shrivastav, R. K. Sharma, E. De Clercq, J. Balzarini, et al., "Design, synthesis and cytotoxic properties of novel 1-[4-(2-alkylaminoethoxy) phenylcarbonyl]-3, 5-bis (arylidene)-4-piperidones and related compounds," European Journal of Medicinal Chemistry, vol. 42, pp. 71-80, 2007.

[8] S. Das, U. Das, P. Selvakumar, R. K. Sharma, J. Balzarini, E. De Clercq, et al., "3, 5-Bis (benzylidene)-4-oxo-1-phosphonopiperidines and related diethyl esters: Potent cytotoxins with multi-drug-resistance reverting properties," ChemMedChem, vol. 4, pp. 1831-1840, 2009.

[9] U. Das, R. Sharma, and J. Dimmock, "1, 5-Diaryl-3-oxo-1, 4-pentadienes: A case for antineoplastics with multiple targets," Current Medicinal Chemistry, vol. 16, p. 2001, 2009.

[10] U. Das, H. Sakagami, Q. Chu, Q. Wang, M. Kawase, P. Selvakumar, et al., "3, 5-Bis (benzylidene)-1-[4-2-(morpholin-4-yl) ethoxyphenylcarbonyl]-4-piperidone hydrochloride: A lead tumor-specific cytotoxin which induces apoptosis and autophagy," Bioorganic and Medicinal Chemistry Letters, vol. 20, pp. 912-917, 2010.

[11] J. M. Reid, S. A. Buhrow, J. A. Gilbert, L. Jia, M. Shoji, J. P. Snyder, et al., "Mouse pharmacokinetics and metabolism of the curcumin analog, 4-piperidinone, 3, 5-bis [(2-

fluorophenyl) methylene]-acetate (3E, 5E)(EF-24; NSC 716993)," Cancer Chemotherapy and Pharmacology, vol. 73, pp. 1137-1146, 2014.

[12] R. S. P. Singh, U. Das, J. R. Dimmock, and J. Alcorn, "A general HPLC–UV method for the quantitative determination of curcumin analogues containing the 1, 5-diaryl-3-oxo-1, 4-pentadienyl pharmacophore in rat biomatrices," Journal of Chromatography B, vol. 878, pp. 2796-2802, 2010.

[13] G. P. Nagaraju, S. Zhu, J. Wen, A. B. Farris, V. N. Adsay, R. Diaz, et al., "Novel synthetic curcumin analogues EF31 and UBS109 are potent DNA hypomethylating agents in pancreatic cancer," Cancer Letters, vol. 341, pp. 195-203, 2013.

[14] S. S. Kanwar, Y. Yu, J. Nautiyal, B. B. Patel, S. Padhye, F. H. Sarkar, et al., "Difluorinated-curcumin (CDF): a novel curcumin analog is a potent inhibitor of colon cancer stem-like cells," Pharmaceutical Research, vol. 28, pp. 827-838, 2011.

[15] F. Faião-Flores, J. A. Q. Suarez, S. S. Maria-Engler, V. Soto-Cerrato, R. Pérez-Tomás, and D. A. Maria, "The curcumin analog DM-1 induces apoptotic cell death in melanoma," Tumor Biology, vol. 34, pp. 1119-1129, 2013.

[16] S. Das, U. Das, D. Michel, D. K. Gorecki, and J. R. Dimmock, "Novel 3, 5-bis (arylidene)-4-piperidone dimers: Potent cytotoxins against colon cancer cells," European Journal of Medicinal Chemistry, vol. 64, pp. 321-328, 2013.

[17] S. Francese, R. Bradshaw, B. Flinders, C. Mitchell, S. Bleay, L. Cicero, et al., "Curcumin: A multipurpose matrix for MALDI mass spectrometry imaging applications," Analytical Chemistry, vol. 85, pp. 5240-5248, 2013.

APPENDIX A
THE SYNTHESIS OF THE DEUTERATED NC CURCUMIN ANALOGUE (3,5-BIS(BENZYLIDENE)-4-PIPERIDONE-D_{10})

The synthesis followed a general scheme previously published by Dr. Dimmock *et al* [1] . The non-deuterated form of the target compound (3,5-bis(benzylidene)-4-piperidone) was first synthesized to adjust the method condition, followed by the synthesis of the deuterated form by the acid-catalyzed condensation between benzaldehyde-d_5 and 4-piperidoine (Appendix A-Scheme 1) as follows:

1. One gram of benzaldehyde-d_5 (99.7 atom % D, CAS Number 14132-51-5, C/D/N Isotopes, Pointe-Claire, Quebec, Canada) was mixed with 12.32 ml of acetic acid followed by the addition of 721.1 mg of 4-piperidone.
2. Dry HCl air was passed through the mixture with stirring for 30 minutes till clear solution was formed. Then the mixture stirred for 24 hours at room temperature.
3. A precipitate was collected by vacuum filtration and washed with ether then mixed with 25% w/v potassium carbonate in water (2.5gm K_2CO_3 in 10ml water).
4. The mixture was stirred for 30 minutes and the precipitate was collected by vacuum filtration and washed with water and dried.

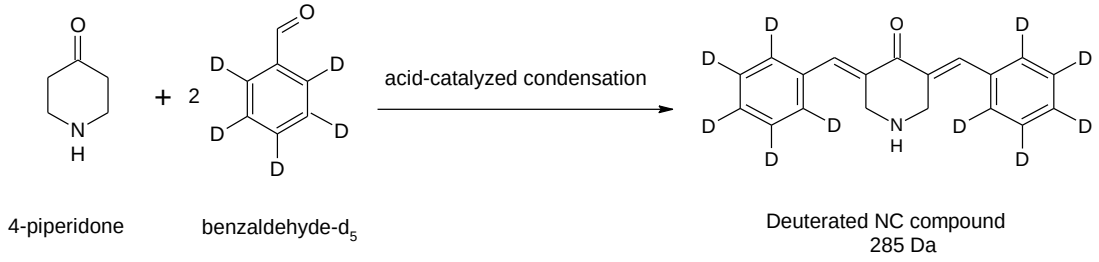

Appendix A-Scheme 1: The synthetic process of the 3,5-bis(benzylidene)-4-piperidone-d_{10} (the dueterated NC curcumin analogue)

The yield% of the deuterated final product was 83.19%. This compound was confirmed by NMR, showing the complete disappearance of the 10 hydrogen atoms of the two benzyl groups in comparison to the NMR of the non-deuterated NC curcumin analogue. The exact mass of the deuterated compound was measured using the ESI-Qq-TOF-MS under the previously mentioned operating condition on pages (79-80), showing the $[M+H]^+$ ion at *m/z* 286.2 with mass accuracy of 5.73 ppm (Appendix A-Figure 1A). No other peaks were detected during the ESI-Qq-TOF-MS analysis of the deuterated compound. As illustrated in Appendix A-Figure 1B, the background at *m/z* values (0 - 285) show signals with maximum intensity of 5.6 ion counts.

References:

[1] U. Das, J. Alcorn, A. Shrivastav, R. K. Sharma, E. De Clercq, J. Balzarini, et al., "Design, synthesis and cytotoxic properties of novel 1-[4-(2-alkylaminoethoxy) phenylcarbonyl]-3, 5-bis (arylidene)-4-piperidones and related compounds," European journal of medicinal chemistry, vol. 42, pp. 71-80, 2007.

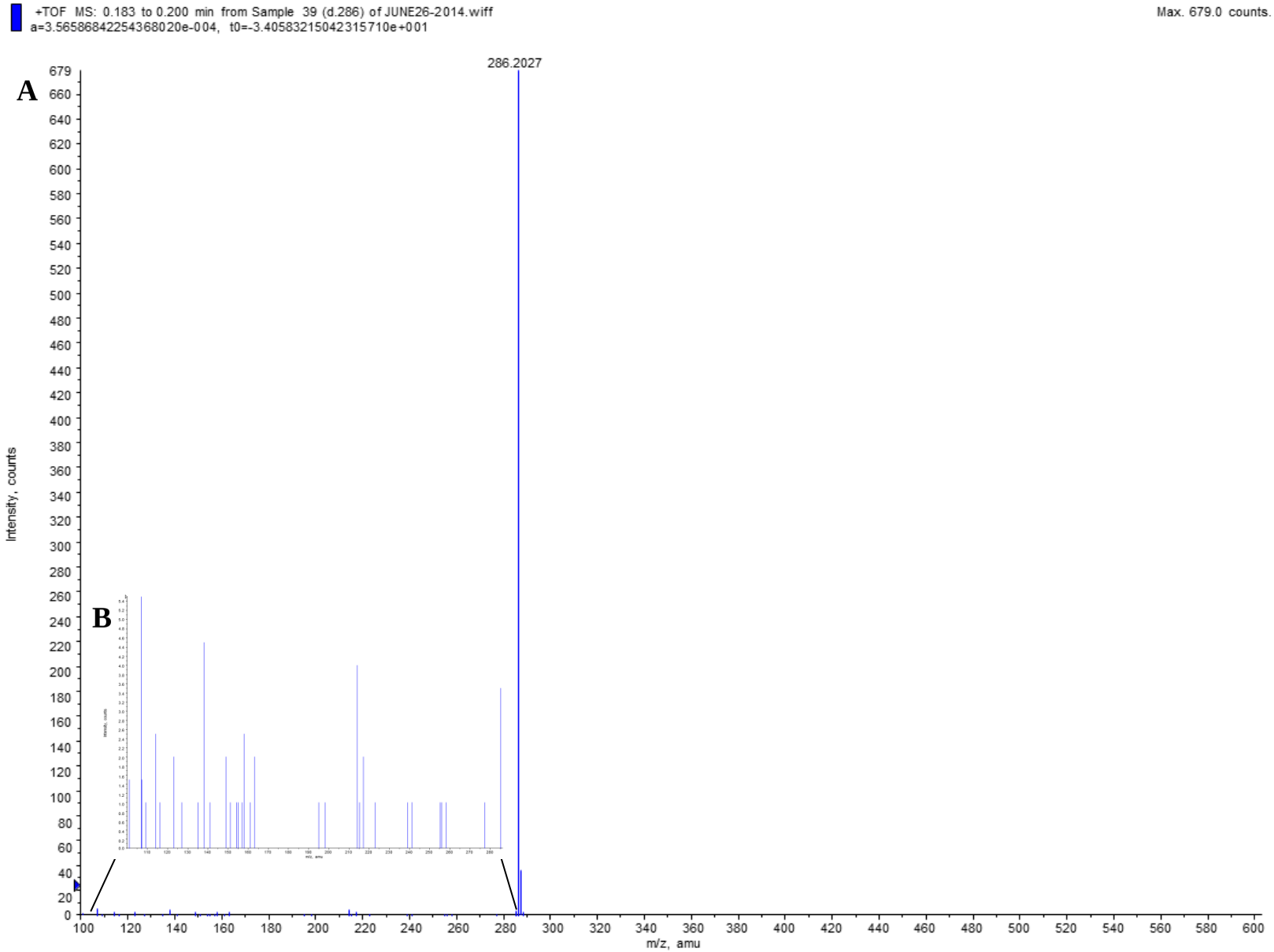

Appendix A-Figure 1: The ESI-Qq-TOF-MS spectrum of the 3,5-bis(benzylidene)-4-piperidone-d_{10}, showing the $[M+H]^+$ ion at *m/z* 286.2 **(A).** The baseline in the range of 0 to 285 Da was presented in **(B)**

APPENDIX B
THE FRAGMENTATION PATTERNS AND SPECTRA OF THE $[M+H]^+$ IONS OF CURCUMIN ANALOGUES DURING ESI-MS/MS ANALYSIS

(The *m/z* values of the diagnostic product ions of each curcumin analogue were underlined)

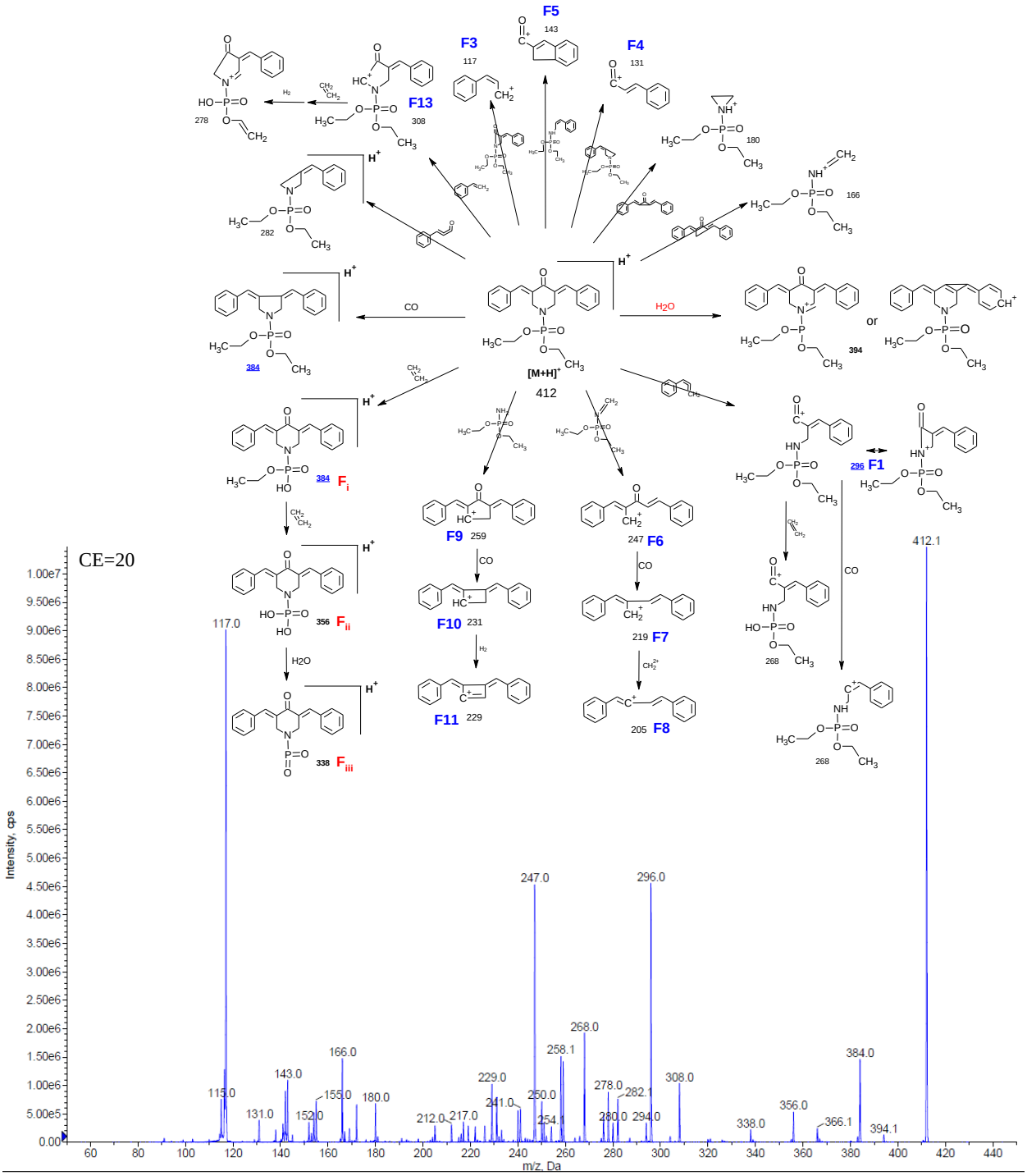

Appendix B-Scheme 1. ESI-MS/MS fragmentation pattern of $[M+H]^+$ of NC2311

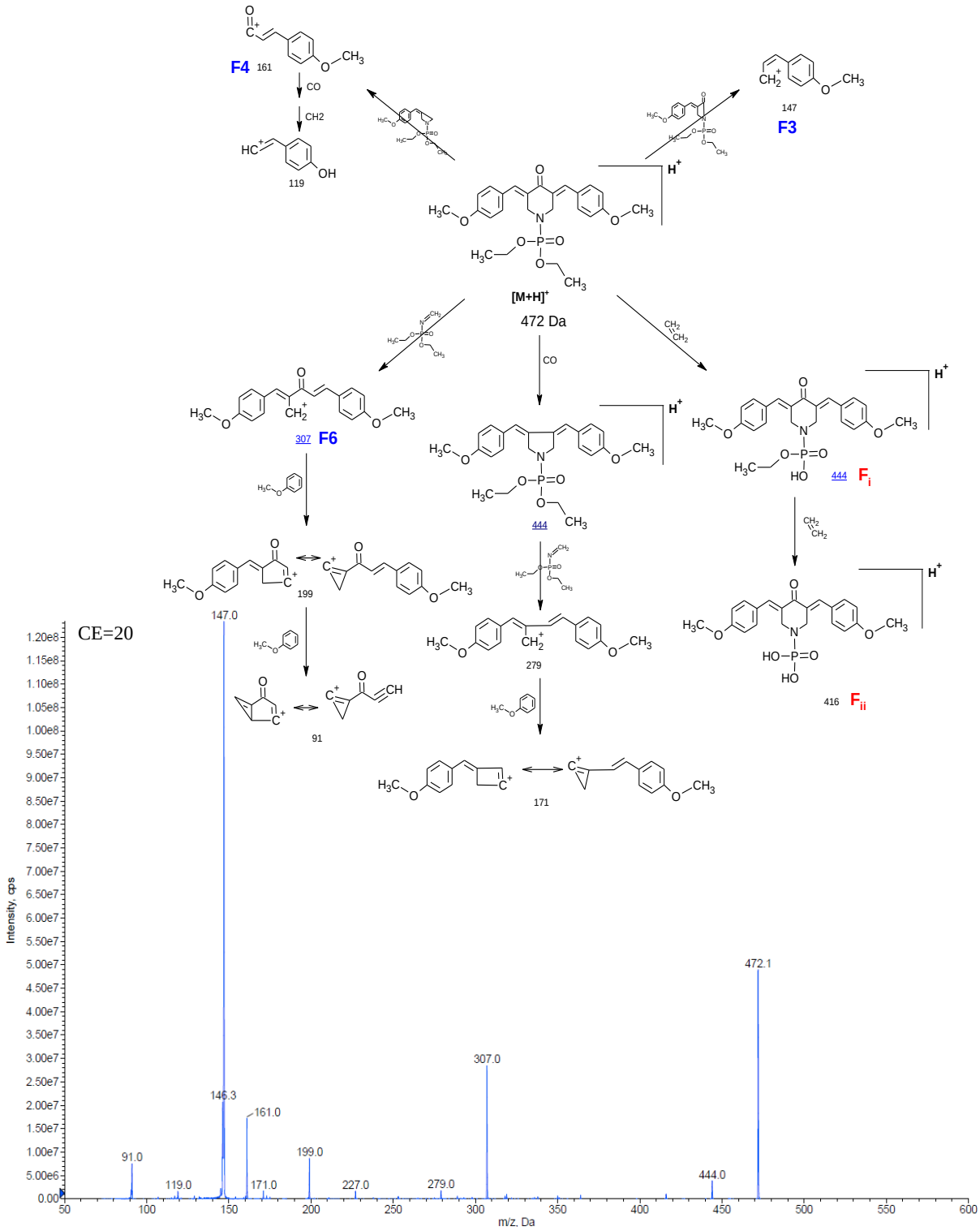

Appendix B-Scheme 2. ESI-MS/MS fragmentation pattern of $[M+H]^+$ of NC2313

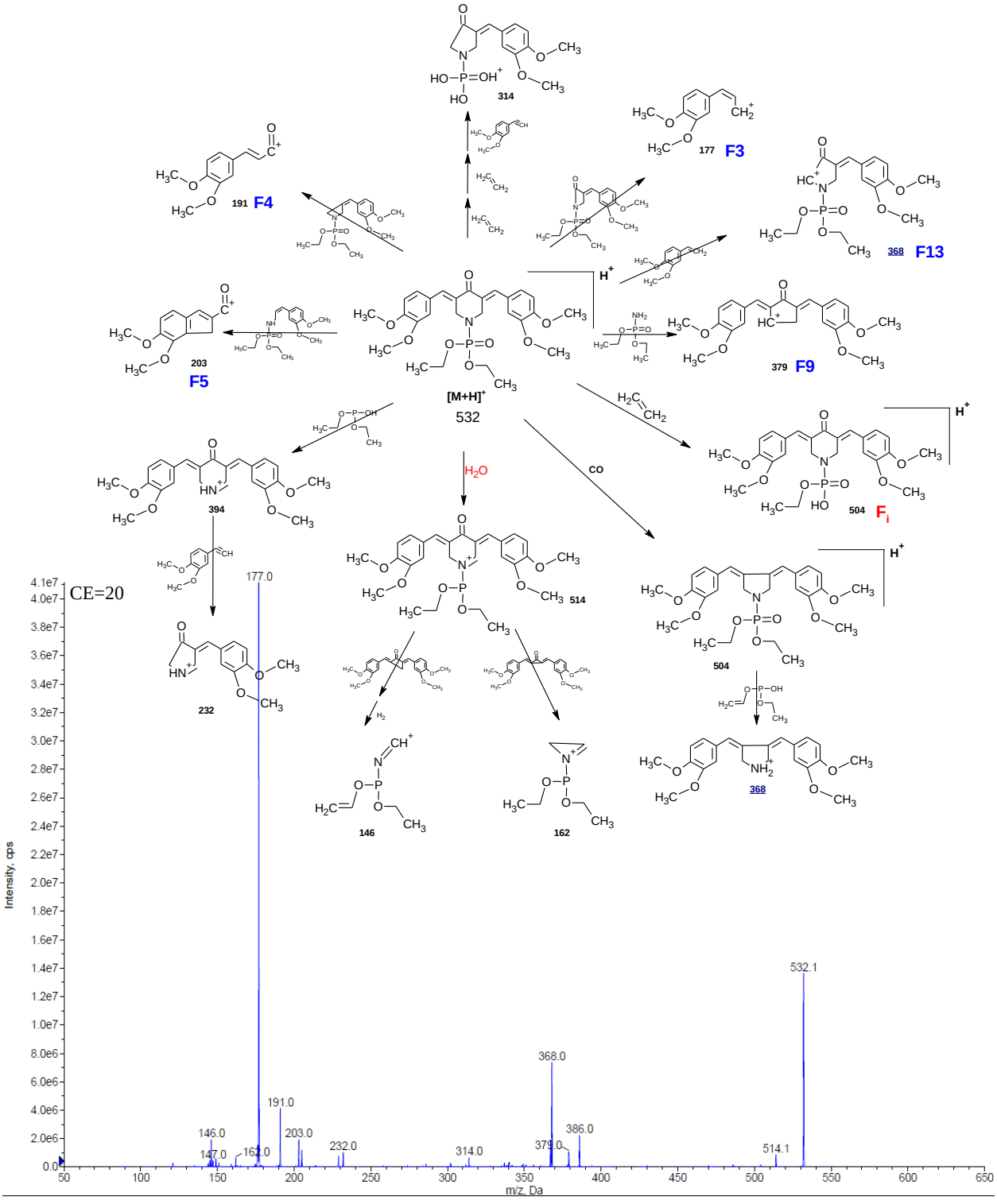

Appendix B-Scheme 3. ESI-MS/MS fragmentation pattern of $[M+H]^+$ of NC2314

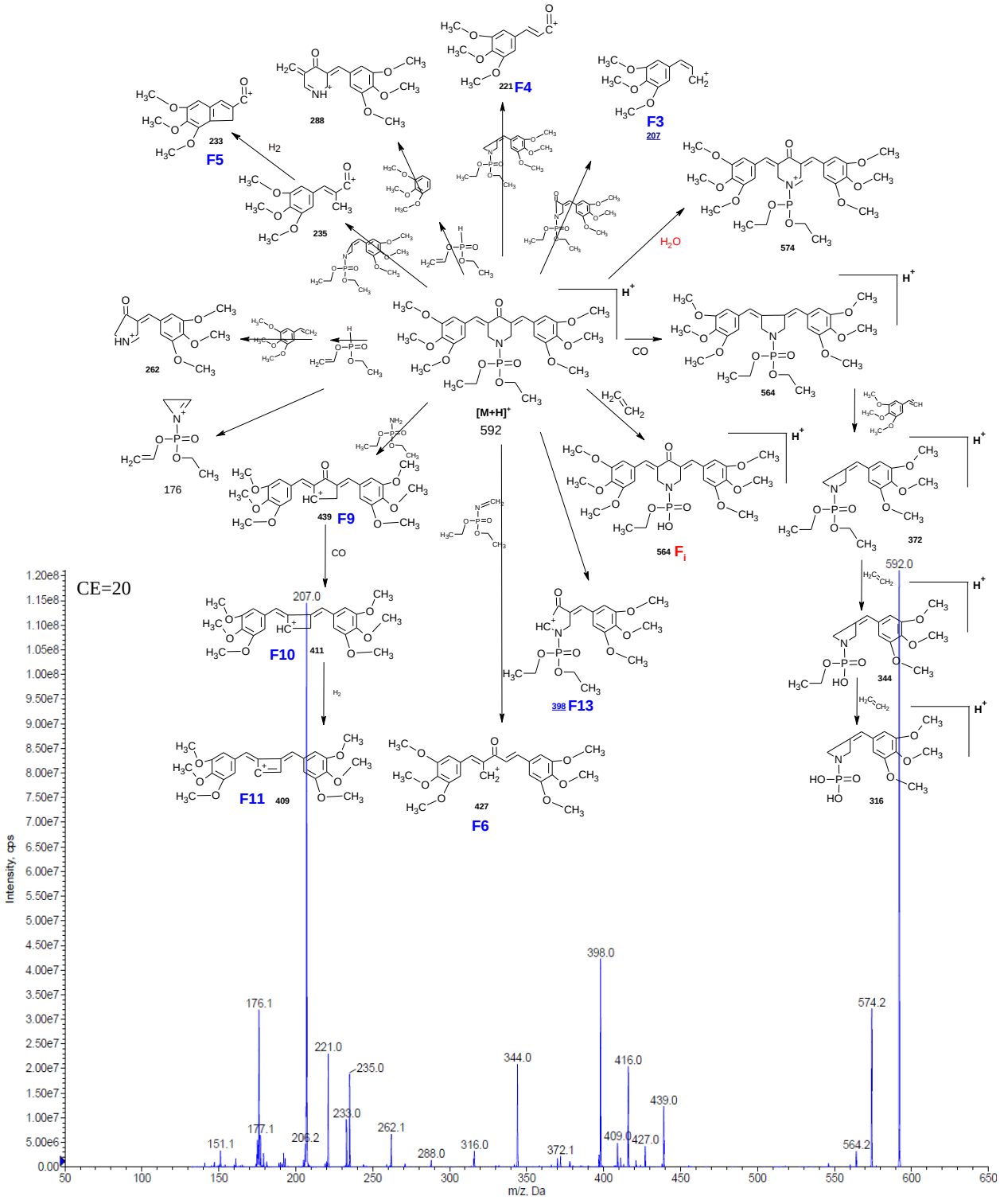

Appendix B-Scheme 4. ESI-MS/MS fragmentation pattern of $[M+H]^+$ of NC2315

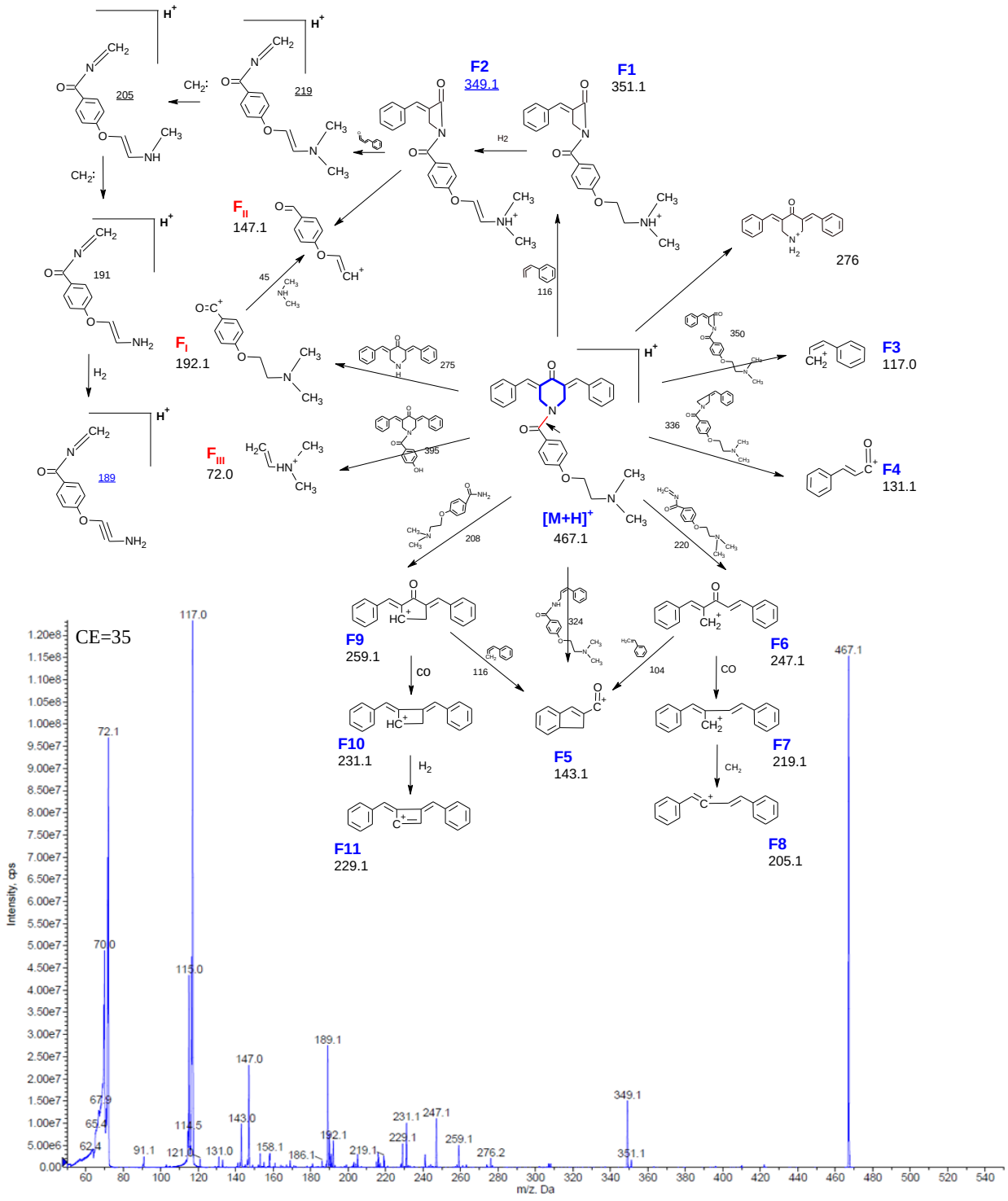

Appendix B-Scheme 5. ESI-MS/MS fragmentation pattern of $[M+H]^+$ of NC2067

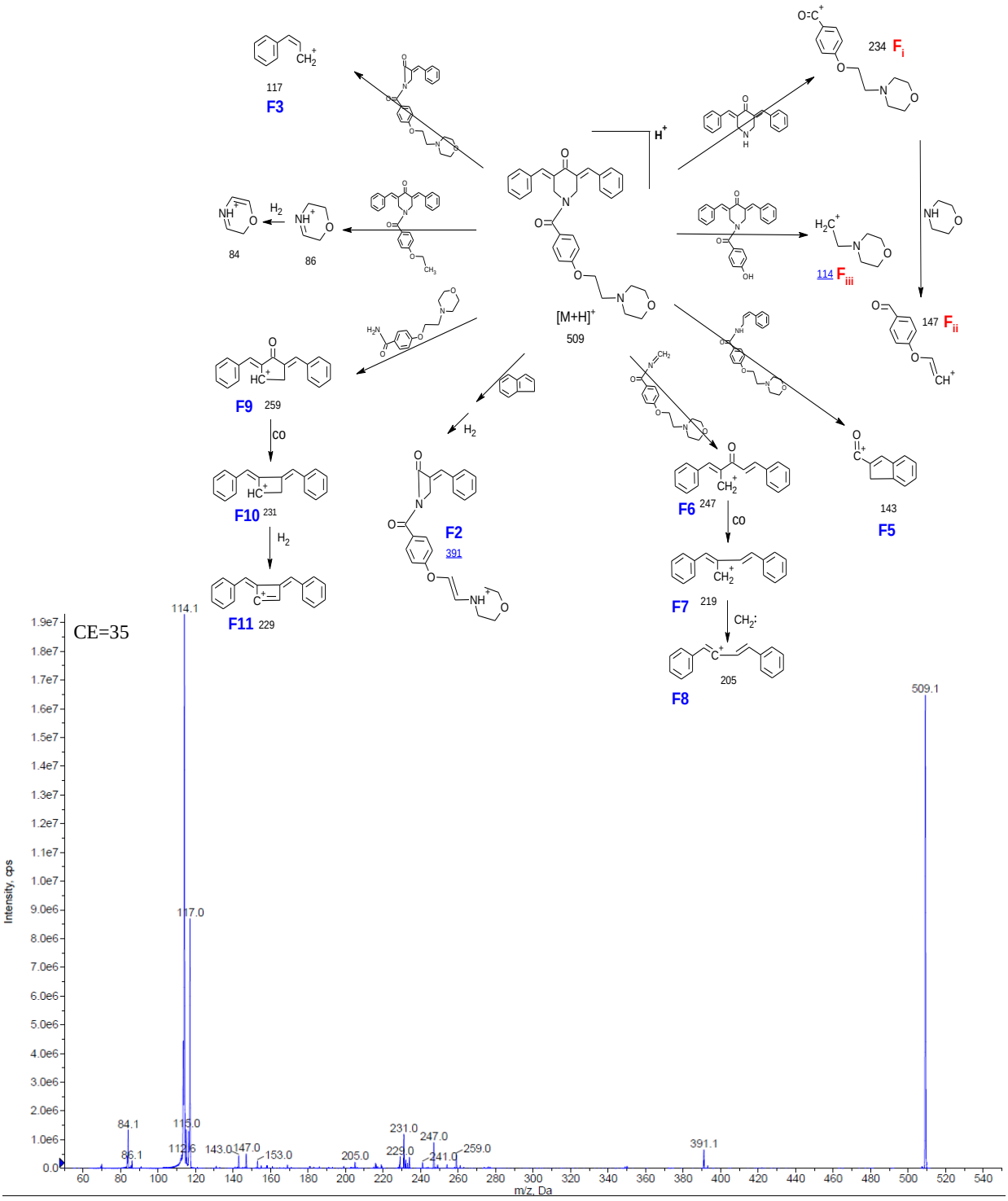

Appendix B-Scheme 6. ESI-MS/MS fragmentation pattern of $[M+H]^+$ of NC2081

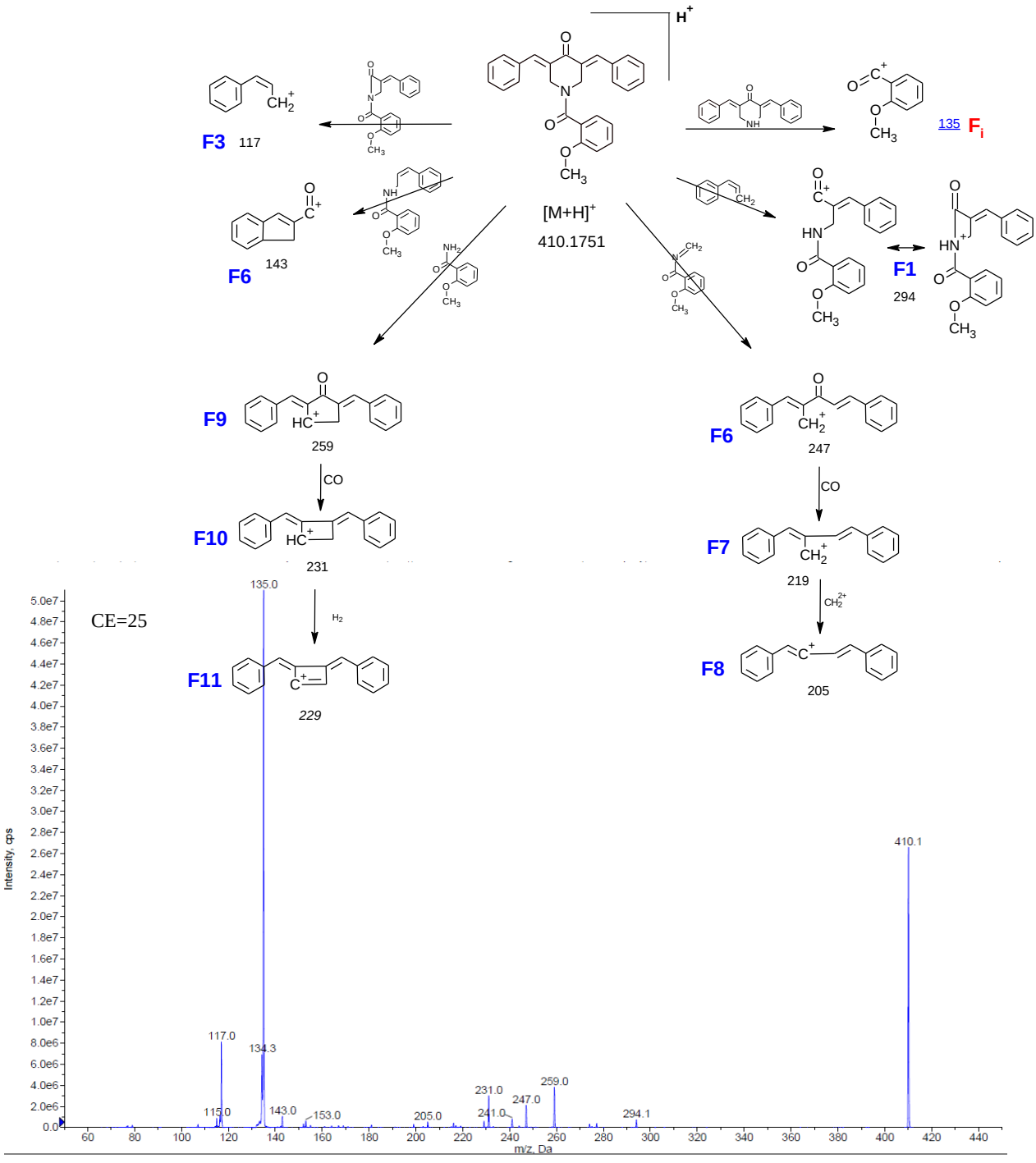

Appendix B-Scheme 7. ESI-MS/MS fragmentation pattern of $[M+H]^+$ of NC2144

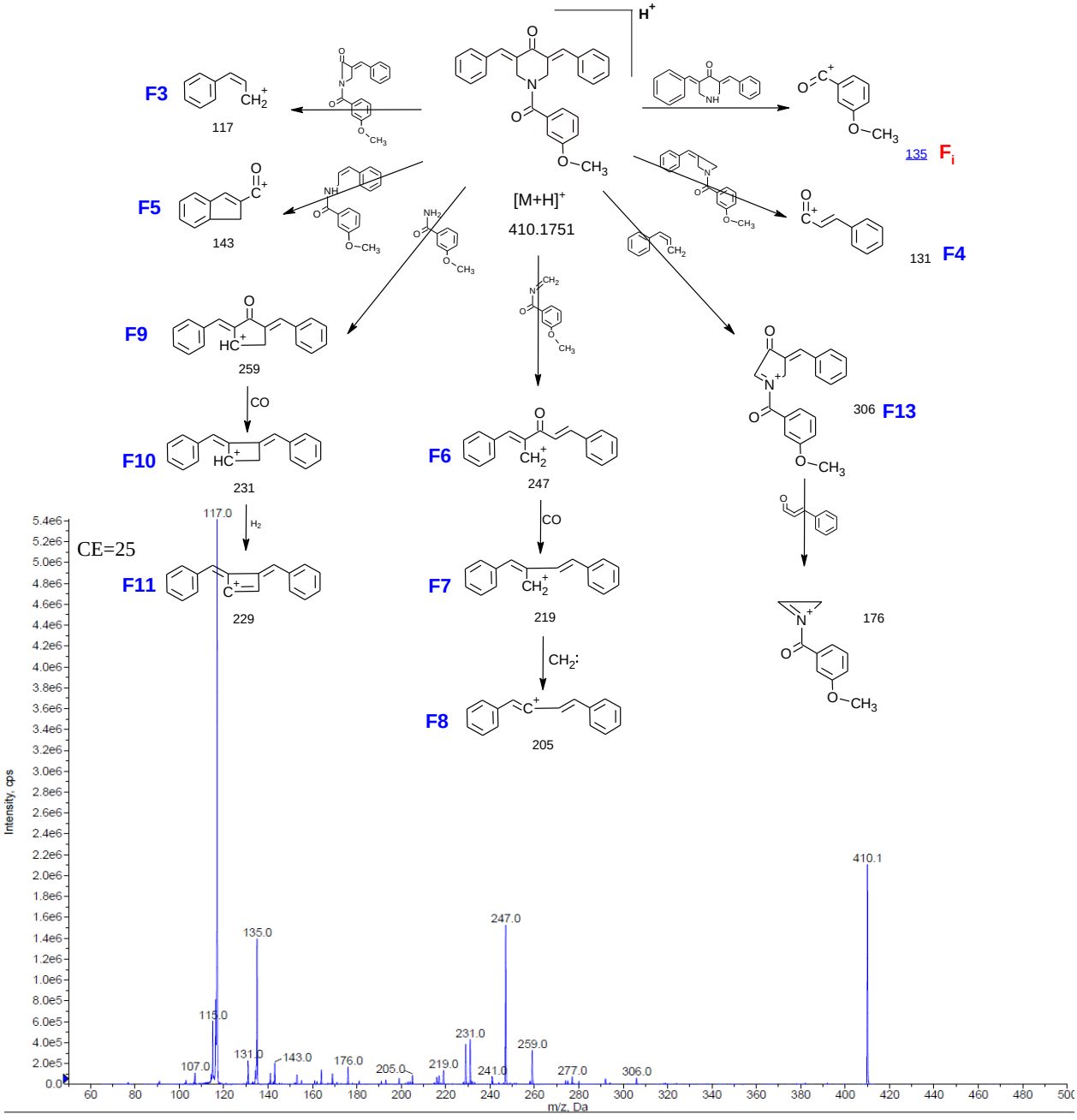

Appendix B-Scheme 8. ESI-MS/MS fragmentation pattern of $[M+H]^+$ of NC2138

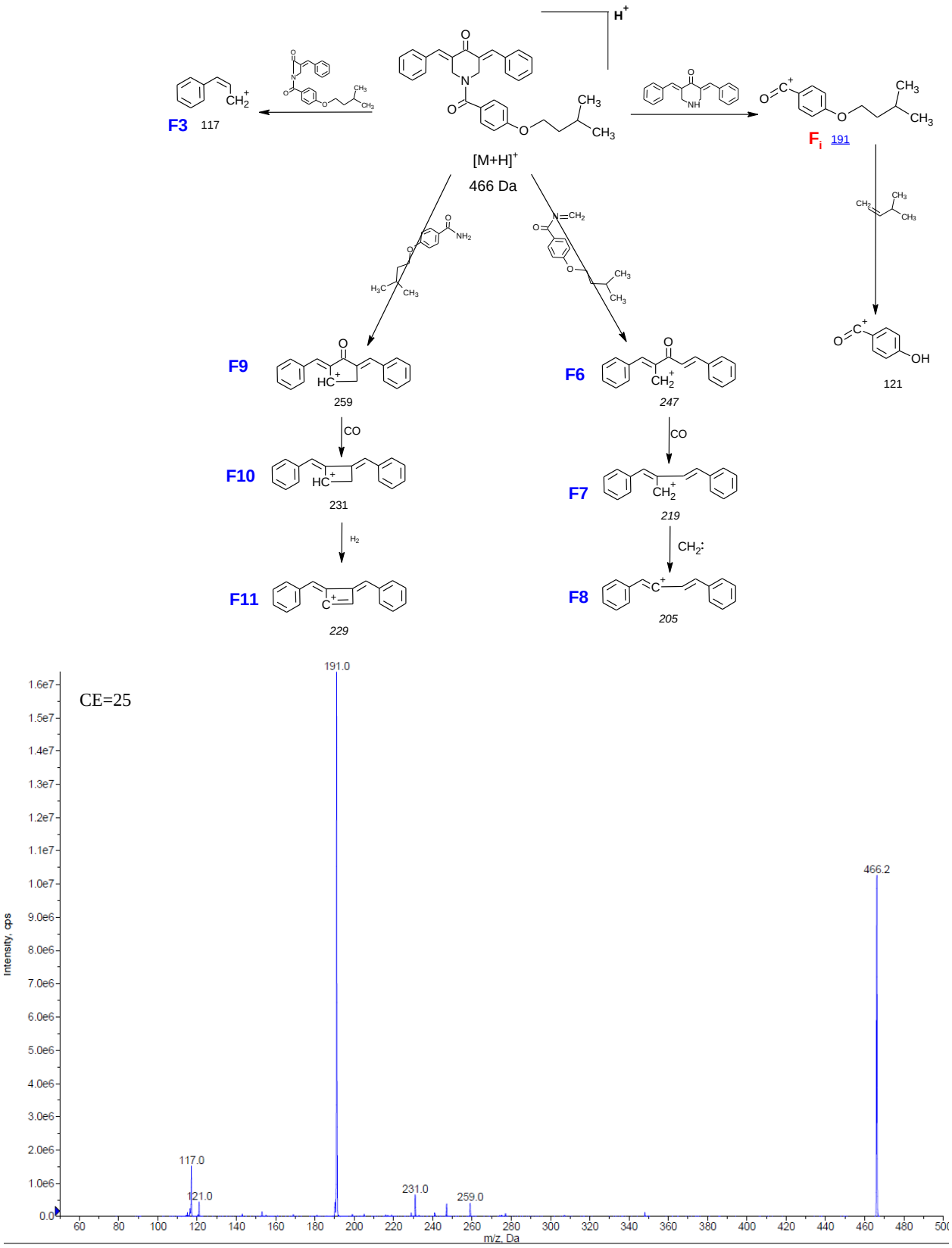

Appendix B-Scheme 9. ESI-MS/MS fragmentation pattern of $[M+H]^+$ of NC2094

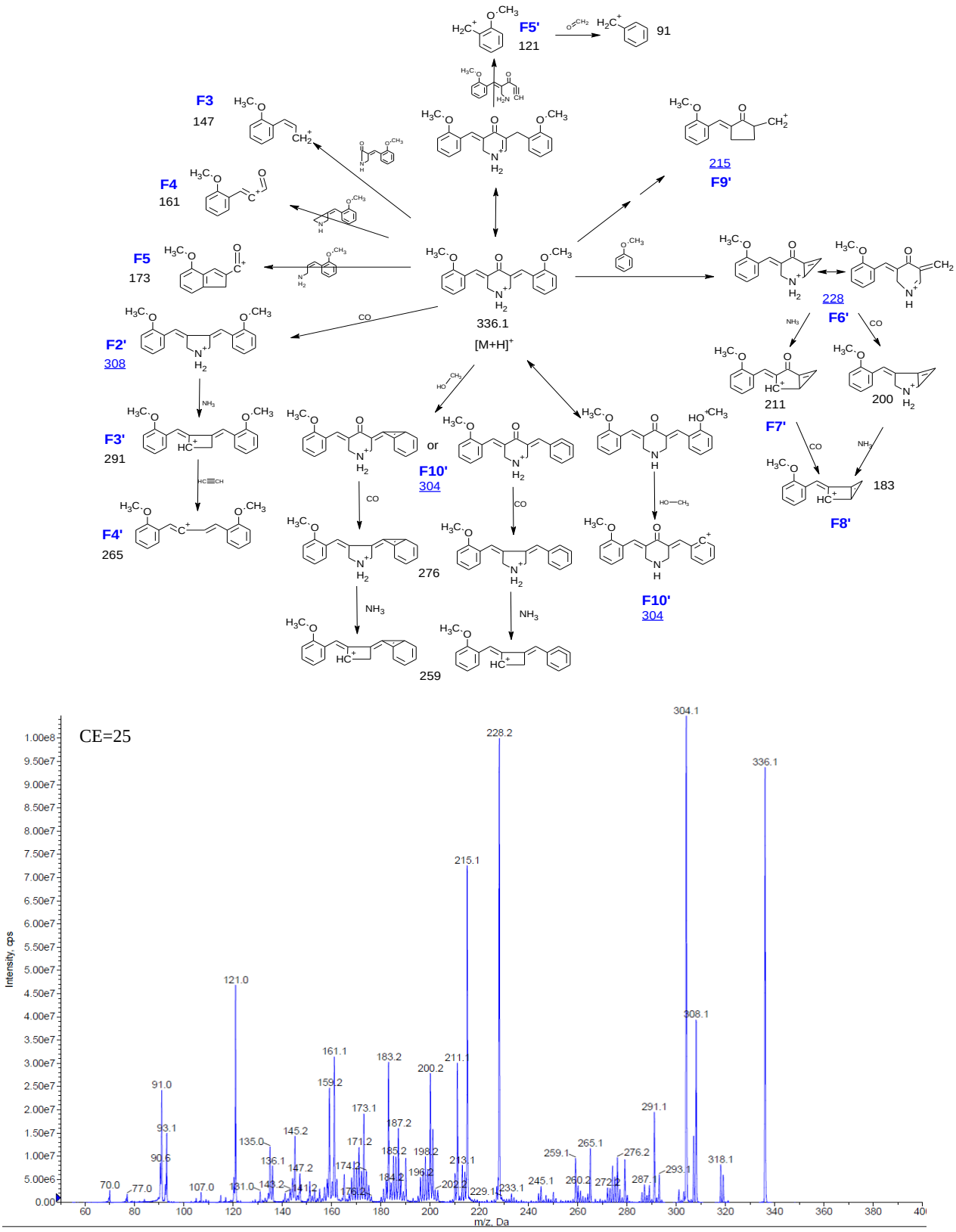

Appendix B-Scheme 10. ESI-MS/MS fragmentation pattern of $[M+H]^+$ of NC2453

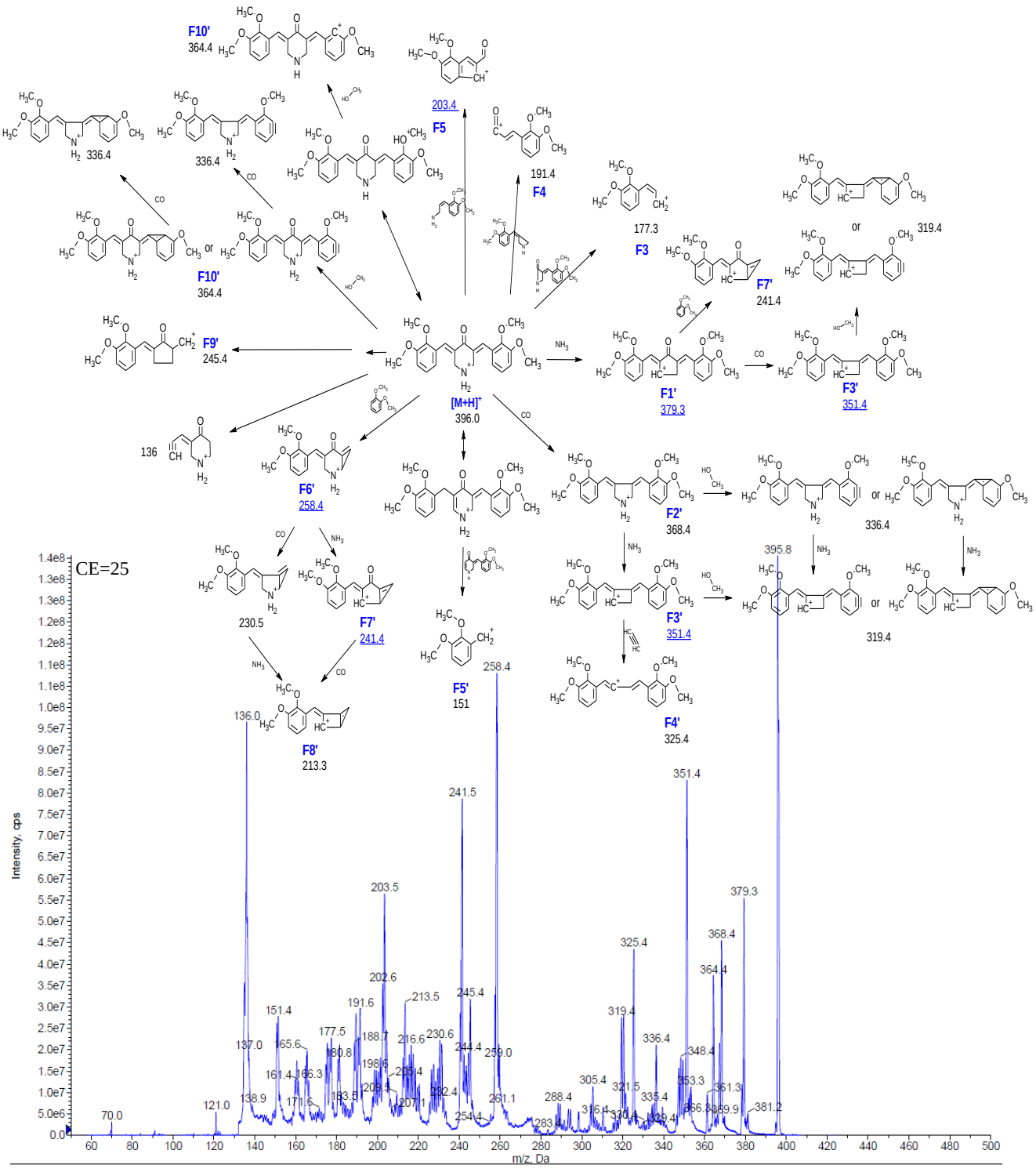

Appendix B-Scheme 11. ESI-MS/MS fragmentation pattern of $[M+H]^+$ of NC2454

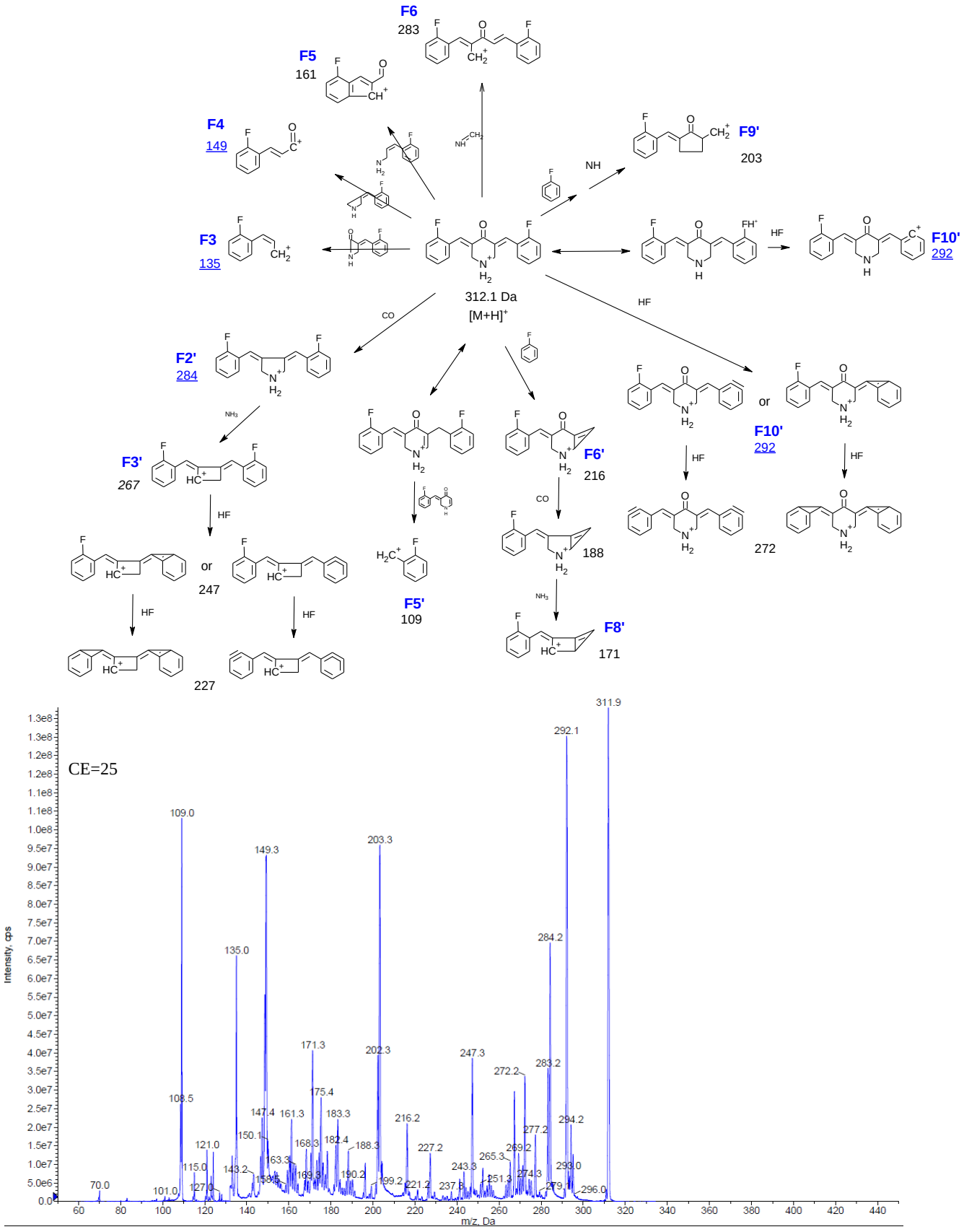

Appendix B-Scheme 12. ESI-MS/MS fragmentation pattern of $[M+H]^+$ of EF24

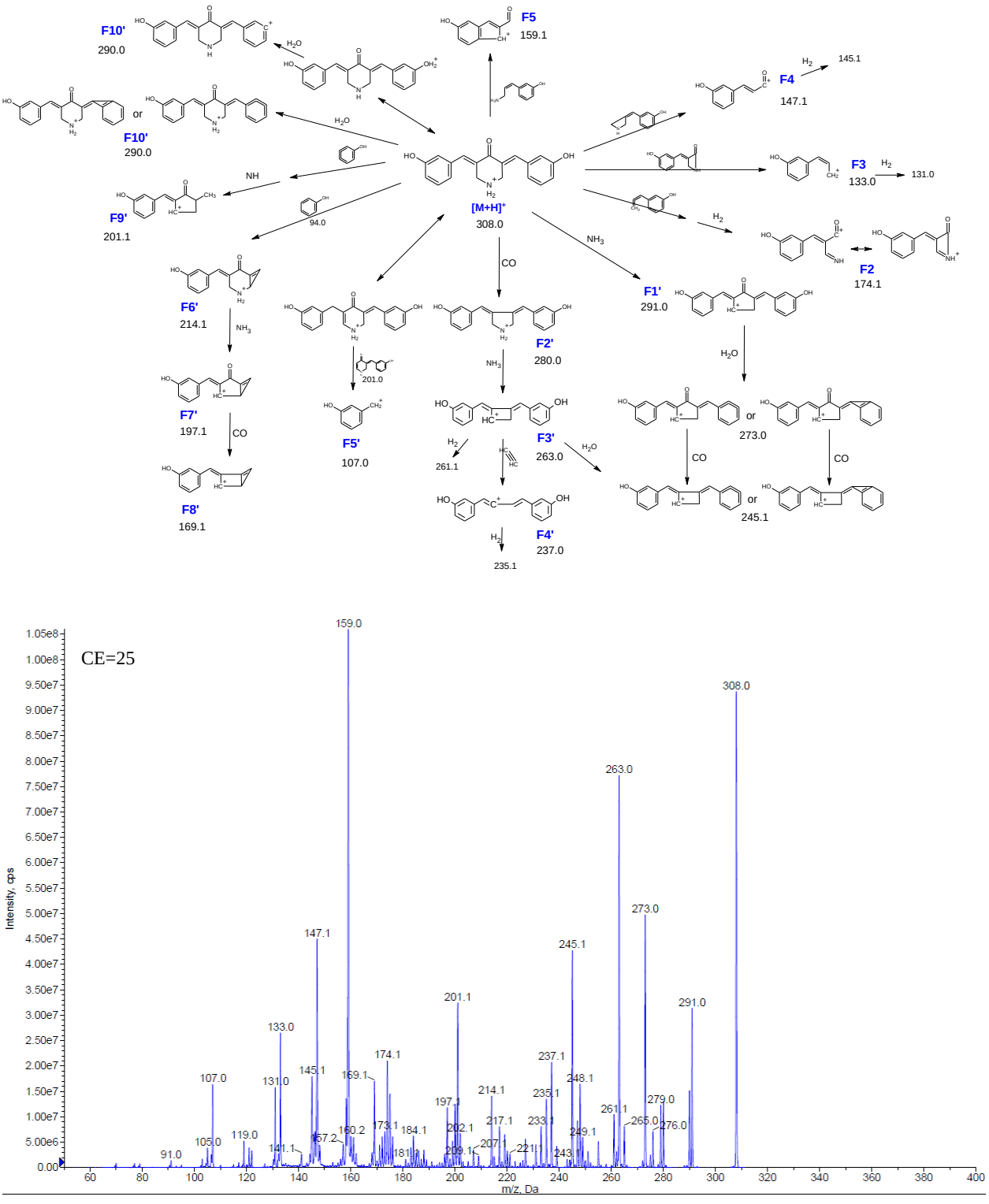

Appendix B-Scheme 13. ESI-MS/MS fragmentation pattern of $[M+H]^+$ of NC2128